ÄSPÖLABORATORIET

INTERNATIONAL COOPERATION REPORT 93-04

Scoping calculations for the Multiple Well Tracer Experiment - efficient design for identifying transport processes

Rune Nordqvist, Erik Gustafsson, Peter Andersson
Geosigma AB, Uppsala, Sweden

December 1993

Supported by SKB, Sweden

SVENSK KÄRNBRÄNSLEHANTERING AB
SWEDISH NUCLEAR FUEL AND WASTE MANAGEMENT CO
BOX 5864 S-102 40 STOCKHOLM
TEL. +46-8-665 28 00 TELEX 13108 SKB TELEFAX +46-8-661 57 19

102.8

9505040286 950424
PDR WASTE
WM-11 PDR

ISSN 1104-3210
ISRN SKB-ICR--93/4--SE

Rec'd with letter dtd 4/28/95

SCOPING CALCULATIONS FOR THE MULTIPLE WELL TRACER EXPERIMENT - EFFICIENT DESIGN FOR IDENTIFYING TRANSPORT PROCESSES

Rune Nordqvist, Erik Gustafsson, Peter Andersson

Geosigma AB, Uppsala, Sweden

December 1993

Supported by SKB, Sweden

This document concerns a study which was conducted within an Äspö HRL joint project. The conclusions and viewpoints expressed are those of the author(s) and do not necessarily coincide with those of the client(s). The supporting organization has reviewed the document according to their documentation procedure.

102.8

GEOSIGMA
MARK BERG VATTEN

Client: **SKB**
Grap: 93 082
1993-12-21

SCOPING CALCULATIONS FOR THE MULTIPLE WELL TRACER EXPERIMENT - EFFICIENT DESIGN FOR IDENTIFYING TRANSPORT PROCESSES

Rune Nordqvist
Erik Gustafsson
Peter Andersson

GEOSIGMA AB
Uppsala

December 1993

ABSTRACT (ENGLISH)

This report concerns scoping calculations for the proposed Multiple Well Tracer Experiment (MWTE), part of the experimental plan for "Flow and transport processes in the detailed scale" at the Äspö Hard Rock Laboratory. The general objective of this report is to provide information that can be used for design of the experiment. The scoping calculations are carried out in a multi-objective optimization framework, and are directed towards the following specific objectives; 1) Model discrimination, 2) Parameter estimation, 3) Influence of the experiment on natural hydraulic conditions. The main design ideas considered are: induced uniform hydraulic gradient, repeated tracer tests with varying water velocities, sampling boreholes between injection and collection points, and combination of tracers with different transport properties. Three conceptual models were considered, formulated mathematically in their one-dimensional forms, representing different types of processes; advection-dispersion, transient solute storage, and matrix diffusion. The optimization calculations are aimed at investigating how the objectives of discrimination and estimation may benefit from the simultaneous evaluation of data from more than one sampling distance, and from repeated tracer tests with different water velocities. In addition, two-dimensional flow calculations are carried out with the purpose of quantifying some hydraulic effects on water velocities of the presence of boreholes inside a flow field. For the models considered, the results indicate that both multiple sampling distances and using tracer tests with different velocities will significantly enhance the possibilities for both parameter estimation and model discrimination. Specifically, the calculations indicate that an experiment involving two sampling distances, and two or three repeated tracer runs with different velocities would provide data with a significantly increased interpretation potential, compared to a traditional single-velocity, single-distance, tracer test. It is also indicated, however, that the presence of boreholes inside the transport field may have a significantly negative hydraulic effects. Based on the results of the scoping calculations a tentative outline of the test program and borehole layout for the MWTE is presented. This also includes discussions of criteria for fracture selection, requirements for the characterization of experimental area, and tracer considerations.

ABSTRACT (SWEDISH)

Denna rapport behandlar inledande beräkningar för det föreslagna "Multiple Well Tracer Experiment" (MWTE), vilka är en del av experimentplanen för "Flow and transport processes in the detailed scale" i Äspö HRL (Äspö Hard Rock Laboratory). Den generella målsättningen med denna rapport är att bidra med information som kan användas vid utformningen av MWTE. Beräkningarna har gjorts i form av en optimeringsanalys, inriktat på följande specifika syften; 1) Modelldiskriminering, 2) Parameterskattning, 3) Inverkan av experimentet på hydrauliska förhållanden. De huvudsakliga designkoncepten är följande: inducerad uniform hydraulisk gradient, upprepade spårförsök med varierande hastighet, provtagning mellan injektions- och uttagspunkter, samt kombination av spårämnen med olika transportegenskaper. Tre konceptuella modeller studerades, matematiskt formulerade i en dimension, representerande olika typer av processer; advektion-dispersion, lagring i stagnanta zoner, och matrisdiffusion. Optimeringsberäkningarna fokuserades huvudsakligen kring hur modelldiskriminering och parameterskattning kan underlättas genom simultan utvärdering av data från mer än ett provtagningsavstånd, och från upprepade spårförsök med olika vattenhastigheter. Dessutom gjordes tvådimensionella flödesberäkningar för att kvantifiera negativa effekter av borrhål inuti ett flödesfält. För de modeller som studerades indikerar resultaten att både flera provtagningsavstånd och upprepade försök med olika hastighet väsentligt underlättar både modelldiskriminering och parameterskattning. Beräkningarna visar också, emellertid, att närvaron av borrhål inuti det flödesfält där spårämnestransporten skall studeras kan innebära en väsentlig störning på hydrauliska förhållanden. Baserat på beräkningsresultaten presenteras också ett preliminärt testprogram och borrhålskonfiguration för MWTE. Detta inkluderar även diskussion av kriterier för urval av lämplig spricka, krav för karaktärisering av experimentområdet, samt spårämnesaspekter.

TABLE OF CONTENTS

SUMMARY

This report concerns scoping calculations for the proposed Multiple Well Tracer Experiment (MWTE), part of the experimental plan for "Flow and transport processes in the detailed scale" at the Äspö Hard Rock Laboratory /Olsson, 1992/. The main objectives for the latter are /Olsson, 1992/:

- to improve understanding of transport processes and refine conceptualization of radionuclide transport in single fractures
- to determine in-situ parameters for the processes which control transport of sorbing nuclides in single fractures
- to quantify variability in flow and transport parameters for fractures of different character

The other sub-tasks of the overall experimental plan are the Pore Volume Characterization and the Matrix Diffusion Experiment.

The objective of the MWTE is to test the validity of different conceptual and numerical models of tracer transport in single fractures. The intention is that the data provided should facilitate discrimination among different conceptual models, and provide bounds for where these models provide reasonable approximations.

The general objective of the scoping calculations in this report is to provide information that can be used for designing an efficient experiment, with respect to the overall objectives of the MWTE. The scoping calculations in this report are intended to give general results, since the hydraulic properties of the fracture are not yet known. The scoping calculations should show in principle how experimental approaches can be applied to increase the possibilities of an unambiguous evaluation of the experiment. In this analysis, the calculations are carried out in a multi-objective optimization framework, and are directed towards the following specific objectives:

- Model discrimination
- Parameter estimation
- Minimize the influence of the experiment on natural hydraulic conditions

The objective of model discrimination includes identification of dominant transport processes and chemical processes, as well as dominant features of the flow system. A good design should favor a "correct" model, and simultaneously discredit "incorrect" models. In this case no prior estimates on parameter values are available, and the scoping calculations have to allow for a parameter-robust design.

The objective of parameter estimation entails finding a design that will give low estimation variance of parameters, which is dependent on the locations

and times of observations. A parameter-robust design should ensure low variance estimates over some plausible range (based on experience) of parameter values. This needs to be done for any considered model as well, since the "best" model also in unknown.

The third specific objective, minimizing hydraulic disturbance, means basically that the number of boreholes and the number of observations in each boreholes should be minimized. The hydraulic influence of the boreholes may be significant for at least two reasons: 1) The diameter and volume of the boreholes may be significant relative to the scale of the experiment 2) water volumes required for sampling and analysis of tracer content may be significant relative to the volume of the fracture.

The following main design ideas have been considered for this study:

- Induced uniform hydraulic gradient
- Repeated tracer runs with varying flow rates (water velocities)
- Sampling boreholes between injection and collection points
- Combination of tracers with different transport properties

One reason for studying transport in a uniform flow field is simply that it is the situation that resembles natural, unstressed, flow and transport conditions the most. There are indications that flow and transport behavior (for example evaluated dispersion characteristics) during natural conditions are quite different from those performed under significant hydraulic stress, such as radially converging experiments.

Repeated experiments using different flow rates, with the same experimental configuration otherwise, is here considered to be more or less a necessary requirement for identifying non-equilibrium (time-dependent) transport processes.

Sampling between injection and collection points is intended to provide data that will give a picture of the two-dimensional spreading pattern, which is determined by the resulting flow pattern. Previous experiments indicate that spatial variability in flow properties cause more or less channelized transport between injection and collection points. If this will be the case also during the MWTE, it should be verified by observation boreholes within the "undisturbed" flow field. If flow is highly channelized, one should allow for the possibility to have enough boreholes to ensure that data can be collected at several locations along an approximately one-dimensional flow path, which also should be advantageous for the model discrimination process.

The combined use of tracers with different transport properties should be obvious for any experiment aiming at identifying transport processes, but listed here because of its importance. For example, apparently time-dependent transport processes interpreted from experiments with varying velocity may actually be caused by mechanisms not related to tracer transport properties. Such ambiguities may be resolved by simultaneous

injection of tracers with different properties, for example diffusion coefficients or chemical sorption properties.

Three models, representing different types of processes, were considered in this study:

- Advection–dispersion
- Transient solute storage
- Matrix diffusion

These models were formulated mathematically in their one–dimensional form. The intention is that considered models should be as simple as possible in order to gain insight into how the basic physics of each model affects parameter estimation and model discrimination possibilities.

The main result of the scoping calculations in this report is the multi–objective optimization analysis in chapter 9. In the preceding chapters (6, 7 and 8), the objectives of parameter estimation, model discrimination and hydraulic influence are illustrated and investigated separately. In chapter 7 (model discrimination) it is also shown how tracer breakthrough curves from repeated tests with different velocities can be used simultaneously for parameter estimation, and how the model discrimination potential is enhanced. Chapter 8 (hydraulic influence) not only looks at effects on fracture transmissivity and porosity caused by the presence of boreholes, but also how the boreholes required to create a uniform flow area may be arranged as efficiently as possible.

The optimization calculations entails the selection of a relatively large number of designs, and evaluate how each design performs with respect to the objectives, thereby identifying non–inferior designs. A design consists of the number of repeated tracer tests with different velocities, the number of sampling distances used, and the sampling frequency. The designs are selected by an initial evaluation using single–objective criteria of parameter estimation and model discrimination, yielding a total 162 designs to be evaluated. The results of the optimization calculations may be summarized as:

- Repeated tracer tests with varying velocities are probably necessary for identifying time–dependent processes, if both the objectives of parameter estimation and model discrimination are to be satisfied.

- Using two different velocities may be sufficient, although optimization calculations indicate that three velocities will give even better possibilities.

- Using two sampling distances rather than one gives a considerable improvement for both the parameter estimation and the model discrimination objectives.

- The method of selecting observation points have a significant effect on the values of the objective functions. It turns out that points selected using the single-objective criterion for parameter estimation does relatively well for both the objectives of parameter estimation and model discrimination.

- Independent information of fracture volume (or cross-section area of transport channel) will enhance the model discrimination possibilities, although this may not be necessary since it is shown that there is a substantial discrimination potential also without a priori knowledge of the fracture volume.

- A relatively large number of sampling points in time are needed for each distance sampled to ensure low correlation between parameters for all the models considered in this study.

- Hydraulic influence of boreholes and pumping for sampling will have a significant effect on the final design decision.

Based on the scoping calculations presented in this report, a tentative outline of the test program and the borehole layout for the MWTE is presented. The main features of the proposed design is that:

- The selected fracture and surrounding rock should be characterized as fully as possible with respect to hydraulics, geology, hydrochemistry, and geomety before tracers are added to the system.

- Repeated tracer tests with different flow velocities should be possible to perform.

- The tracer tests should be possible to perform in different directions using the same borehole array.

- A relatively large number of sampling points at different distances within the flow field should be drilled.

- A linear flow field should be established.

- The influence of sampling procedures and sampling boreholes should be minimized.

The proposed setup includes a discussion of suitable borehole configurations for pilot holes to identify and characterize the geometry and hydraulics of the fracture, "flow" boreholes for creating a controlled hydraulic environment during the transport experiment, and "migration" boreholes for the tracer injection and collection. Further, criteria for the selection of a suitable fracture are presented, as well as recommendations for the detailed characterization of the experimental area, along with discussions of tracer

selection, injection and sampling strategies, and supporting research.

1 INTRODUCTION

This report concerns scoping calculations for the proposed Multiple Well Tracer Experiment (MWTE), defined as Task 2A in the experimental plan for "Flow and transport processes in the detailed scale" at the Äspö Hard Rock Laboratory /Olsson, 1992/. The main objectives for the latter are /Olsson, 1992/:

- to improve understanding of transport processes and refine conceptualization of radionuclide transport in single fractures
- to determine in-situ parameters for the processes which control transport of sorbing nuclides in single fractures
- to quantify variability in flow and transport parameters for fractures of different character

The other sub-tasks of the overall experimental plan are the Pore Volume Characterization and the Matrix Diffusion Experiment.

The objective of the MWTE is to test the validity of different conceptual and numerical models of tracer transport in single fractures. The intention is that the data provided should facilitate discrimination among different conceptual models, and provide bounds for where these models provide reasonable approximations.

The basic experimental concept is that significant transport attributes can be evaluated from cross-hole tracer and hydraulic tests in a number of boreholes intersecting a single transmissive fracture, under different boundary conditions and experimental procedures. For example, injection and abstraction rates may be varied, and tracers with different sorption capacity may be used.

A general observation from tracer experiments is that data may be interpreted with equal plausibility with a number of different conceptual models /Andersson et al, 1993a/. Some of the reasons for this may be that:

- Models contain too many model coefficients and assumptions
- Data is only collected at the beginning and at the end of a flow path
- Independent information supporting the substantial number of assumptions that have to be made is not available

- The experiment was only carried out for one specific set of boundary conditions

- Insufficient control and characterization of hydraulic conditions during the tracer experiment

Thus, for repository safety considerations there is still a need for in–situ experimental data that can be used to test the validity of models, and to determine the magnitude of different transport processes. The underlying idea for the MWTE is that the selected fracture will be used for a sequence of experiments where experimental conditions are varied in such a way that best possible data is obtained for unambiguous interpretation of transport processes.

The main project tasks for the MWTE consists of the following:

- Scoping calculations by a number of project teams coordinated by the Task Force of modelling groundwater flow and transport of solutes
- Site selection and preparation
- Site characterization
- Cross–hole hydraulic testing
- Tracer testing – conservative tracers
- Tracer testing – reactive tracers
- Numerical model development

2 OBJECTIVES OF SCOPING CALCULATIONS

The general objective of the scoping calculations should be to provide information that can be used for designing an efficient experiment, with respect to the overall objectives of the MWTE. The scoping calculations in this report are intended to give general results, since the hydraulic properties of the fracture are not yet known. The scoping calculations should show in principle how experimental approaches can be applied to increase the possibilities of an unambiguous evaluation of the experiment. In this analysis, the calculations are directed towards the following specific objectives:

- Model discrimination
- Parameter estimation
- Minimize the influence of the experiment on natural hydraulic conditions

The objectives of parameter estimation and model discrimination generally conflict with the third objective (the more observations the better), and the scoping calculations are aimed at finding a reasonable balance. Thus, the main task for these scoping calculations is a multi-objective optimization analysis.

Again, the scoping calculations should provide a rather general design of the tracer experiment, and the final design will be based on the results from the hydraulic tests and other initial investigations of the target fracture. In addition, any design considered should be flexible enough to allow for any practical considerations that may arise during the actual planning and performance of the MWTE.

The objective of model discrimination includes identification of dominant transport processes and chemical processes, as well as dominant features of the flow system. A good design should favor a "correct" model, and simultaneously discredit "incorrect" models. The best possibilities of a good design for model discrimination arise if prior estimates from previous experiments exist. As in this case no prior estimates on parameter values are available, the scoping calculations have to allow for a parameter-robust design.

The objective of parameter estimation entails finding a design that will give low estimation variance of parameters, which is dependent on the locations and times of observations. In this case, very little or no prior information on parameter values exists. Therefore a parameter-robust design should ensure low variance estimates over some plausible range (based on experience) of parameter values. This needs to be done for any considered model as well,

since the "best" model also in unknown. Thus, the results from the scoping calculations are expected to be model–robust, as well as parameter–robust.

The third specific objective, minimizing hydraulic disturbance, is actually very similar to minimizing cost, and means basically that the number of boreholes and the number of observations in each boreholes should be minimized. The hydraulic influence of the boreholes may be significant for at least two reasons: 1) The diameter and volume of the boreholes may be significant relative to the scale of the experiment 2) water volumes required for sampling and analysis of tracer content may be significant relative to the volume of the fracture.

The objectives and the mathematical formulation of their objective functions are discussed in detail in chapters 6–9.

3 APPROACH

3.1 GENERAL CONSIDERATIONS FOR DESIGN SELECTION

The actual steps taken to obtain a good design includes the selection of a number of possible designs (number of and location of boreholes, times of observations, sequence and types of tests, type of tracer injection, etc). The selection of possible design concepts are made subjectively, based on experience from similar experiments. This selection will by necessity be rather limited, and the following main design ideas have been considered for this study:

- Induced uniform hydraulic gradient
- Repeated tracer tests with varying flow rates (water velocities)
- Sampling boreholes between injection and collection points
- Combination of tracers with different transport properties

The scoping calculations should show how parameter estimation and model discrimination may benefit from these considerations, which will be discussed briefly below.

One reason for studying transport in a uniform flow field is simply that it is the situation that resembles natural, unstressed, flow and transport conditions the most. There are indications that flow and transport behavior (for example evaluated dispersion characteristics) during natural conditions are quite different from those performed under significant hydraulic stress, such as radially converging experiments. Further, since the uniform flow field is assumed to be maintained by regulating the pressure in relatively peripheral boreholes outside the actual tracer test area, it is expected that hydraulic conditions may be controlled and characterized better than when tracer is injected and/or collected at points coniciding with major hydraulic controls.

Repeated experiments using different flow rates, with the same experimental configuration otherwise, is here considered to be more or less a necessary requirement for identifying non-equilibrium (time-dependent) transport processes.

Sampling between injection and collection points is intended to provide data that will give a picture of the two-dimensional spreading pattern, which is determined by the resulting flow pattern. Previous experiments indicate that spatial variability in flow properties cause more or less channelized transport between injection and collection points. If this will be the case also during the MWTE, it should be verified by observation boreholes within the "undisturbed" flow field. If flow is highly channelized, one should allow for the possibility to have enough boreholes to ensure that data can be collected

at several locations along an approximately one-dimensional flow path, which also should be advantageous for the model discrimination process.

The combined use of tracers with different transport properties should be obvious for any experiment aiming at identifying transport processes, but listed here because of its importance. For example, apparently time-dependent transport processes interpreted from experiments with varying velocity may actually be caused by mechanisms not related to tracer transport properties. Such ambiguities may be resolved by simultaneous injection of tracers with different properties, for example diffusion coefficients or chemical sorption properties.

DETAILED APPROACH

The actual steps involved in the present analysis may be divided in two major parts. First, one-dimensional models of flow and transport were considered for the main part of the analysis by studying:

- Behavior of parameter sensitivities and "physical" correlation between parameters
- Estimation using data from repeated tracer tests simultaneously
- Defining discriminative regions among models for a range of parameter values
- Test of discrimination potential by applying wrong models to synthetic data
- Optimization of sampling design for parameter estimation, model discrimination, and hydraulic influence of the experiment

Of the above steps, the last one is clearly the most important, and the previous steps may be seen as initial considerations finally resulting in a complete optimization analysis.

Second, two-dimensional flow and transport model analysis was carried out to complement the optimization analysis. In this case the following was studied:

- Hydraulic influence of boreholes and sampling
- Test of design using data from synthetic tracer tests in a simulated heterogeneous fracture plane

The hydraulic influence of boreholes and sampling was studied in order to, if possible, provide quantitative input to the optimization calculations, as well as to provide general suggestions for the practical considerations of the design. Finally, the test of the obtained design is an attempt to synthetically

mimic an actual experiment, according to the obtained design, with subsequent evaluation. This will not show if the suggested design indeed is effective, but it will give some insight into the applicability of the design.

Finally, based on the results of the scoping calculations, a tentative test program including borehole layout, criteria for fracture selection, site characterization, test sequence, etc, for the MWTE is presented.

MODELS CONSIDERED

Common to all models considered in this study, is that they should be as simple as possible in order to gain insight into how the basic physics of each considered model affects estimation and discrimination possibilities. Three different conceptual transport models were considered in this study, representing three different types of processes:

- Advection–dispersion (AD) model
- Transient solute storage (ADTS) model
- Matrix diffusion (MDIF) model

The one–dimensional mathematical formulation of these models, along with a brief description of some of their properties, will be given in the following sections. Although different types of tracer injection procedures may be considered, this study assumes that tracer is injected instantaneously as an ideal pulse. This is the simplest assumption that allows consideration of both the rising and tailing parts of the resulting breakthrough curves.

ADVECTION–DISPERSION MODEL

The simple advection–dispersion model is probably the most commonly applied model for evaluation of tracer tests. It may be formulated using the well known equation:

$$\frac{\partial C}{\partial t} = -v\frac{\partial C}{\partial x} + D_L\frac{\partial^2 C}{\partial x^2} \qquad (4\text{–}1)$$

where C is tracer concentration, t is time, x is distance along transport path, v is the average water velocity along the flow path, and D_L is the dispersion coefficient. Equation (4–1) may be solved for a variety of boundary conditions. In this analysis, boundary conditions for a semi–infinite domain are assumed:

$$C(x,0) = 0 \qquad (4\text{–}2)$$

$$-D_L\frac{\partial C}{\partial x}(0,t) + vC(0,t) = M_A\delta(x) \qquad (4\text{–}3)$$

$$C(+\infty,t) = 0 \qquad (4\text{–}4)$$

where M_A is the injected tracer per unit area of stream tube section normal to flow.

The solution to eq. (4–1) may be formulated as /Raven et al., 1988/:

$$C(x,t) = \frac{M_{inj}}{V_f}\left[\frac{x}{(\pi D_L t)^{1/2}}\exp\{-\frac{(x - vt)^2}{4D_L t}\} - \frac{vx}{2D_L}\exp\{\frac{vx}{D_L}\}\,erfc\{\frac{x + vt}{2(D_L t)^{1/2}}\}\right] \quad (4–5)$$

where V_f is the total volume of the one–dimensional transport channel, and M_{inj} is the total injected tracer mass.

The properties of the advection–dispersion model are well documented for example /Kreft & Zuber, 1978/, and need not be discussed further here.

4.2 MATRIX DIFFUSION MODEL

This type of model is also well documented, and differ from the simple advection–dispersion model by allowing tracer to diffuse into a practically impermeable, but porous, rock matrix. It may for a single fracture be formulated mathematically as:

$$\frac{\partial C_f}{\partial t} = -v\frac{\partial C_f}{\partial x} + D_L\frac{\partial^2 C_f}{\partial x^2} + \frac{n_p D_{eff}}{b}\frac{\partial C_p}{\partial y} \quad (4–6)$$

$$\frac{n_p \partial C_p}{\partial t} - n_p D_{eff}\frac{\partial^2 C_p}{\partial y^2} + (1 - n_p)\rho\frac{\partial C_s}{\partial t} = 0 \quad (4–7)$$

where n_p is porosity of the rock matrix, D_{eff} is the effective diffusion coefficient, b is the half–fracture aperture, C_p is tracer concentration in the rock matrix, ρ is the bulk density of the matrix, C_s is the tracer concentration sorbed on the rock surfaces inside the matrix, y is a coordinate into the matrix perpendicular to the fracture, and remaining parameters and variables are the same as for the advection–dispersion model.

A solution to equations (4–6) and (4–7) for tracer concentration in a semi–infinite domain with an instantaneous pulse input may be written as /Maloszewski & Zuber, 1990/:

$$C_f(t) = \frac{M_{inj}A}{2\pi Q}(Pe\ t_0)^{1/2}\int_0^t \exp[-\frac{Pe(t_0 - u)^2}{4ut_0} - \frac{A^2u^2}{t - u}]\frac{du}{[u(t-u)^3)]^{1/2}} \quad (4–8)$$

where Pe is the Peclet number (vx/D_L), t_0 the residence time, M_{inj} is the total injected tracer mass, Q is the flow rate through the system, and the

parameter A is defined as:

$$A = n_p \frac{D_p^{1/2}}{2b} \tag{4-9}$$

Similar to non-equilibrium sorption processes, the matrix diffusion process basically affects the peak level and tailing parts of breakthrough curves, and causes a delay of tracer.

TRANSIENT SOLUTE STORAGE MODEL

This type of model is considered because it represents a somewhat different type of non-equilibrium mass transfer than matrix diffusion. The difference consists of that this model assumes instantaneously and completely mixed stagnant volumes, where the matrix diffusion model assumes a concentration gradient outward from the flowing part of the fracture. Thus, the transient solute storage model may be expected to give more rapid effects compared to matrix diffusion.

These kind of processes may be thought of as a result of stagnant water occupying dead-end pores or volumes that, although part of the interconnected void space and the continuous water phase, do not take part in the flow of water. Alternatively, stagnant zones may also be thought of as local zones of considerably lower permeability than the main flow conduits. It may be argued /Raven et al., 1988/, that stagnant zone storage is significant only during induced gradient tracer test, and that its importance becomes smaller as natural flow conditions are approached. Nonetheless, from a tracer test interpretation point of view, it is still important to distinguish such processes from other that may be more important for safety repository consideration, such as matrix diffusion.

The transient storage model may be formulated in one dimension as /Bear & Verruijt, 1987/:

$$\frac{\partial C}{\partial t} + \frac{(1-\phi)}{\phi}\frac{\partial C_s}{\partial t} = -v\frac{\partial C}{\partial x} + D\frac{\partial^2 C}{\partial x^2} \tag{4-10}$$

$$(1 - \phi)\frac{\partial C_s}{\partial t} = K(C - C_s) \tag{4-11}$$

where C is the tracer concentration in the mobile water, C_s is the concentration in the immobile water, ϕ is the volume fraction occupied by mobile water, and K is a transfer coefficient.

The transfer coefficient K depends on the coefficient of molecular diffusion and on the geometry of the contact area between the water in the mobile and

immobile zones. Thus, the main driving force for the exchange of solutes between zones, just as for matrix diffusion, is usually assumed to be molecular diffusion.

A solution to equations (4–10) and (4–11), using similar boundary conditions as for the advection–dispersion model and the matrix diffusion model, may be written as /Villermaux & Van Swaaij, 1969/:

$$E(\theta) = \exp\{-\frac{N\theta}{\phi}\}h(\theta,\phi) + \int_0^\theta g(z,\theta,\phi)dx \qquad (4\text{–}12)$$

with

$$h(z,\phi) = [\frac{Pe}{\pi\phi z}]^{1/2} \exp\{-\frac{Pe(z-\phi)^2}{4\phi z}\} - [\frac{Pe}{2\phi}] \exp(Pe)\, erfc\{[\frac{Pe}{\phi z}]^{1/2}\frac{(z+\phi)}{2}\} \qquad (4\text{–}13)$$

$$g(z,\theta,\phi) = [\frac{N}{\phi}][\frac{\phi z}{(1-\phi)(\theta-z)}]^{1/2} I_1\{2N[\frac{z(\theta-z)}{\phi(1-\phi)}]^{1/2}\} \exp\{-N\frac{(z-2\phi z+\phi\theta)}{\phi}(1-\phi)\} h(z,\phi) \qquad (4\text{–}14)$$

using the following transformed variables: z is dimensionless distance equal to 1.0 at the point of measurement, θ is dimensionless time equal to $\phi t/t_0$, N is dimensionless exchange coefficient equal to Kt_0/ϕ, with K being the mass transfer coefficient (s^{-1}), and I_1 is the modified Bessel function of order one.

In order to transform the dimensionless residence time distribution $E(\theta)$ to ordinary concentration (actual concentration in mobile part), the following conversion is done:

$$\frac{C(t)V_f}{M_{inj}} = \phi E(\theta) \quad at\ t = \theta\frac{t_0}{\phi} \qquad (4\text{–}15)$$

where t_0 is water residence time in the mobile part, V_f is the volume of the mobile part, and M_{inj} is total injected tracer mass.

The solution for C in the mobile part of the flow volume is generally a function of four parameters: t_0, Pe, ϕ and K. The need for two parameters to describe the transient storage terms arises from the assumption that the volume available for storage is not independent of the mobile volume, as the parameter ϕ appears both in equations (4–10) and (4–11). Thus, this model requires one extra parameter compared to the matrix diffusion model, in order to describe the tracer exchange with the immobile part of the flow system. A somewhat analogous case for matrix diffusion would arise for example if multiple parallel fractures were considered, where an extra parameter would be required to describe the distance between fractures.

The effect of transient solute storage on tracer breakthrough curves are

similar to matrix diffusion at moderate rates of the diffusion into the stagnant zones. As the transfer rate into stagnant zones become more rapid, in relation to the residence time in the flowing fraction, the transient solute storage model effectively approaches the equivalent of an equilibrium linear sorption transport model.

5 GENERAL CONSIDERATIONS FOR INTERPRETING TRACER TESTS

This section discusses some general aspects of the interpretation of tracer tests, as this is central to all analysis described in this report. First, some general comments on inverse modeling are given, which essentially is the main task that the analyst performs when evaluating a tracer test (as well as any other experiment). Second, properties of models in general that are related to the possibilities of evaluating collected data will be described in the framework of non-linear regression.

5.1 INVERSE MODELING

Any mathematical model of flow and solute transport is made up of a number of elements such as a geometrical description of the considered domain and its boundaries, equations for mass balances and fluxes, constitutive behavior that define the behavior of fluids and solids, initial and boundary conditions. The resulting set of model equations will always contain some model parameters, that in some way describes fundamental properties of for example the medium, the fluid or a solute. Such parameters, are for example the hydraulic conductivity, porosity, diffusion coefficients, etc. Model parameters can in general never be measured directly, but has to be interpreted given a certain model. Thus, the interpretation of a model parameter differ from one model to another, and one should not use interpreted values of coefficients in another model than they were derived from. When using parameter values interpreted with a certain model in a different model, the error will depend on the differences between the two models.

Thus, estimation of model parameters, given a certain model with all its assumptions, is actually what is done during the inverse modelling, also referred to as solving the identification problem /Bear & Verruijt, 1987/. The term calibration is also often used instead of inverse modelling. In order to determine the parameter values of interest one needs measured values of some variable such as tracer concentration, along with simulated values of the same values, using some assumed mathematical model with as much known information as possible. Then one finds the parameter values that make the observed and simulated values be so close to each other as possible.

The method employed to estimate the "best-fit" parameters may vary. Commonly the so called "trial-and-error" technique is used, where the model is run many times with the analyst updating parameter values in between runs until an acceptable fit to observed data is obtained. Other

methods use some automatic scheme for determining the parameters that best explains measured data. In principle, it is not important which method is used, the basic problem is the same. However, automatic estimation methods are often designed to give statistical measures of parameter uniqueness. A unique set of parameters, given an assumed model, means that there is no other significantly different set of values for those parameters that explain data equally well. The cause of non-uniqueness is often that a model contains too many adjustable parameters or simply that the wrong model is applied.

NON-LINEAR REGRESSION

The application of non-linear least-squares regression for parameter estimation is central to much of the discussion in this report, and is also used specifically in some of the analysis in section 7.3 and chapter 10. The purpose of least-squares regression is basically to fit observations to a model by minimizing the squared sum of differences between observed data and the applied model:

$$\textit{Minimize } S = \sum_{i=1}^{n} (C_i^o - C_i^m)^2 \qquad (5\text{-}1)$$

where C^o and C^m are the observed and computed concentrations at observation point i, and n is the number of sampling points. The difference $C^o - C^m$ is also called the residual, and is assumed to consist of random error as well as systematic error. The systematic error is usually considered to be a result of applying an incorrect model to data, although both types of errors are combined to a single term during the actual regression calculations, since they may not be distinguished in advance. Systematic model errors may be tested using the regression results for an analysis of residuals. Such testing however, require some assumptions of the statistical distribution of random errors in data. Typically, which is also the case in this report, random errors are assumed to be normally distributed.

Under the assumption that the applied model is correct, a general regression model in vector form may be written as:

$$\boldsymbol{C^o} = \boldsymbol{C^m} + \boldsymbol{E_R} \qquad (5\text{-}2)$$

where $\boldsymbol{C^o}$ and $\boldsymbol{C^m}$ are vectors of observed and calculated concentrations, respectively, $\boldsymbol{E_R}$ is the vector of residuals representing random errors only. By a Taylor expansion of $\boldsymbol{C^m}$ about an initial parameter set $\boldsymbol{B_0}$, eq. (5-2) may be modified and combined with (5-1) resulting in the so called normal equations /Draper & Smith, 1981/:

$$X^T X(B - B_0) = X^T(C^o - C_0^m) \tag{5-3}$$

where X is a matrix of parameter sensitivity coefficients evaluated using parameter set B_0. Eq. (5–3) is applied in an iterative form for non–linear problems, and an estimate of B at the (r+1)th iteration is given by:

$$B_{r+1} = B_r + (X_r X)^{-1} X_r (C^o - C_r^m) \tag{5-4}$$

Equation (5–4) is the simplest form of the so called Gauss–Newton algorithm /Cooley, 1985/. It is applied iteratively until some convergence criterion is satisfied. Whenever it is applied in this report, convergence of eq. (5–4) is further enhanced by restricting the parameter step length from one iteration to another, scaling of sensitivities and the $X^T X$ matrix, as well as by the application of the so called Marquardt modification /Marquardt, 1963/.

The parameter sensitivity matrix is the most important part of the regression procedure. An element in the sensitivity matrix is generally defined as:

$$X_{ij} = \frac{\partial C_i^m}{\partial B_j} \tag{5-5}$$

Equation (5–5) states that the sensitivity coefficient for parameter j at observation point i, is the partial derivative of the computed dependent variable, C^m, with respect to parameter B_j. When used in eq. (5–4), the derivatives are evaluated using parameter set B_r. The sensitivity matrix depends solely on the physical properties of the applied model, and on the number and locations (in time and space) of observation points. This matrix will actually to a large extent control the estimation variance of the estimated parameters, as well as the co–variance between parameters. Thus, the information contained in this matrix will be central to any experimental design considerations. Parameter sensitivities and implications for design, with respect to the physical models considered in this report, will be discussed in more detail in Chapter 6.

BASIC CONCEPTS

As was seen in section 5.2, the parameter sensitivities are central to the parameter estimation process, when evaluating observed data with different models. The values of the sensitivities at a given observation point (in time and space) generally depend on the applied model, and also varies with the actual parameter values. A complete sensitivity matrix for a simple example with only two parameters v and a_L and m observation points, with elements as defined in eq. (5–5) may be written as:

$$X = \begin{bmatrix} \frac{\partial C_1}{\partial v} & \frac{\partial C_1}{\partial a_L} \\ \frac{\partial C_2}{\partial v} & \frac{\partial C_2}{\partial a_L} \\ \cdot & \cdot \\ \frac{\partial C_m}{\partial v} & \frac{\partial C_m}{\partial a_L} \end{bmatrix} \qquad (6\text{–}1)$$

This sensitivity matrix may be defined for any set of observed data. For example, concentration data from several tracers with different sorption properties may be used simultaneously in the same estimation, or breakthrough curves at several locations in space may be used simultaneously /Andersson et al., 1993b/.

As mentioned, the sensitivity matrix contains the most essential information for design considerations. The co–variance matrix of an estimated set of parameters is given by the matrix $s^2(X^TX)^{-1}$ /Cooley, 1979/, where s^2 is the variance of the residuals. In this matrix, the diagonal contains the estimation variance of each parameter and the off–diagonal elements are the co–variances between parameters. The correlation $r(p_1,p_2)$ between two parameters p_1 and p_2 is expressed by:

$$r(p_1,p_2) = \frac{Cov(p_1,p_2)}{\sqrt{Var(p_1)\ Var(p_2)}} \qquad (6\text{–}2)$$

where the variance and co–variance terms are elements of the $(X^TX)^{-1}$ matrix. The correlation between two parameters may be seen as an indication of

linear dependence in the sensitivity matrix. It can be shown that the sensitivities and correlations are related to the estimation variances of the parameters. Using the parameter v in the simple system above, an expression for the variance of v can be derived /Knopman & Voss, 1987/:

$$Var(v) = \frac{s^2}{a_{11}(1 - r_{12}^2)} \tag{6–3}$$

where for n sampling points a_{11} is defined as:

$$a_{11} = \sum_{i=1}^{n} (\frac{\partial C_i}{\partial v})^2 \tag{6–4}$$

and r_{12} is the correlation between parameters v and a_L, as defined by eq. (6–2). Equations (6–3) and (6–4) demonstrates that the variance of an estimated parameter is reduced if observation points with high sensitivities are chosen, while a high correlation between parameters will increase the variance.

Thus, from a design point of view, it is desirable to identify observation points that have high parameter sensitivities, that at the same time will give low correlations between parameters. The identification of points with high sensitivities is rather straight–forward, as this is simply accomplished by computing the partial derivative of the dependent variable to each parameter across the entire design space. Correlations, on the other hand, are defined by the entire set of observation points, and it is not possible to determine if a single observation point is advantageous with regard to parameter correlations. In addition, correlation between parameters also depends on the total number of parameters being estimated. Correlation between parameters may be considered to be a property of the particular physical model selected, in combination with the locations of the available observation points and also the parameter values themselves. For some models, correlations among parameters may cause significant problems when determining a good design, and may require careful attention. In chapter 9, an approximate design measure containing both sensitivities and correlations will be defined and used. In the remainder of this chapter, the behavior of sensitivities for the models considered will be discussed.

2 BEHAVIOR OF SENSITIVITIES OF THE STUDIED MODELS

This section gives some examples of how the parameter sensitivities, defined by eq. (5–5), vary with time for each model considered, given some assumed set of parameter values. It should be recalled that the behavior of the sensitivities also vary with the values of the model parameters, and that the plots presented here do not attempt to cover the entire range of plausible parameter values.

The sensitivities are obtained using the models and solutions described in chapter 4, assuming an ideal tracer pulse input.

From a design point of view, it is generally desirable to locate observation points that have large absolute values of the sensitivities.

2.1 Advection–Dispersion Model

An example of parameter sensitivities in the advection–dispersion (AD) model is illustrated in Figure 6–1. Three parameters, the average water velocity v, the dispersivity a_L , and the injected tracer mass/fracture volume, M/V. The latter parameter is proportional to the breakthrough curve itself, and is usually a required parameter for estimation. Since this parameter is proportional to the concentration breakthrough curve, its main purpose in Figure 6–1 is to facilitate a direct comparison between the sensitivities of the other parameters and the breakthrough curve. An assumed transport distance of 3 m, a residence time of 100 hours and a dispersivity of 0.3 m is used for Figure 6–1. The sensitivities in Figure 6–1, and similar figures for the other models, are scaled by multiplying the sensitivity with the parameter value itself, in order to make the sensitivity curves have similar magnitudes.

As mentioned, observation points with high absolute values of the parameter sensitivities generally is beneficial to estimation. For the simple advection–dispersion, the interpretation of the sensitivities in Figure 6–1 is relatively straightforward. It is well known that the velocity parameter is estimated with the most certainty using data before and after the residence time ($t/t_0 = 1$), at the rising and descending parts of the breakthrough curve, corresponding to the absolute maxima for the sensitivity curve of parameter v in Figure 6–1. The point in between where the sensitivity is zero, corresponds to the peak of the breakthrough curve, where a very small change in v does not have any effect on the concentration. Consequently, observation points at the peak of the breakthrough curve have very little information value for estimation of the velocity. The sensitivity curve for a_L is somewhat different, and actually is close to zero where the sensitivity for v has its maxima. One may also note that the dispersivity sensitivity has a maximum close to the residence time, corresponding to the peak of the breakthrough curve.

The correlation between parameters are generally low for this model, and in

practice reliable estimation can be accomplished with relatively few observation points.

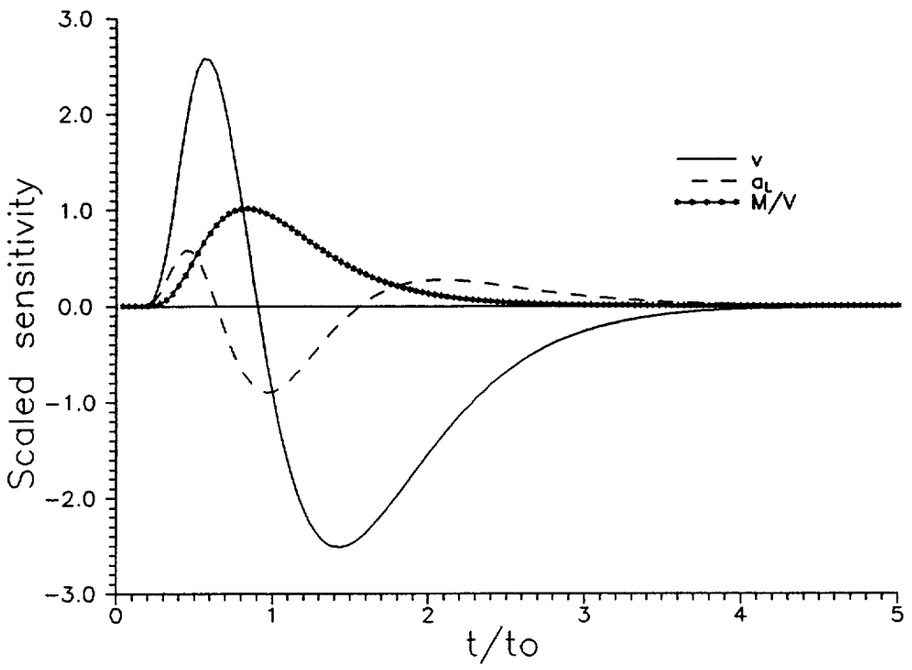

Figure 6–1. Example of parameter sensitivities in the advection dispersion model.

6.2.2 Transient Solute Storage Model

Four parameters are considered for the transient solute storage model (ADTS): the average water velocity, v, longitudinal dispersivity (or Peclet number), a_L, the flowing fluid fraction and the exchange coefficient, K. As for the advection–dispersion model, it is assumed that the transport distance is 3 m. Figure 6–2 shows how these four parameters vary with dimensionless time, for the following values:

- residence time = 100 hours
- a_L = 0.3 m (Pe = 10)
- flowing fraction = 0.8
- K = 0.01 h^{-1}

The sensitivities for the velocity and dispersivity are similar to the advection–dispersion model. The flowing fraction parameter, is in some aspects a mirror image of the velocity. A maximum occurs around the residence time, where the sensitivity to v is roughly zero, and is zero at approximately 1.5 times the residence time, where the sensitivity to v has a maximum (in absolute values). The sensitivity to the transfer coefficient, K,

also has two maxima, but it may be noted that the sensitivity is practically zero for times longer than approximately twice the residence time.

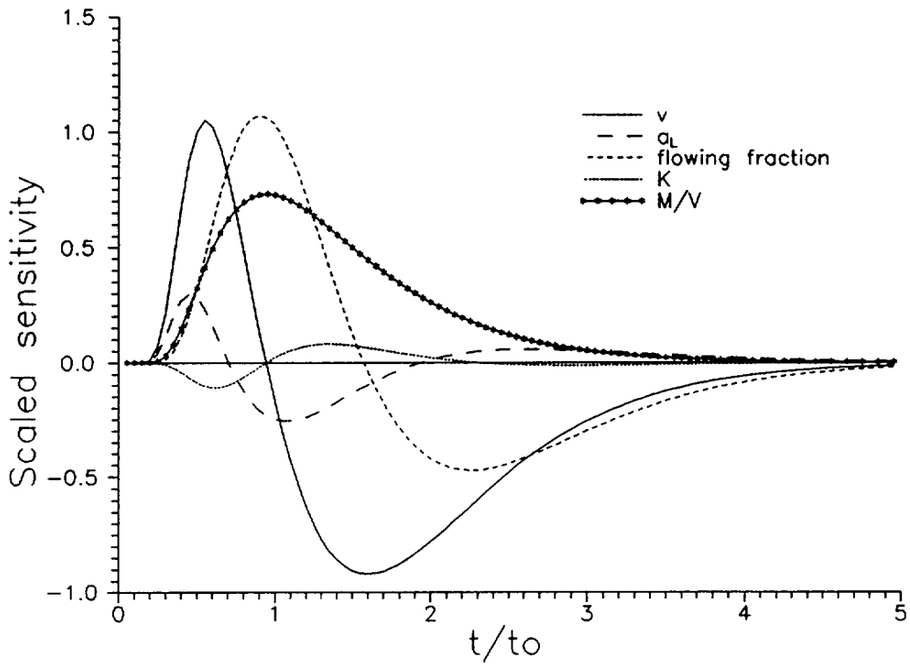

Figure 6–2. Example of parameter sensitivities in the transient solute storage model.

Correlation between parameters is generally a problem for this model, which means that it is difficult to estimate the parameters in the ADTS–model, even if stagnant zone storage effects were significant and high–quality data were available. For some combinations of parameter values in the ADTS–model, the correlation may be well above 0.9 between many, or sometimes all, parameters.

.3 Matrix Diffusion Model

Three parameters were considered for the matrix diffusion model; the velocity, v, the dispersivity, a_L, and the parameter A, as defined in section 4.3. Sensitivities were calculated for the matrix diffusion model (MDIF), assuming the following values:

- residence time = 100 hours
- dispersivity = 0.3 m (Pe = 10)
- A = 5 x 10^{-4} $s^{-1/2}$

The value of the parameter A is selected so that a moderate but significant

effect of matrix diffusion is obtained. The computed scaled sensitivities in this case is shown in Figure 6–3.

The sensitivities to the velocity and dispersivity are similar to the previous models. However, although they are similar, one may note that the sensitivity curves for these parameters are slightly different for the three models. Thus, even for the parameters that all three models have in common, the observation points with the highest sensitivities may occur at different times. The sensitivity to the diffusion parameter, A, has a maximum in absolute sensitivity around half the residence time, at about the time as the velocity has a maximum. At longer times, it may be noted that while both the velocity and the A–parameter have non–zero sensitivities, the dispersivity sensitivity is practically zero.

Correlation between parameters are generally less of a problem than for the ADTS–model, but may be relatively high also for the matrix diffusion model.

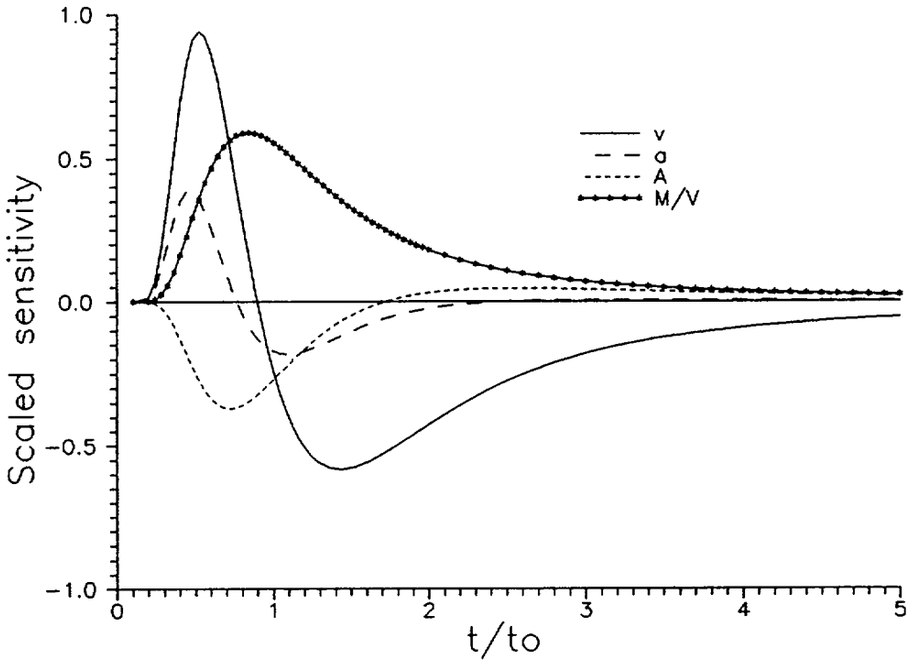

Figure 6–3. Example of parameter sensitivities in the matrix diffusion model.

In summary, these examples of sensitivities in the three models illustrate the difficulties in choosing the best points that will give good possibilities for estimation, if a number of candidate models are considered. In addition, the sensitivities are greatly dependent on the parameter values themselves, introducing additional difficulties if no prior estimates on parameters exist. The latter case is actually what is assumed in this analysis, and an attempt to identify parameter–robust sampling designs will be discussed in chapter 9.

MODEL DISCRIMINATION

BASIC CONCEPTS

There may be a number of steps involved during the process of model discrimination. The identification of models most likely includes some comparison of observation data with models. Here it is assumed that parameter estimation, using methods similar to what was outlined in section 6.2, forms a basis for the process of model discrimination. When several competing models are considered for interpreting a set of field data, best–fit parameters for each model are determined. Several criteria for discrimination may then be applied, such as /Knopman & Voss, 1988/:

1. Common measures of model fit such as mean squared error or correlation coefficient.

2. Estimation statistics of the estimated parameters, such as standard errors and correlation between parameters.

3. Analysis of residuals for indications of systematic model error.

4. If multiple rounds of sampling are made, comparison of prediction errors and estimated parameter values from one sampling round to another.

From a design perspective observation points should be chosen so that differences between predictions with competing models are maximized. Thus, observation points where model differences are large are better than those with small differences. The discrimination process is significantly improved by having initial estimates on parameter values, from an initial sampling round. In this case however, no such information is available, and the actual design calculations in chapter 9 are done in a parameter–robust manner.

The purpose of this chapter is to point to the fundamental differences in the three models considered, advection–dispersion, transient solute storage, and matrix diffusion. Although in some cases trivial, it may be seen as an illustration of the applied measure for the objective function for model discrimination applied in chapter 9. Further, the discrimination potential of applying repeated tracer tests with different velocities is tested and demonstrated.

7.2 DISCRIMINATIVE REGIONS BETWEEN THE STUDIED MODELS

As the purpose of section 6.2 is to demonstrate the basic model properties that are used for the estimation of parameters for a model, this section will demonstrate the basic features of the applied models that are used for model discrimination. Three model comparisons are made here: advection–dispersion (AD) vs transient solute storage (ADTS), advection–dispersion vs matrix diffusion (MDIF), and transient solute storage vs matrix diffusion. In principle, this may be done in a parameter–robust manner by calculating model results for complete ranges of the parameters associated with each model, and thereby identify model differences, if any, no matter what the values of the parameters are. Thus, this is nothing more than a complete sensitivity analysis, where uncertainty in all parameters for all models are evaluated simultaneously. In this case this is simplified so that the only parameter that is allowed to vary within a range is the dispersivity (or Peclet number) for each model. For the non–equilibrium models (ADTS and MDIF), parameter values are defined so that there is a moderately significant effect of either process on the breakthrough curves. This will show potential discriminative regions, independent of the value of the dispersion coefficient. A discriminative region is here defined by all observation points (in time and space) where there is a non–zero difference between model predictions.

A further assumption is also that the ratio (injected mass)/(transport volume) is known, which is basically a parameter proportional to the tracer breakthrough curve. In reality , this is generally not the case, which makes the process of model discrimination considerably more difficult than it may appear from the comparison of model behavior in this section.

The three model pairings are studied by plotting tracer breakthrough curves covering the assumed range in dispersivity. The curves are plotted using a normalized concentration (C x injected mass/transport volume) vs normalized time (t/t_0), where t_0 is the residence time for a conservative tracer. For all pairings, the assumed residence time was 50 hours, and the Peclet number was set at two different values, 5 and 25.

In order to illustrate how the discriminative regions between the models are determined, the advection–dispersion model only is plotted in Figure 7–1, for the two values of the Peclet number. The marked region in Figure 7–1 is the total envelope of possible outcomes, assuming all uncertainty in the system is covered by the range of Pe values. When comparing two models, the discriminative region is made up of points with non–zero differences between the total envelopes of possible outcomes for each model.

For the comparison of the AD–model vs ADTS, the remaining parameters in the ADTS–model, the flowing fraction (ϕ), and the transfer coefficient (K) were assumed to be 0.5 and 0.5 h^{-1}, respectively. The potential discriminative region for the model pairing AD–ADTS is demonstrated in Figure 7–2. Note that the marked area defines the difference between the total envelope of possible outcomes for each model.

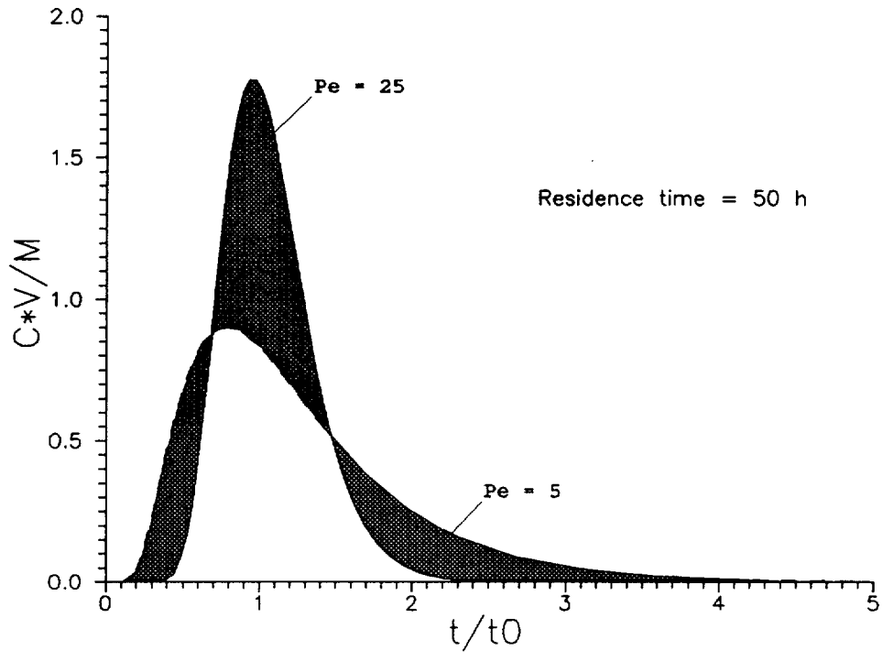

Figure 7–1. Total envelope of possible outcomes of the advection–dispersion model (AD), assuming all uncertainty is covered by the range in Pe values.

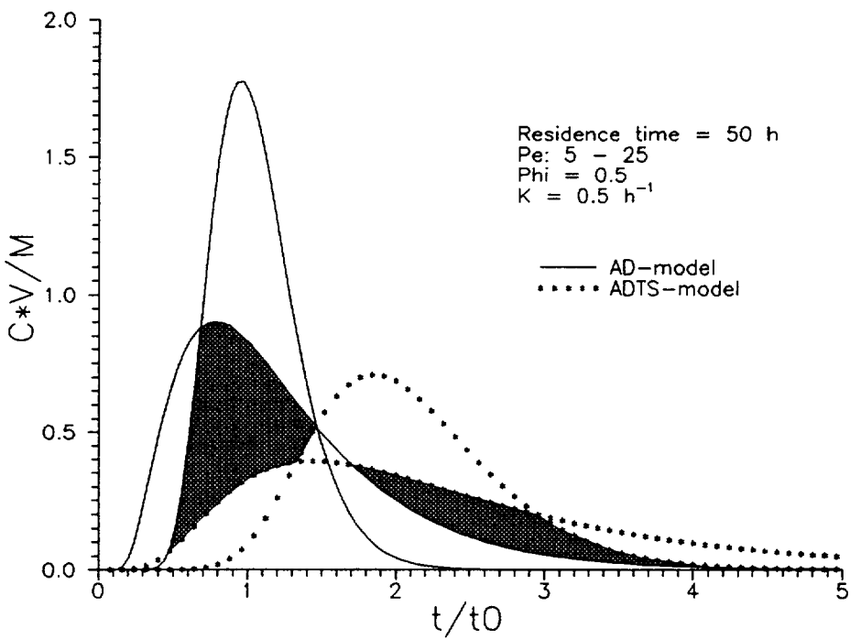

Figure 7–2. Discriminative region for the AD–ADTS model pairing.

The discriminative region indicated in Figure 7–2 is a potential one, since the ADTS–parameters are intentionally set so that there is a significant effect on this type of process on the breakthrough curve. Changing the parameter values for ϕ and K so that the transient solute storage effect becomes less, will gradually decrease the indicated regions in Figure 7–2. Thus, Figure 7–2 may not be directly used for model discrimination design without consideration of uncertainty in all parameters. However, what Figure 7–2, as well as the corresponding figures for the other pairings, shows is the basic principle for the selection of "good" observation points for model discrimination. In this case the discriminative region is divided into two clearly separate areas. One area is approximately between 0.5 and 1.5 times the residence time, and the other approximately between 2 and 3 times the residence time. Thus, if the results in Figure 7–2 would be used for model discrimination design, observations points within these intervals would be considered to have the greatest information value.

The physical interpretation is fairly straight–forward in this case. Tracer transfer into the stagnant zones is relatively rapid, causing a delay of tracer and considerably lower concentrations than the AD–model around $t/t_0 = 1$. As the tracer diffuses out from the stagnant zones at an equal rate, a delayed peak results from the stagnant zone storage.

The corresponding discrimination potential for the AD–MDIF pairing is demonstrated in Figure 7–3. Again, the residence time is set to 50 hours, while the parameter A, as defined in eq. (4–9), is set to 1×10^{-3} $s^{-1/2}$.

The potential discriminative region in Figure 7–3 is somewhat similar to the AD–ADTS pairing, with two separate areas around the residence time and in the tailing parts of the curves. The most important difference is that for the AD–MDIF pairing, the discriminative region in the tailing parts, although relatively small in this case, extend to much longer observation times than for the AD–ADTS pairing. The apparently large model differences around t/t_0 for both examined pairings so far, will probably have limited information value for discrimination in practice unless the tracer transport volume in the fracture (or the flow rate through the tracer conduit) is known a priori.

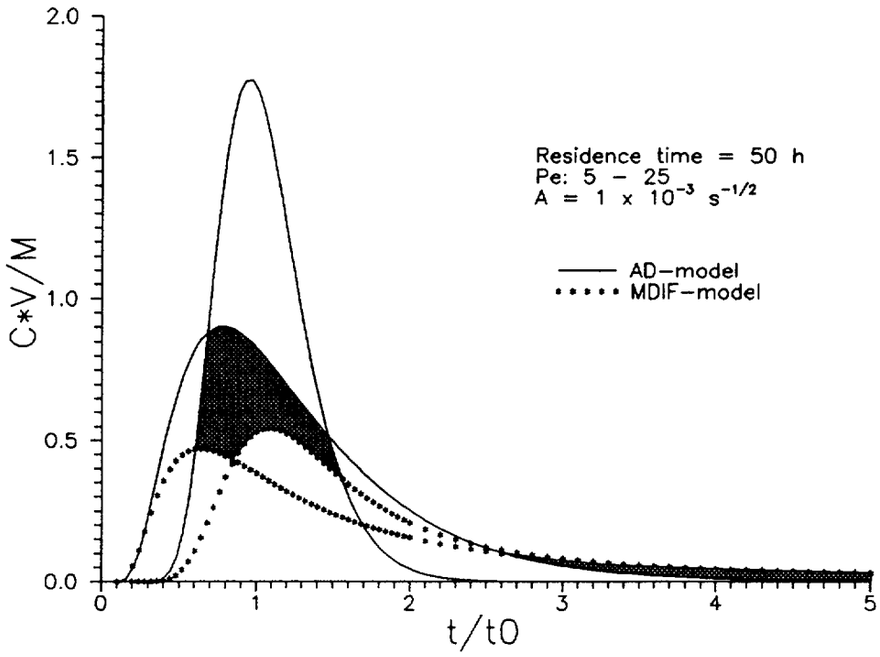

Figure 7–3. Discriminative region for the AD–MDIF model pairing.

Finally, the discriminative region for the ADTS–MDIF model pairing, given the same assumed parameter ranges and values as above, is demonstrated in Figure 7–4.

Both models in Figure 7–4 have the common feature of causing tailing effects to the breakthrough curves. The most dominant part of the discriminative region is in this case roughly between 1.5 and 3 times the residence time, similar to the AD–ADTS pairing. One may also expect that towards very long times (outside the graph) the tailing effects of the MDIF–model are greater. Based on the physical properties of these models, one may speculate that the greater the residence time, the greater the differences between these models will become. When the residence time becomes very large relative to the transfer rate in and out of stagnant zones, the ADTS–model will approach an equivalent equilibrium sorption model.

The analysis in this section has shown, even for the considerable simplifications made, that fundamental model differences for the pairings studied vary significantly from one pairing to another. In other words, identifying efficient designs (high discrimination potential with as few observations as possible) would be a difficult task already in this simple case.

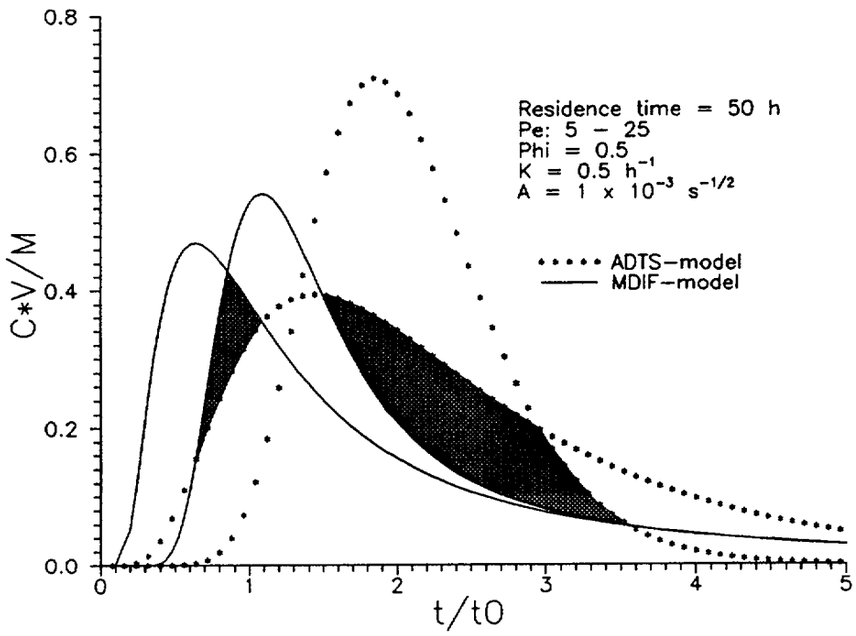

Figure 7–4. Discriminative region for the ADTS–MDIF model pairing.

A complete analysis considering total ranges for all parameters is applied for the actual design calculations in chapter 9, where also all the model pairings are considered simultaneously.

7.3 TEST OF DISCRIMINATION POTENTIAL

As a test and demonstration of the discrimination potential of using observation data from repeated tracer tests with varying residence times in combination, synthetic data from one model was fitted with an incorrect model. The principal model differences identified in the preceding section assumed that the transport volume, or the flow rate through the transport conduit, was known. This is not likely to be the case for a uniform gradient experiment, and a proportionality factor affecting the concentration magnitude in the breakthrough curves will have to be estimated also. This means that the differences between the models will be significantly smaller than in section 7.2. A more strict test of the discrimination potential, of using variable velocity experiments, is thus to simply apply wrong models to synthetic data sets, and look for systematic model errors.

As before, the evaluation is done by parameter estimation, in this case using all data sets from experiments with different velocities simultaneously. The method used is a straight–forward extension of the concepts outlined in section 5.2, with the only major difference being a modification of the parameter sensitivity matrix. For an example of two data sets evaluated with the simple advection–dispersion model used (section 4.1), the following form of the sensitivity matrix is used in this case:

$$\boldsymbol{X} = \begin{bmatrix} \frac{\partial C_1}{\partial v} & \frac{\partial C_1}{\partial a_L} & \frac{\partial C_1}{\partial F} & 0 & 0 \\ . & . & . & . & . \\ . & . & . & . & . \\ \frac{\partial C_m}{\partial v} & \frac{\partial C_m}{\partial a_L} & \frac{\partial C_m}{\partial F} & 0 & 0 \\ \frac{\partial C_{m+1}}{\partial v} & \partial\frac{C_{m+1}}{\partial a_L} & \frac{\partial C_{m+1}}{\partial F} & \frac{\partial C_{m+1}}{\partial f_{v2}} & \frac{\partial C_{m+1}}{\partial f_{F2}} \\ . & . & . & . & . \\ . & . & . & . & . \\ \frac{\partial C_{m+n}}{\partial v} & \frac{\partial C_{m+n}}{\partial a_L} & \frac{\partial C_{m+n}}{\partial F} & \frac{\partial C_{m+n}}{\partial f_{v2}} & \frac{\partial C_{m+n}}{\partial f_{F2}} \end{bmatrix} \qquad (7\text{–}1)$$

with m observation points for the first data set and n for the second data set. Note that the sensitivity in the first column, which corresponds to the average water velocity for the first data set, has a non–zero value for all data points in both sets. The velocity (or residence time) for the second data set is represented by a factor (f_{v2}), proportional to the velocity for the first tracer test. This implies the assumption that the tracer transport conduit has some basic properties that governs the travel time for a conservative tracer, given a certain hydraulic gradient. For example, such a property would for an equivalent porous medium be the ratio hydraulic conductivity/porosity.

The second and third columns are the sensitivities to the dispersivity (a_L) and the ratio injected mass/transport volume (F), respectively, and are considered common parameters for both data sets. This implies that the assumed dispersion model has the dispersion coefficient (D in equation 4–1) being proportional to the average water velocity. It may be more appropriate for single fracture transport with a more general dispersion model, but for reasons of simplicity the dispersion model with only one parameter (a_L) is considered here.

The last (fifth) column in the matrix is an analogous scaling factor for the fracture transport volume (f_{F2}), assuming that the injected tracer mass is considered known for each experiment. The parameters in column 4 and 5 in the matrix may be excluded from estimation (considered known and set to fixed values) under some further assumptions. If the transport volume is assumed to be the same for both experiments, the fracture volume proportionality factor is set to one and is not estimated. Further, if the average water velocity in each experiment is assumed to be proportional to the flow rate (or the hydraulic gradient), the velocity proportionality factors may be considered known, and would then not be estimated.

As an example of the simultaneous estimation of three data sets (from tracer tests where the residence times were varied) and the discrimination potential, synthetic data was produced with the ADTS-model. It was then estimated with the AD-model, under different assumptions. The synthetic data was simulated for residence times, for a conservative tracer, of 5, 20 and 50 hours. Other parameters were as follows: ϕ = 0.6, K = 0.05 h^{-1}, the injection mass/transport volume proportionality factor = 0.7, and Peclet number = 10. the ADTS-data used for estimation is shown in Figure 7-5.

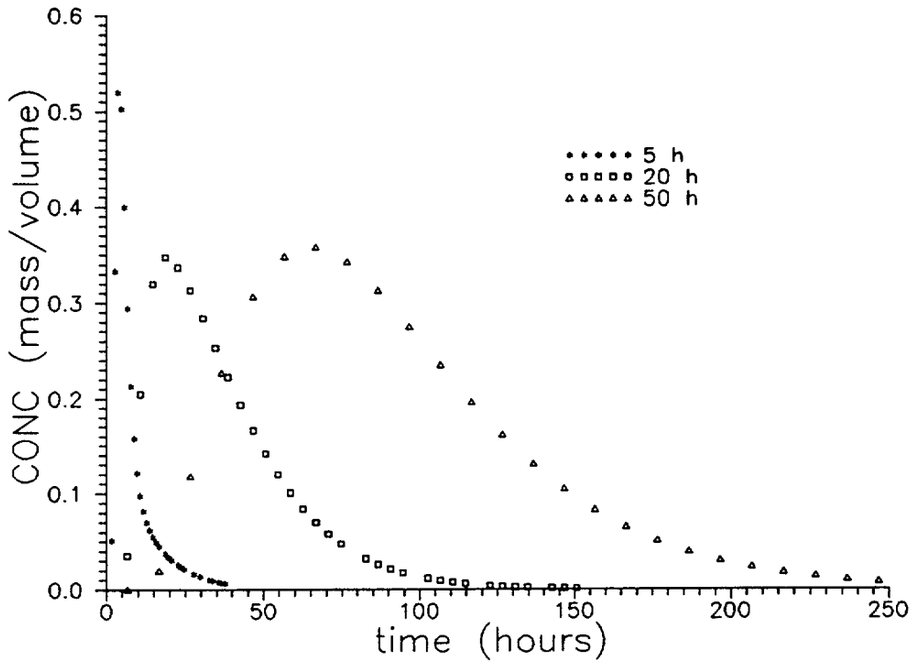

Figure 7-5. Synthetic ADTS-data used for estimation with the AD-model.

The advection-dispersion model was applied to the synthetic data using each curve separately, as well as two and all three in combination. The resulting best-fit model estimate to the 50 h residence time ADTS-data is shown in Figure 7-6. By looking at the agreement between model and data in Figure 7-6, one would no doubt conclude that the applied model was successful in explaining the observed data. Although the estimated residence time is greatly in error, approximately 97 hours compared to the "true" 50 hours, one would likely not have any possibility to detect this error in practice. The estimated Peclet number is 6.3 (compared to 10), and the injection mass/transport volume is 0.37 (compared to 0.7). In spite of the small systematic model errors at the peak and in the tail, one would probably conclude that the applied advection-dispersion model is the correct one.

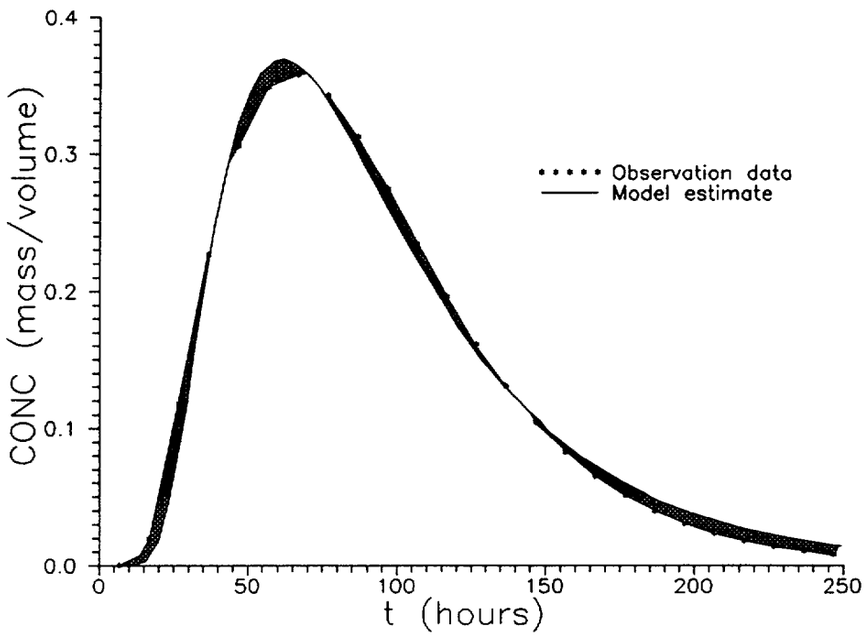

Figure 7–6. Best–fit model estimate using the AD–model to synthetic ADTS–data with a residence time of 50 hours.

In Figure 7–7, the AD–model is applied to all three curves simultaneously. In this case the transport volume is allowed to vary between the different residence times, which means that proportionality factors as described above are estimated. Although still seemingly small, model systematic errors are greater than the case of using the 50 hour residence time data set only. The most significant systematic error appears to be in the peak values and tailing parts of the 5 hour residence time curve.

The estimated residence times (with the AD–model) are 6.5, 36.2 and 98.8 hours, respectively. The estimated residence time of 98.8 hours is consistent with the evaluation in Figure 7–6. In addition, the estimated values for the Peclet number and the mass injected/transport volume are also relatively consistent with the previous case. Thus, based on criterium number four in section 7.1 for model discrimination, the advection–dispersion model seems to be quite acceptable. However, the transport volume proportionality factors are estimated to approximately 0.75 for both the 20 and 50 hours residence time ADTS–data. This means that if the injection mass is considered known with certainty, the volume of the tracer conduit is about 1/0.75 times greater during the 20 and 50 hours tests than during the 5 hour test. Assuming that it would be reasonable to expect that the tracer volume should be the same during all three tests, this may point to that the AD–model may not be correct.

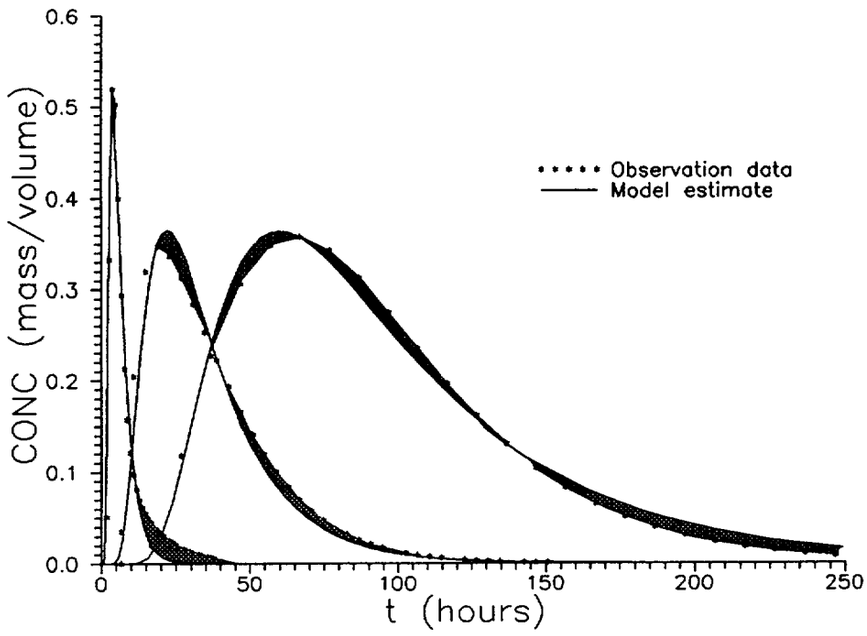

Figure 7–7. Best–fit model estimate using the AD–model to synthetic ADTS–data with residence times of 5, 20 and 50 hours, allowing for different transport volumes.

The evaluation illustrated in Figure 7–7 was repeated, but this time with the assumption that the transport volume is the same for all tests, which means that the number of parameters to estimate decreases by two. Figure 7–8 shows the best–fit model estimate in this case. The systematic model errors are larger compared to Figure 7–7, especially around the peaks of the breakthrough curves. The estimated parameter values, residence times for each test, Peclet number and mass injected/transport volume, are relatively close to what was obtained for the previous case. If the assumption of equal transport volume for different velocities is reasonable, it would seem likely that the advection–dispersion model is definitely rejected in this case.

Although real data will have noise caused by random and other errors not associated with systematic model error, a reasonable conclusion from this exercise is that the possibilities for identification of non–equilibrium transport processes is improved by using data from repeated tracer tests with different velocities. In practice, this would be accomplished by controlling the hydraulic gradient (across a uniform flow field) by maintaining some specified hydraulic heads at both ends of the flow field. If the additional assumption is made that the average water velocity along the transport conduit is proportional to the hydraulic gradient, one would expect that the systematic model errors resulting from an evaluation with the AD–model will be severe. In other words this means that one would, when estimating parameters, require that the relation between the different residence times would be 1:4:10, rather than the estimated 1:6:16 (approximately).

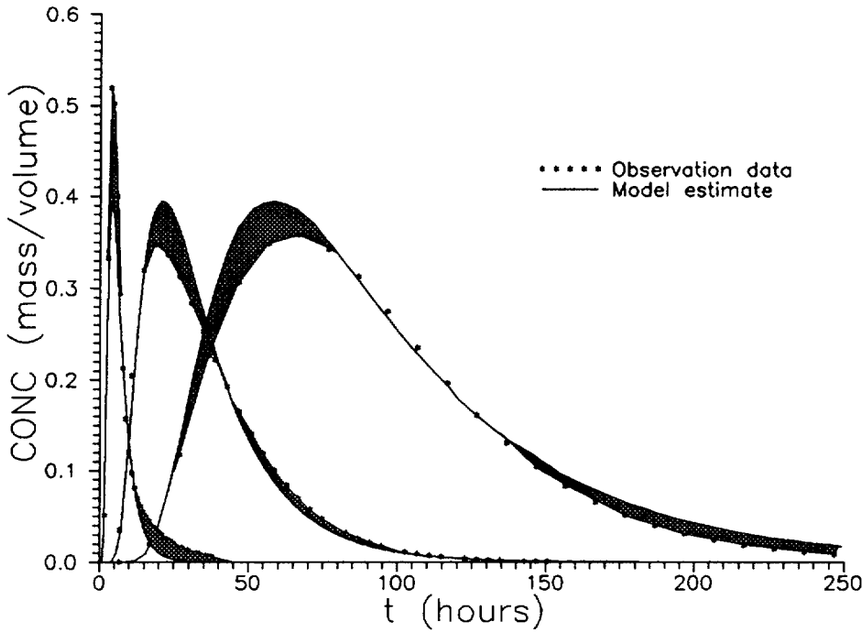

Figure 7–8. Best–fit model estimate using the AD–model to synthetic ADTS–data with residence times of 5, 20 and 50 hours, assuming that the transport volumes is the same for all residence times.

8 HYDRAULIC INFLUENCE OF BOREHOLES AND SAMPLING

8.1 PROBLEM DEFINITION

The 1-D modelling performed has shown that many observation points are favorable in respect to the work of model discrimination, i.e. to distinguish between transport processes. However, by necessity every observation point requires the drilling of a borehole and the borehole penetrating the fracture to be studied will create an anomaly within the fracture. It is also supposed that tracer breakthrough can be measured at several locations along an essentially one-dimensional flow path. The implications of these statements are:

- The area and the volume of the fracture flow path occupied by the observation holes may be significant in relation to the scale of the fracture investigated.
- Tracer transport may be significantly delayed when flowing through the observation boreholes.
- The flow field is distorted due to the presence of the boreholes and due to the water volumes removed from the fracture for tracer analysis.

In order to study the hydraulic influence of boreholes and sampling two-dimensional flow and transport model analysis was carried out as a complement to the optimization analysis. In addition, design simulations of the flow field was made in order to optimize the number and locations of boreholes used to control the flow field, c.f. Section 11. The model analysis presented in this section was made for a homogeneous fracture.

8.2 2-D FLOW AND TRANSPORT CALCULATIONS

8.2.1 Flow Field Simulations

A series of 7 simulations were run using the two-dimensional analytical element code SLAEM (Strack, 1988). The scope of the simulations was to determine how to create a linear flow field across the area for tracer tests ("migration area", c.f Section 11) with as few boreholes and within as small area as possible. The basic idea was to use a dipole flow field and place the "migration area" in the centre of the dipole where flow may be considered to be linear.

The model simulations were performed in a homogeneous fracture plane with the following hydraulic properties:

Hydraulic conductivity: $K = 2.2 \times 10^{-5}$ m/s
Aperture (cubic law): $e = 6.0 \times 10^{-6}$ m
Flow porosity: $\theta = 6 \times 10^{-5}$

These values represent a very narrow, low transmissive ($T = 1.3 \times 10^{-10}$ m^2/s) fracture which, in practice, may be difficult to identify at Äspö. However, the reason for choosing such a fracture is that effects of boreholes will be larger than in a more transmissive fracture. Hence, these simulations may be seen as "worst case" simulations.

The simulations, summarized in Table 8–1, were made using either one injection hole and one pumping hole or a pair of injection and pumping holes. Injection and pumping was simulated by applying a constant head of 2 and –2 m, respectively. Injection and pumping well diameters were assumed to be 76 mm.

Table 8–1. Flow simulations of the dipole field across the "migration area".

Simulation No	No of flow holes	Distance between paired holes	Distance between inj. and pumping	Size of migration area
1	2	–	16 m	4 x 4 m
2	4	2 m	16 m	4 x 4 m
3	4	4 m	16 m	4 x 4 m
4	4	6 m	16 m	4 x 4 m
5	4	6 m	16 m	8 x 8 m
6	4	8 m	16 m	8 x 8 m
7	4	4 m	8 m	4 x 4 m

The main result of these simulations is that a uniform gradient can be established over a small area inside a dipole flow field. By using a pair of boreholes, the distance between injection and pumping holes can be kept small compared to the size of the "migration area". In practice, this means that the total fracture area needed for the experiment can be kept small which decreases the risk of intersections with other transmissive fractures within the experimental area. Examples of the simulations are shown in Figures 8–1 and 8–2 for simulation no 1 and 7.

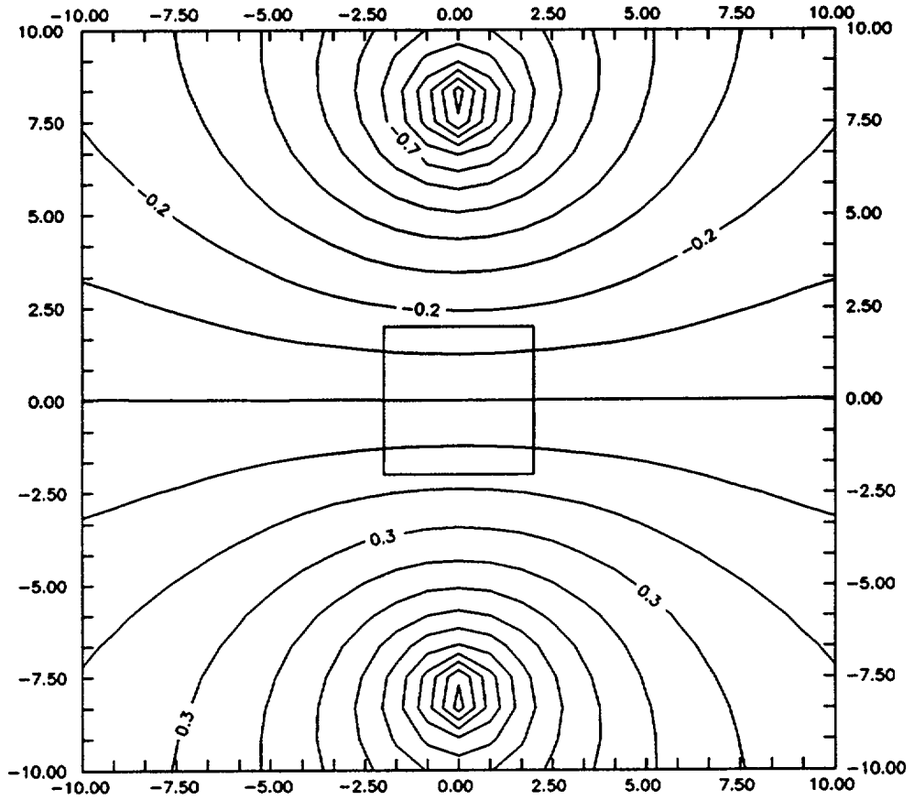

Figure 8–1. 2–D model simulation of a fracture plane in a dipole flow field. Solid lines represent piezometric head, 0.1 m isolines. Proposed test area in the centre.

Figure 8–1 shows that a fairly uniform gradient can be obtained using only one injection and one pumping hole. However, the distance between the holes need to be in the order of 4 times the side length of the "migration area". When using pairs of holes for injection and pumping a uniform gradient may be obtained with a distance between injection and pumping of only twice the side length of the "migration area" as shown in Figure 8–2.

It should be noted that these simulations only are examples. The transmissivity may very well be one or two orders of magnitude higher, flow porosity might be different but these are only scale factors and will not change the general results. The most difficult problems envisaged are the heterogeneity of the fracture and the influence of the "natural" gradient. These problems along with practical considerations such as pump capacities, etc., will have to be carefully considered.

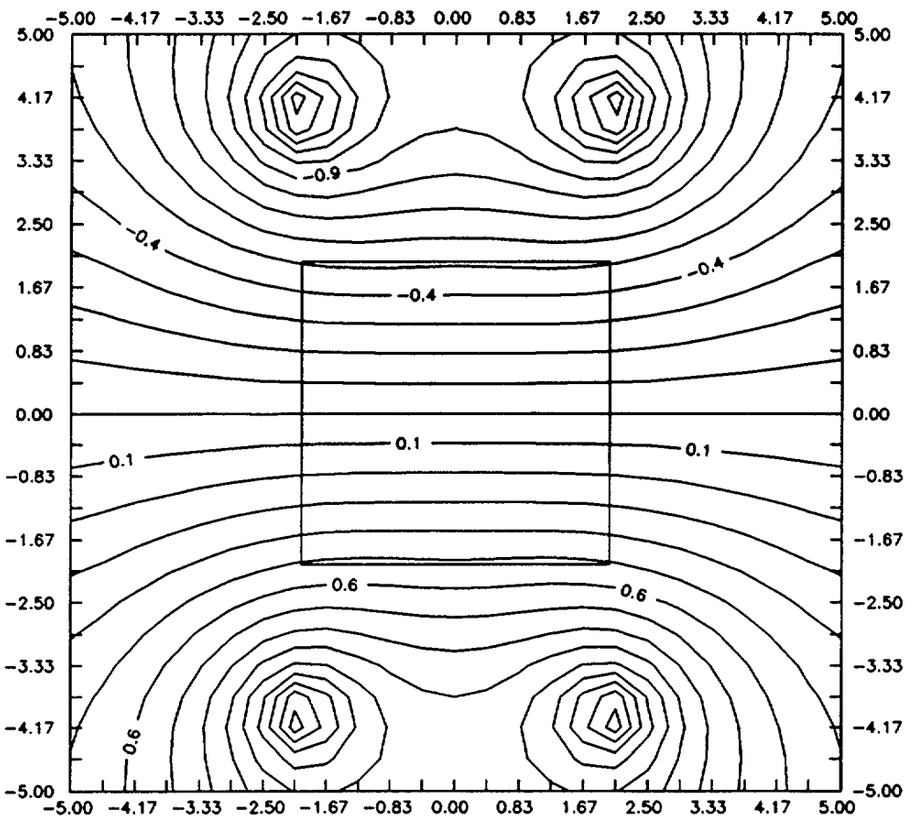

Figure 8–2. 2–D model simulation of a fracture plane in a dipole flow field created by pairs of boreholes. Solid lines represent piezometric head, 0.1 m isolines. Proposed test area in the centre.

.2 Influence of Boreholes

An observation borehole with a diameter of 38 mm occupies about 0.1 % of a square meter fracture area. If a fracture, having the same hydraulic properties as in the simulations in Section 8.2.1, can be straddled with a packer spacing of 0.01 m, the volume in the borehole is about twice as large as the volume in one square meter of fracture. This simple calculation suggests that the borehole volume is a crucial parameter for the test design.

One way of diminishing the borehole volume would be to use dummies inside the section. Theoretical work (Institut fur Radiohydrometrie, 1965) has shown that a dummy could fill about 95 % of the borehole area without disturbance of the flow field. Assuming that this could be done, the borehole volume would be about 20% of the volume in one square meter of fracture.

In order to assess the influence of a sampling borehole on tracer transport simulations with the 2–D model was made using the same fracture properties

and borehole configuration as in Simulation no 7 shown above (Figure 8–2). Particles were released from the lower boundary of the "migration area" and travel times were compared for particles going through a simulated borehole and without passing a borehole. The travel distance was 4 meters and the hydraulic gradient 0.25. The result presented in Figure 8–3 shows a significant delay for the particle going through the borehole. The travel time for the undisturbed particle is 187 hours while the particle passing through the borehole is delayed for about 370 hours in the borehole volume leading to a total travel time of 569 hours. Hence, tracer breakthrough downstream the observation borehole will show significant errors.

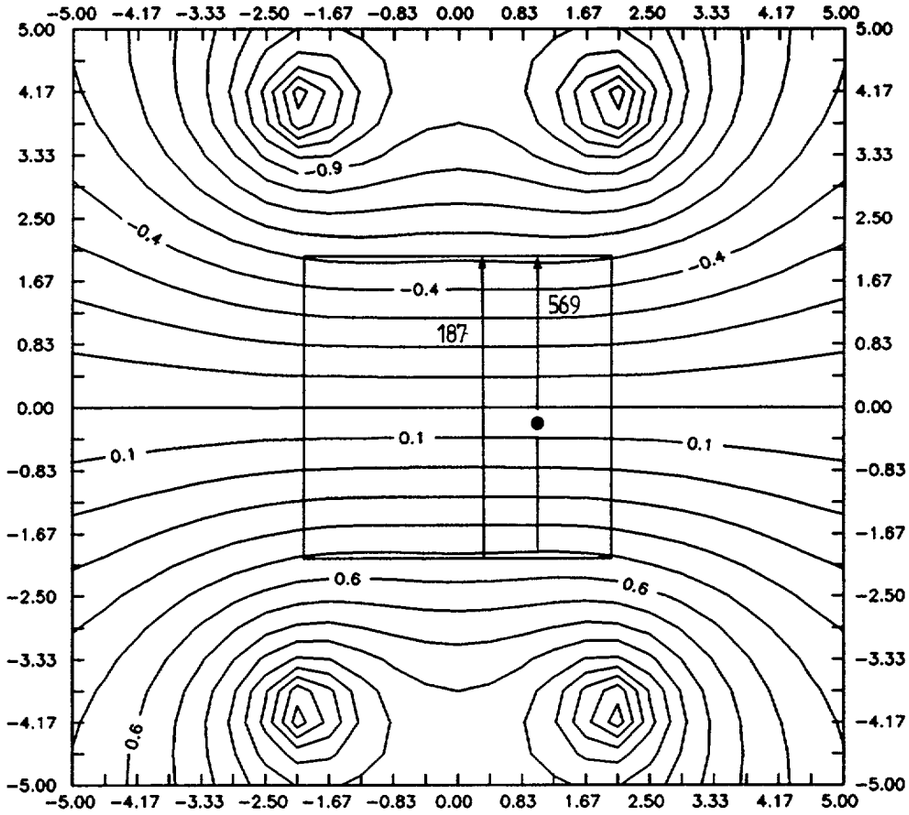

Figure 8–3. 2–D model simulation of particle transport in a fracture plane in a dipole flow field. Solid lines represent piezometric head, 0.1 m isolines.

However, this example is probably the "worst case" considering the choice of hydraulic parameters. If the transmissivity of the fracture was two orders of magnitude higher, the borehole volume would only be about 4% of the volume in one square meter of fracture and the delay will be reduced.

One way of reducing the delay through the observation holes is to decrease the porosity of the borehole by filling the straddled section with a porous material with an artificial fracture. Another way is to install specially

designed packers where the observation borehole can be plugged when not sampled.

Another effect that need to be considered for the final design of the MWTE is the effect of sampling by withdrawal of water. Given the properties of the "worst case fracture" above, the volume of one square meter of fracture is only about 6 ml. Two orders of magnitude higher transmissivity yields a volume of 27 ml. Hence, sampling has to be made in such a way that only extremely small volumes are removed from the system. The possibility of down-hole, in situ measurements of tracer concentration, without extraction of water samples, seems very favorable considering the limited reliability of the measured results according to the hydraulics.

9 MULTI-OBJECTIVE OPTIMIZATION

This chapter describes the combined evaluation of the considered objectives for parameter estimation, model discrimination, and hydraulic disturbance. The general approach is to select a relatively large number of designs, and evaluate how each design performs with respect to the objectives. The expected outcome of the optimization calculations is that non-inferior designs may be identified, meaning that, for a given hydraulic disturbance, there are no designs that perform better with respect to the objectives of parameter estimation and model discrimination. The interpretation of the results should be made in a general manner, and provide insight into the entire process of how to design an experiment that is likely to meet the defined objectives.

Section 9.1 describes the mathematical formulation of each objective function in detail. Section 9.2 contains a description of the procedure used for selecting all designs, as well as all values of parameters and other design variables used for generating the data used for the optimization calculations. Finally, the analysis and results of the optimization are given in section 9.3.

9.1 DEFINITION OF OBJECTIVE FUNCTIONS

9.1.1 Parameter Estimation

The objective of parameter estimation in general is to estimate parameters with a resulting low estimation variance. The objective function that is used here utilizes the parameter sensitivity matrix (see section 6). It can be shown that in the matrix $(X^TX)^{-1}$, the diagonals are proportional to the estimation variance while the off-diagonals are proportional to the covariance between parameters. The matrix $s^2(X^TX)^{-1}$ is called the variance-covariance matrix, where s^2 is the variance in the random error of the dependent variable. Thus, the variance-covariance matrix contains information both about the estimation errors, and also about the correlation between parameters. The correlation between two parameters are defined in section 6.1.

In order to use the information contained in the variance-covariance matrix, one may use the determinant of the X^TX matrix /Draper & Smith, 1990/. This measure is used in the so called D-optimality, and is an approximate measure proportional to the volume of a confidence ellipsoid surrounding the parameter estimates /Knopman & Voss, 1991/. The D-optimality objective function, for a model m, may be written in its simplest form as:

$$Maximize\ Z_D^m = |X^T X| \tag{9-1}$$

For the design calculations, the X matrix contains the sensitivities at the observation points considered for a particular design considered. A good design is generally one that includes many points with high parameter sensitivities. In addition, low overall values of parameter correlations will also contribute to a high value of the determinant of the $X_T X$ matrix. However, the D-optimality criterion will not guarantee that all parameter correlations are low for a considered design. A design that results in a high linear dependence between two parameters will give data that is difficult to evaluate, that is, to find a unique set of model parameters that give as good fit of observed data for a considered model. More specifically, in the case of non-linear regression, this results in a least-square space with a poorly defined minimum or multiple minima.

In order to account for differences in magnitude between parameter values in a model, each element in the sensitivity matrix is scaled by multiplying the sensitivity by the value of the parameter B_j itself:

$$S_{ij} = \frac{\partial C_i}{\partial B_j} B_j \tag{9-2}$$

Using eq. (9-2), a scaled objective for a model m can be written as:

$$Maximize\ Z_{SD}^m = |S^T S| \tag{9-3}$$

The simple expression for D-optimality in eq. (9-3) is for a single model being considered. In the multi-objective analysis applied here, the parameter estimation objective need to be satisfied independently of which model turns out to be the most valid. Thus, a model-robust criterion need to be formulated. This may be accomplished by various types of scaling. Since the magnitude of Z_{SD} varies with the number of parameters in a model, the Z_{SD} for each model is divided by the number of parameters. This results in a composite D-optimality objective for multiple models:

$$Maximize\ Z_{CSD} = \sum_{m=1}^{M} \left[\frac{|S^T S|}{p}\right]_m \tag{9-4}$$

Where M is the number of models, and p the number of parameters in model m.

If the design calculations were based on an initial sampling round, and thus initial estimates of the parameter values were available, the objective function in eq. (9-4) would be what was actually used for optimization. However, in this case it is assumed that prior estimates on parameter values are only available in ranges, and a parameter-robust expression is needed. In this study this is accomplished by, prior to the summation over models, calculating:

$$Z^m_{RSD} = \min_{\beta} \{(Z_{SD})_\beta\} \tag{9–5}$$

Thus, for each design and for each model, the expression in eq. (9–4) is evaluated for each parameter set $\boldsymbol{\theta}$, and the smallest such value is desired to be as high as possible for a good design.

Finally, since the parameter values are assumed to be known only in ranges, the magnitude of the resulting tracer concentration is also unknown. This means that the composite D–optimality measure may contain models with calculated concentration and sensitivity values varying significantly in magnitude from one model to another. Therefore, before the final summation over all models, each model component of the expression in eq. (9–4) is scaled to its maximum value:

$$Maximize\ Z_{PE} = \sum_{m=1}^{M} \delta^*_m\, Z^m_{RSD} \tag{9–6}$$

where the scaling factor δ^*_m is the inverse of the maximum value of Z^m_{RSD} among all possible designs, and Z_{PE} is the final measure for parameter estimation actually used in this analysis. Thus, the largest value of the contribution of each model to the objective function in eq. (9–6) becomes equal to one. The objective function in (9–6) assumes that each model, as well as each parameter set for a particular model, has an equal chance of occurring.

9.1.2 Model Discrimination

The purpose of model discrimination is to, from among a set of possible candidate models, identify the model that most adequately describes observed data from a performed field experiment. The general design strategy to find the best points for model discrimination, is to select observation points where predicted differences between models are as large as possible. For a simple case of discrimination between two models, the objective function for model pairing γ, with models m and m', may be written:

$$Maximize\ Z^\gamma_M = \sum_{i=1}^{n} Y^\gamma_i \tag{9–7}$$

with

$$Y^\gamma_i = (C^m_i - C^{m'}_i)^2 \tag{9–8}$$

where i is an index of an observation point in time and space in a design, n is the total number of points, $C^m{}_i$ and $C^{m'}{}_i$ is the solute concentration predicted by model m and m', respectively.

For any model pairing considered, the objective function in eq. (9–7) needs

to be modified to a parameter–robust form. This is done by, for each observation point considered in a design, determining the smallest difference in predicted concentrations using any of the assumed parameter intervals. This is equivalent to defining complete envelopes of possible outcomes for each model (given a set of parameter intervals), and computing the interval between the envelopes. A modified objective function that maximizes this interval may be written as:

$$Maximize\ Z_{RM}^{\gamma} = \sum_{i=1}^{n} \underset{\beta}{Min}\ Y_i^{\gamma} \qquad (9\text{–}9)$$

Equation (9–9) states that for every point in time and space that concentrations are computed for, the smallest difference in computed concentration considering all parameter sets for each model. An illustration of (9–9) may be seen in Figures 7–1 to 7–3 (in section 7.2), for the simple case of only two parameter sets, where Z^{γ}_{RM} corresponds to the discriminative regions indicated in those figures.

Further, the expression in eq. (9–8) has to be modified for multiple pairings of models. This is accomplished simply by summing a scaled form of all the parameter–robust pairings:

$$Maximize\ Z_{MD} = \sum_{\gamma=1}^{M} d^{\gamma}\ Z_{RM}^{\gamma} \qquad (9\text{–}10)$$

where d^{γ} is a scaling factor, giving equal weight to all models, defined as the inverse of the maximum value of the terms in the summation in eq. (9–9).

The objective function, Z_{MD}, in eq. (9–10) is what is actually used for the optimization calculations.

3 Hydraulic Disturbance

This objective function is considered to be made up of two parts. First, the hydraulic disturbance caused by the existence of a borehole. A borehole intersecting a fracture will affect the transmissivity locally around the borehole, and this effect is likely to be even greater if the target fracture consists of a set of fractures rather than a single one. A borehole will also add to the volume of the fracture, as it will probably be necessary to have a certain distance between packers to ensure that the fracture, or fracture set, is completely sealed off. The increase in transmissivity will affect the flow field, and will contribute to faster transport around the borehole, while the increase in volume will increase the residence time for tracer passing through or close to a borehole. Second, depending on the number of and desired properties of tracers used, water may have to be pumped from the packed–off section for sampling and laboratory analysis. The volumes necessary for this may be significant relative to the volume of the fracture.

The objective function is simply assumed to be a weighted sum of the effect of boreholes and sampling, respectively, and may be written as:

$$Z_C = f_d\, n_d + f_s\, n_s \qquad (9\text{–}11)$$

where f_d is the disturbance introduced by each sampling distance, that is, a row of boreholes perpendicular to the transport direction, n_d is the total number of sampling distances, f_s is the disturbance of discharged water volumes for each sample taken, and n_s is the total number of samples. It can be expected that transport between two points is likely to take place along a tortuous path, and in this analysis it is hypothesized that concentrations may be measured between injection and collection points by installing rows of boreholes, separated by some relatively small distance.

The quantification of the different disturbance factors is the most difficult aspect of this objective function. Any attempt do such a quantification will be of a subjective nature. In this analysis, the 2–D flow and transport calculations in chapter 8 attempts to quantify these effects by explicitly including the boreholes, with different transmissivity and volumes in the flow field. As a "base case" for the optimization calculations, it is assumed that the two disturbance factors are equal, which implies that it is equally disturbing to either install a new row of boreholes as to take an individual sample.

9.2 PROCEDURE FOR THE SELECTION OF POSSIBLE DESIGNS

The approach to the multi–objective design calculations involves some, relatively subjective, decisions about how the experiment should be performed, how potential observation points in space and time should be selected, etc. In this study the decision was made to consider a maximum of three repeated tracer tests with different residence times. Design calculations were carried out for evaluation of either one residence time, or for evaluation of either two or three residence times in combination, using the 1–D models described in section 4. Further, a maximum of three locations in space, or distances, were considered, and a maximum of 60 sampling times for each location. This means that a total of 15 120 concentration values were computed for the optimization calculations.

A total of 162 possible designs were considered, selected by evaluation of single–objective criteria for parameter estimation and model discrimination. The available data, concentrations and sensitivities, to base the selection of design points on, were calculated for 120 simulated time points with a frequency of 1/20 of the residence time, for each distance, for each parameter set, for each model, and for each experiment (residence time). This data was generated by running each model for every parameter set considered for that particular model.

The distances chosen for calculation of concentrations and sensitivities were 3, 1.5, and 4.5 m. Of these, 3 m was considered the primary choice of

distance for a borehole location. The residence times were 400, 100 and 40 hours, where 400 hours was given the highest priority. This means that if only one single residence time experiment was performed, it would be with a 400 hours residence time. If experiments were to be repeated with other residence times, the second residence time would be 100 hours, and a third 40 hours. Similarly, if only one distance was selected, it would be a 3 m. If a second sampling distance was chosen it would be 1.5 m, and the third 4.5 m.

The parameter intervals that were defined for the three models were as follows:

- Advection–dispersion model:
  - dispersivity: 0.1 – 0.3 m

- Transient solute storage model:
  - dispersivity: 0.1 – 0.3 m
  - flowing fluid fraction: 0.6 – 0.8
  - transfer coefficient: 0.00125 – 0.0075 h^{-1}

- Matrix diffusion model:
  - dispersivity: 0.1 – 0.3 m
  - $D_{eff} = 10^{-13} - 10^{-12}$ m^2/s

Thus, two parameter sets for the advection–dispersion model, eight for the transient solute storage model, and four for the matrix diffusion model, a total of 14 parameter sets. The ranges of values are generally based on experience from other experiments. The dispersivity values obtained from tracer tests are typically one magnitude smaller than the scale of the experiment. The transient solute storage parameters are simply chosen so that a significant influence of this type of non–equilibrium process is simulated. Finally, the range of the effective diffusion coefficient, D_{eff}, is taken from literature values given by Abelin et al. (1987), from measurements of diffusion of Uranine in granite. Additional assumptions for the matrix diffusion model were that the fracture aperture was set to 6×10^{-6} m, and the matrix porosity to 0.01.

Parameter sensitivities were calculated for all the parameters listed above, as well as for the water velocity, v. Note that ranges are not considered for the velocity parameter. Further, when tracer tests with different residence time are considered in combination, the transport volume is assumed to be the same for all tests and the residence time is assumed to be proportional to the applied hydraulic gradient. This means that the parameters corresponding to those in column 4 and five in eq (7–1) are not considered in the optimization calculations, and is not included in the calculation of eq (9–6). Thus, the number parameters considered here are 2, 4, and 3, for the advection–dispersion, the transient solute storage, and the matrix diffusion model, respectively. This results in a total of 136 080 computed sensitivity values.

The basic idea of a parameter–robust design is that these parameter ranges covers the total parameter availability in the system. This would be true if

the hypothesized models in this case were the only possible ones. Obviously, a number of other models, assuming other processes and geometrical descriptions, could also be considered to be possible candidate models.

As mentioned, design points were selected based on single–objective criteria for parameter estimation and discrimination, respectively. The order of selecting designs was as follows, for one distance (3 m) the nine best sets of time points for each criteria were calculated. This was then repeated for two distances (3 and 1.5 m) and three distances (3, 1.5 and 4.5 m). The nine sets of time points were defined as the best 10, 15, 20, 25, 30, 35, 40, 50, 60 points, respectively, calculated from each of the single–objective (parameter estimation and model discrimination) selection criteria.

The above procedure was then repeated for one residence time (400 hours), two residence times (400 and 100 hours), and three residence times (400, 100, and 40 hours) in combination. Thus, for example, a design including two distances, two residence times, and the best 25 time points for each distance and residence time, contains a total of 200 observation points (2 x 2 x 25 x 2). The number of sampling distances and residence times for all considered designs are listed in Table 9–1.

Table 9–1. Number of distances and residence times for each evaluated design.

Design no	# of distances	# of residence times	selection criterion*
1 - 9	1	1	1
10 - 18	2	1	1
19 - 27	3	1	1
28 - 36	1	2	1
37 - 45	2	2	1
46 - 54	3	2	1
55 - 63	1	3	1
64 - 72	2	3	1
73 - 81	3	3	1
82 - 90	1	1	2
91 - 99	2	1	2
100 - 108	3	1	2
109 - 117	1	2	2
118 - 126	2	2	2
127 - 135	3	2	2
136 - 144	1	3	2
145 - 153	2	3	2
154 - 162	3	3	2

* 1 = parameter estimation selection criterion
2 = model discrimination selection criterion

ANALYSIS AND RESULTS

The results of the optimization calculations are generally presented as plots of trade–off functions between different objectives. The objectives of model discrimination and parameter estimation in this case is complimentary, with the hydraulic disturbance objective being a competing objective to both. The plots in this section generally contain all the 162 different designs listed in Table 9–1.

The plots of trade–off functions should generally be interpreted as follows: High values for the objective functions for parameter estimation (Z_{PE}) and

model discrimination (Z_{MD}) are desirable for design, while the objective function for hydraulic disturbance (Z_C) should be as low as possible. In each plot involving the hydraulic disturbance objective function, there will generally be a number of designs plotted for approximately the same value of Z_C. For a given Z_C, the point with the highest value of the other objective function plotted (either Z_{PE} or Z_{MD}) represents the best design. By connecting all such points across the entire range of Z_C–values, the so called boundary of non–inferior designs is defined, and all points below this line represent inferior designs. Thus, the concept of optimality is in reality represented by the concept of non–inferiority. This means that at for any given hydraulic disturbance, there is one design that is better than all other considered designs. It should also be pointed out that all residence time values referred to in the plots and in the text, are based on a sampling distance of 3 meters.

Figure 9–1 shows the trade–off between the parameter estimation objective function (Z_{PE}) and hydraulic disturbance objective function (Z_C), using C/C_{max} as the dependent variable, where C_{max} is the peak value of the breakthrough curve at a sampling distance of 3 m. The purpose of using C/C_{max} as the dependent variable is to approximate robustness in the analysis with respect to an unknown value of the parameter representing the mass injected/fracture volume, which essentially acts as a proportionality factor during evaluation of a breakthrough curve. The calculations with C/C_{max} as the dependent variable may be seen as a "base case".

In Figure 9–1, and all other similar plots in this section, calculated results are plotted with different symbols depending on how many repeated tests with different residence times are involved in a certain design, since repeated tests do not increase the hydraulic disturbance objective. By separating designs involving different combinations of residence times in the plot, any improvement in objective functions by repeated tests can easily be seen. For each combination of residence times, the boundary of the non–inferior designs is outlined.

As may be expected, Figure 9–1 shows that the boundary of non–inferior designs is made up entirely by designs involving the combination of three different residence times. One may also conclude that there is a significant improvement in the position of the boundary of the non–inferior design set by adding repeated tracer tests with variable residence times. The addition of a third test (residence time of 40 hours) gives the largest increase in the objective function for parameter estimation (Z_{PE}) in this case. The design with highest objective function value of all in this case is, as expected, the one with three residence times using all possible observation points, and selected using the parameter estimation criterion.

Of the inferior points one may distinguish other clusters, representing other combinations of residence times and sampling distances, or designs selected based on the model discrimination criterion. For example, the best design according to the other criterion used (model discrimination) has a Z_{PE}–value of approximately 1/6 of the best design selected using the parameter estimation objective. This is an indication that the criterion for selection of

observation points has a significant impact on the expected design performance. Among other inferior points, one may note the designs involving three residence times but only two sampling distances, which plots in between the sets of non-inferior designs for three and two residence times, respectively. Thus, one may also conclude that adding a residence time, to a design with two residence times and two sampling distances, will result in a larger gain in the parameter estimation objective function, than adding a third sampling distance.

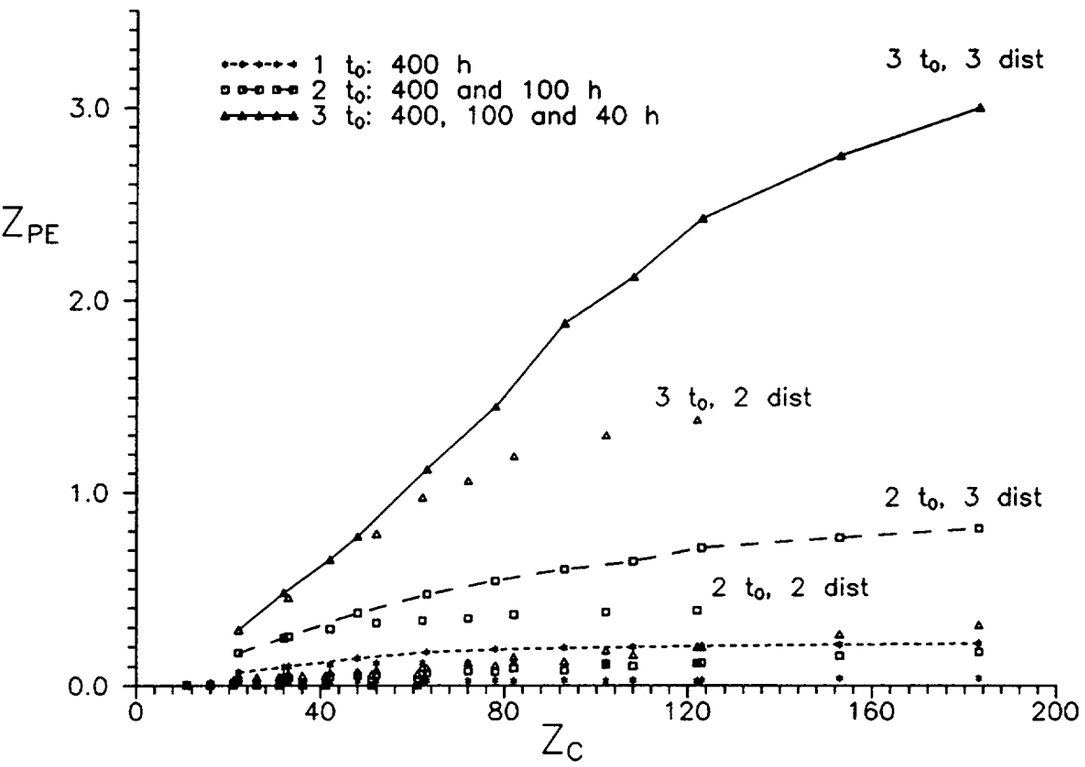

Figure 9–1. Trade-off between the parameter estimation objective function (Z_{PE}) and the hydraulic disturbance objective function (Z_C), using C/C_{max}. The lines indicate the boundaries of non-inferior designs for each combination of residence times (based on 3 m sampling distance).

Figure 9–1 also shows that there is a large variation in objective function values, if all designs are considered. In order to examine also the designs with relatively low values of Z_{PE}, involving fewer distances and residence times, each residence time combination is plotted separately in Figures 9–2a to 9–2c. These figures combined contain the same information as Figure 9–1, except that all designs with observation points selected based on the model discrimination criterion are omitted for clarity. Each combination of sampling distances is connected with a line, in order to compare the gain in the objective function value by adding sampling distances.

Figures 9–2a to 9–2c all have in common that there is a significant improvement in the parameter objective function, by using two distances rather than only one, while the addition of a third distance is more moderate. Comparing the largest Z_{PE}–value for each combination of distances, the ratio of two distances vs one is approximately a factor 20–25, the ratio of three distances vs two is approximately a factor 2. Using two sampling distances instead of one will actually give a larger relative improvement than adding a residence time, while the addition of a third distance will have a smaller effect that adding another residence time to the design.

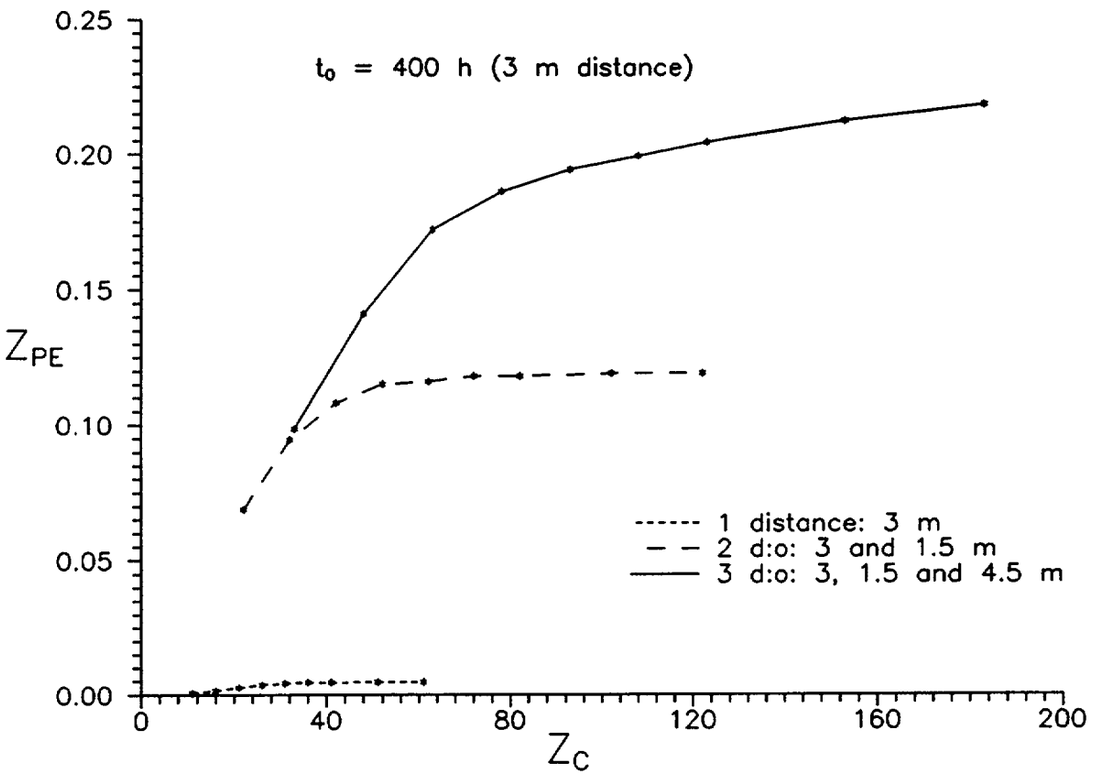

Figure 9–2a. Trade–off between the parameter objective function (Z_{PE}) and the hydraulic disturbance objective function (Z_C) for a residence time of 400 h only. Lines represent the boundary of non–inferior designs for each combination of sampling distances.

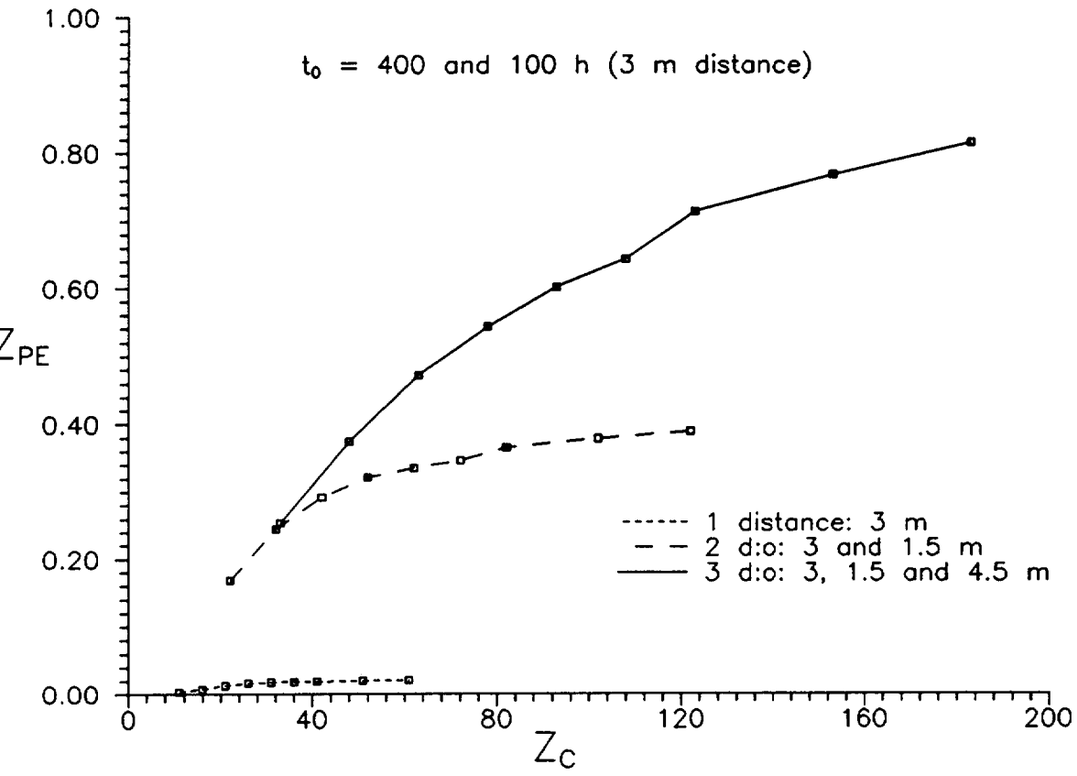

Figure 9–2b. Trade–off between the parameter objective function (Z_{PE}) and the hydraulic disturbance objective function (Z_C) for a combination of residence times of 400 and 100 hours. Lines represent the boundaries of non–inferior designs for each combination of sampling distances.

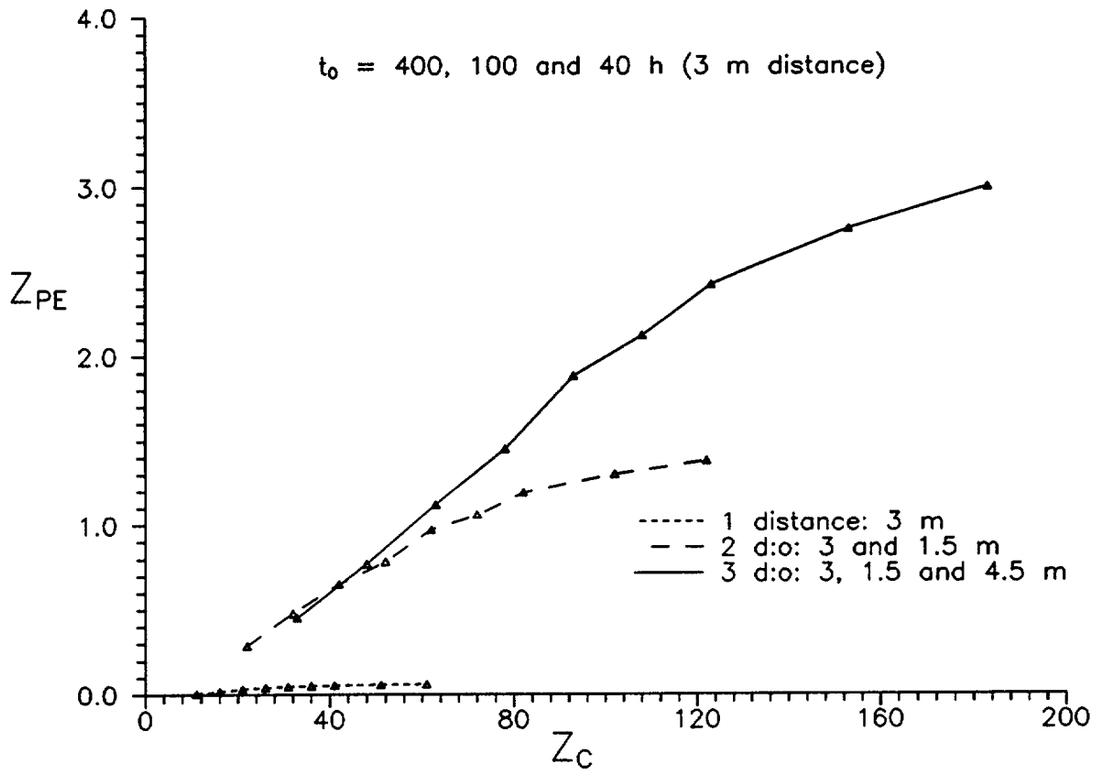

Figure 9–2c. Trade–off between the parameter objective function (Z_{PE}) and the hydraulic disturbance objective function (Z_C) for the combination of residence times of 400, 100 and 40 hours. Lines represent the boundaries of non–inferior designs for each combination of sampling distances.

It may be noted that in Figure 9–2a, that although the gain in the objective function Z_{PE} is considerable when adding sampling distances to the design, the highest values of Z_{PE} still are small in comparison to the total number of designs (Figure 9–1).

Figure 9–3 shows the corresponding plot for the trade–off between the model discrimination objective function (Z_{MD}) and the hydraulic objective function (Z_C). In this case, the results are somewhat different, as it is evident that repeated tracer tests with different residence times only give a marginal improvement to the discrimination possibilities (the value of Z_{MD}). This is not totally unexpected, since the residence time used in the test with only one residence time also is the longest one (400 hours), and where time–dependent features in the ADTS (transient solute storage) and MDIF (matrix diffusion) models may be expected to be most significant.

The cluster of points in the lower left–hand corner of Figure 9–3 represent designs with only one sampling distance used. Thus, the most marked improvement in the model discrimination objective function occurs when increasing the number of sampling distances from one to two. The difference

between two and three sampling distances is relatively marginal in this case. In fact, although not visible in Figure 9–3, the boundary of non–inferior designs below Z_C values of approximately 100 units is made up of designs with two distances, rather than three, for all three combinations of residence times.

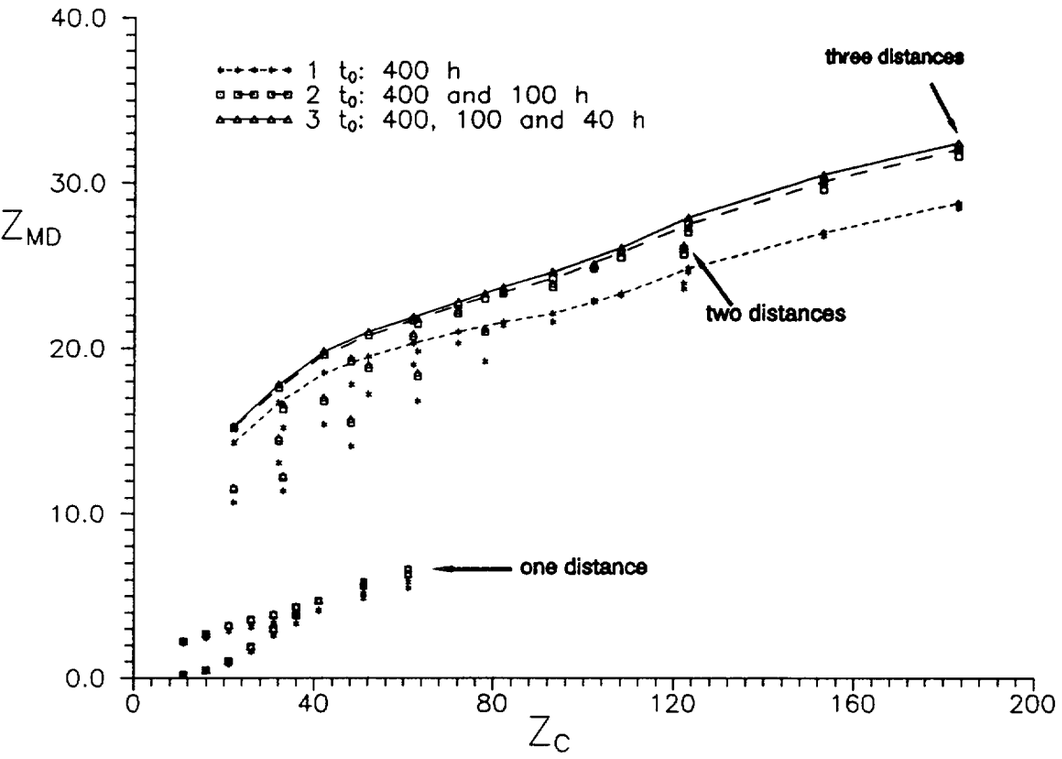

Figure 9–3. Trade–off between the model discrimination objective function (Z_{MD}) and the hydraulic disturbance objective function (Z_C), using C/C_{max}. The lines indicate the boundaries of non–inferior designs for each combination of residence times (based on 3 m sampling distance). Arrows indicate the designs with the maximum Z_{MD}–value for each combination of distances.

The boundary of non–inferior designs, for the different combination of residence times, are made up of points selected using the model discrimination criterion. In contrast to Figure 9–1, the points selected using the parameter estimation function result in only slightly lower values of the objective function Z_{MD}. Thus, it appears as the parameter selection criterion for observation points does well both for parameter estimation and model discrimination.

The combined results of Figures 9–1 to 9–3 indicates that, although repeated tracer tests with different residence times gives little improvement to the model discrimination objective function, given the pre–defined design

selection order one residence time may not be sufficient to estimate parameters with low estimation variance and low correlation between parameters in whatever model turns out to fit data the best. It is also indicated that by using a combination of two sampling distances (3 and 1.5 m), rather than a single one (3 m), may contribute significantly to both the objectives of parameter estimation and model discrimination.

Figure 9–4 shows the trade–off between the model discrimination objective function (Z_{MD}) and the model discrimination objective function (Z_{PE}). Although these objectives generally are complimentary, it is desirable to choose a design that gives relatively high values in both objective functions simultaneously. Thus, points located towards the upper right corner in the plot are good points for design. In this case, the designs involving three repeated tests with different residence times are better than other designs. In general, the best designs in this case are those where observation points have been selected based on the parameter estimation criterion. Thus, the results in Figure 9–4 generally agree with the results in Figures 9–1 and 9–3.

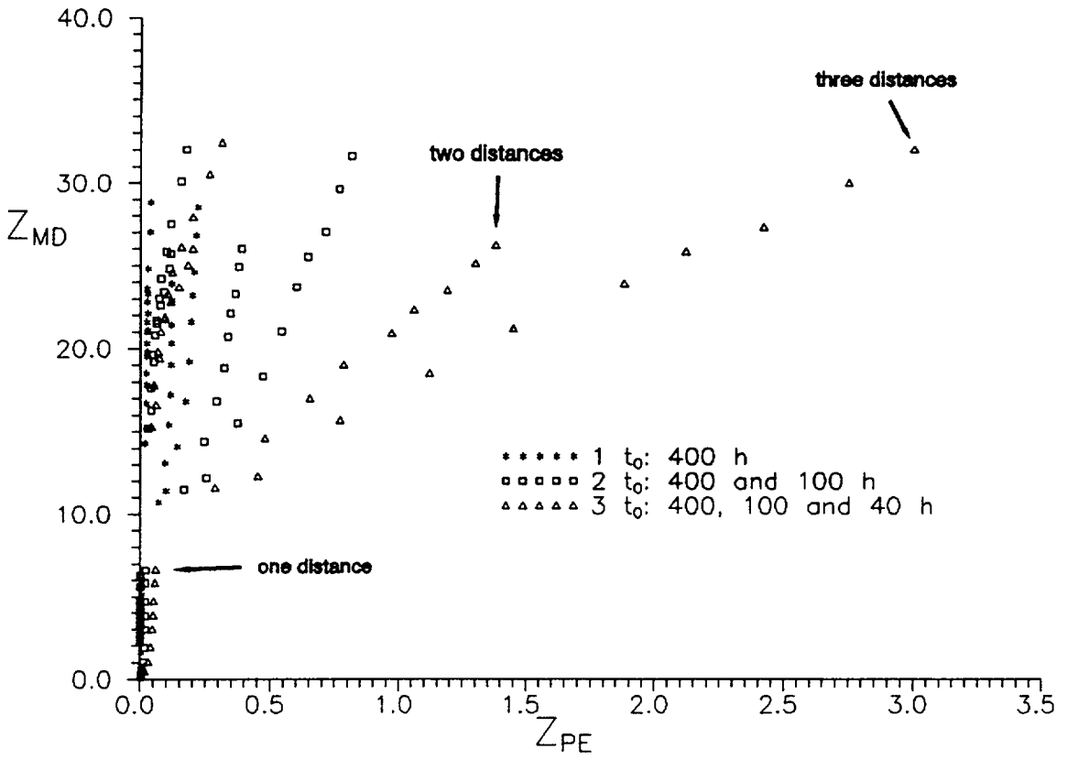

Figure 9–4. Trade–off between the model discrimination objective function (Z_{MD}) and the parameter estimation function (Z_{PE}), using C/C_{max}. The different residence times are based on a sampling distance of 3 meters. Arrows indicate the designs with the maximum Z_{PE}–values for each combination of distances.

The results so far indicate that the success of a design is sensitive to the choice of selection criteria for observation points. An explanation for this may be found in the results shown in Figures 9–5 and 9–6. The plotted values in Figure 9–5 are the same as in Figure 9–1 but where the terms, one for each model, in the objective function Z_{PE} (see equation 9–6) are plotted separately. These values are plotted as Z_{PE}^{m} in Figure 9–5. In this case the boundaries for the non–inferior designs (among all designs) for individual models are drawn, and reveal marked differences between the three models. Evidently it is the Z_{PE}^{m}–values of the AD–model that contributes the most to the Z_{PE} objective function value at relatively low values of Z_C. The AD–model reaches its maximum potential for estimation already at approximately 100 ZC–units, while the other models do not reach a maximum Z_{PE}^{m} value at all within the given set of available observation points. As the difference between the connected points in Figure 9–5 essentially consists of increasing sampling frequency, this means that a relatively large number of samples is probably required for each tracer breakthrough curve, for a reliable estimation of ADTS and MDIF parameters.

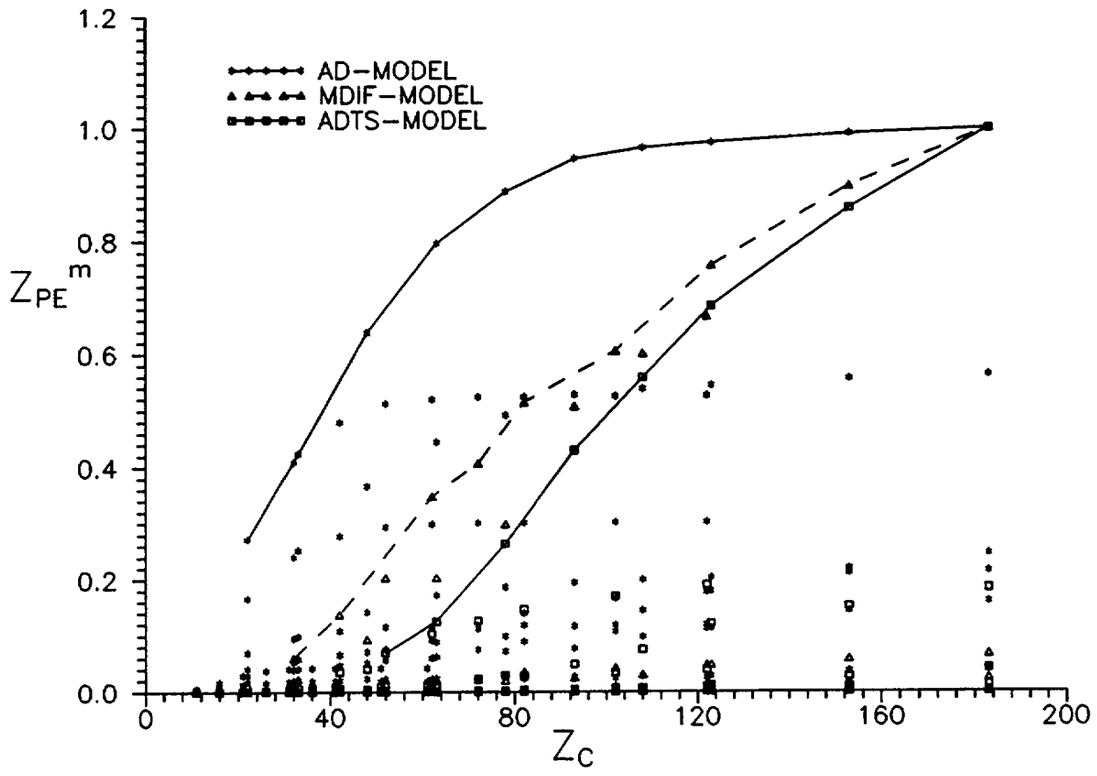

Figure 9–5. Trade–off between the parameter estimation objective function for each model (Z_{PE}^{m}) and Z_C. The designs connected by lines are based on three distances and three residence times.

An interpretation of Figure 9–5, as also indicated in chapter 6, is that correlation between parameters is a more serious problem for the MDIF and ADTS–models. As mentioned, the correlation between parameters is determined by the mathematical description of the model, the values of the parameters considered for estimation, and the whole set of spatially and temporally distributed observation points. The single–objective criterion for parameter estimation used for the selection of observation points is in this case only based on the selection of points with high parameter sensitivities. These sensitivities, although tending to minimize estimation variance, will not guarantee that the entire set of observations will give low values of correlation between parameters, and thus facilitate estimation of a unique set of parameters.

Figure 9–6 is the corresponding plot to 9–5 with the terms in model discrimination objective function (eq. 9–10), plotted as Z_M, split up between the three pairings of models. The non–inferior boundary reach increases in a similar way for all three models, but the maximum levels differ. It may be noted that the difference between AD (advection–dispersion) model and the ADTS (transient solute storage) model, and the ADTS and the MDIF (matrix diffusion) models are much smaller than the difference between the AD and the MDIF models, and thus most crucial for design selection. This is not

entirely unexpected, since the AD and ADTS models become more similar the greater the transfer coefficient between mobile and immobile zones is relative to the residence time, while the ADTS and the MDIF models both represent apparently similar non–equilibrium processes.

The objective function (Z_M) for the AD – ADTS and MDIF – ADTS pairings have very similar values for almost all of Z_C (at least above approximately 40 units), indicating that the maximum discrimination potential for these pairings is essentially reached already with a design involving two sampling distances (3 and 1.5 m) and one residence time (400 hours). Another interesting result is that the apparent lack of points for the MDIF – ADTS pairings is simply due to that many points have identical Z_M–values, that is, there is no change in the Z_M–value for this pairing when using more than one residence time. In other words, for the residence times of 100 and 40 hours, there are no non–zero values of the differences between the transient solute storage model and the matrix diffusion model, when using C/C_{max} as the dependent variable.

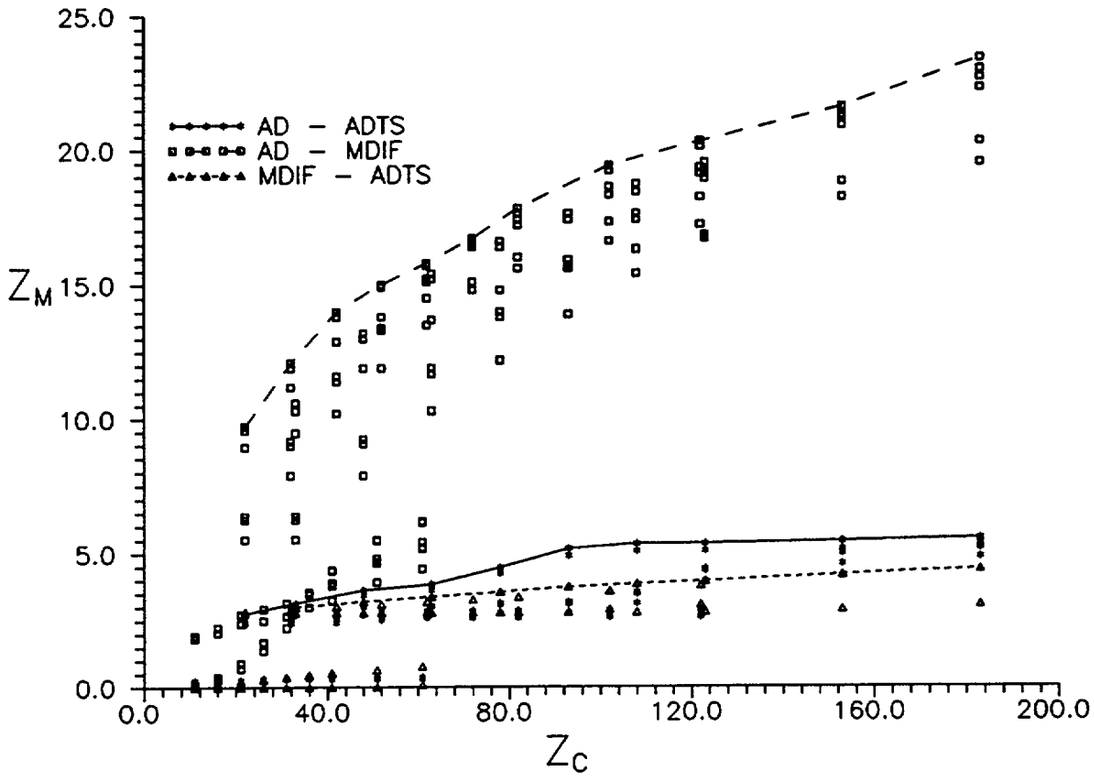

Figure 9–6. Trade–off between Z_M and Z_C for each pairing of models, using C/C_{max} as the dependent variable. The designs connected by lines are based on three distances and three residence times.

In the results above, it was assumed that the parameter representing injected mass/fracture volume was not known. In principle it may be possible to estimate this parameter a priori by running a tracer tests using a step–input injection concentration. In order to investigate the effects on estimation and discrimination possibilities if such information was available, a plot analogous to Figure 9–6 (model discrimination for each pairing vs hydraulic disturbance), but using the concentration, C, as the dependent variable was produced. The parameter estimation objective function is not affected by the change of dependent variable in this case, as that objective function is solely calculated using the parameter sensitivities.

The use of C as the dependent variable implies that the concentration magnitude of the resulting breakthrough is assumed to be approximately known beforehand, and that estimation of a proportionality factor (injected mass/fracture volume) is not needed.

Figure 9–7 shows the trade–off between the model discrimination objective function split up between the model pairings (Z_M) and the hydraulic disturbance objective function (Z_C). Figure 9–7 show some significant

differences compared to Figure 9–6. The actual values of the objective function Z_M are generally somewhat higher, compared to the case with unknown injected mass/fracture volume. This is especially the case for the MDIF – ADTS pairing, while the AD – ADTS pairing have similar Z_M–values as in Figure 9–6.

The boundary lines for the non–inferior sets of designs reach near maximum values at approximately 70 Z_C units, compared to Figure 9–6 where a maximum is not reached at all for the AD – MDIF pairing, within the given set of available observation points.

As for the case when C/C_{max} was used as the dependent variable, the model discrimination objective function is not improved at all when using more than one residence time for the MDIF – ADTS pairing, which is actually also the case for the AD – ADTS model pairing. This is simply a reflection of that, given the assumed sets of parameter ranges for the different models, significant parameter–robust model differences for these pairings are only obtained with the tracer test with a residence time of 400 hours.

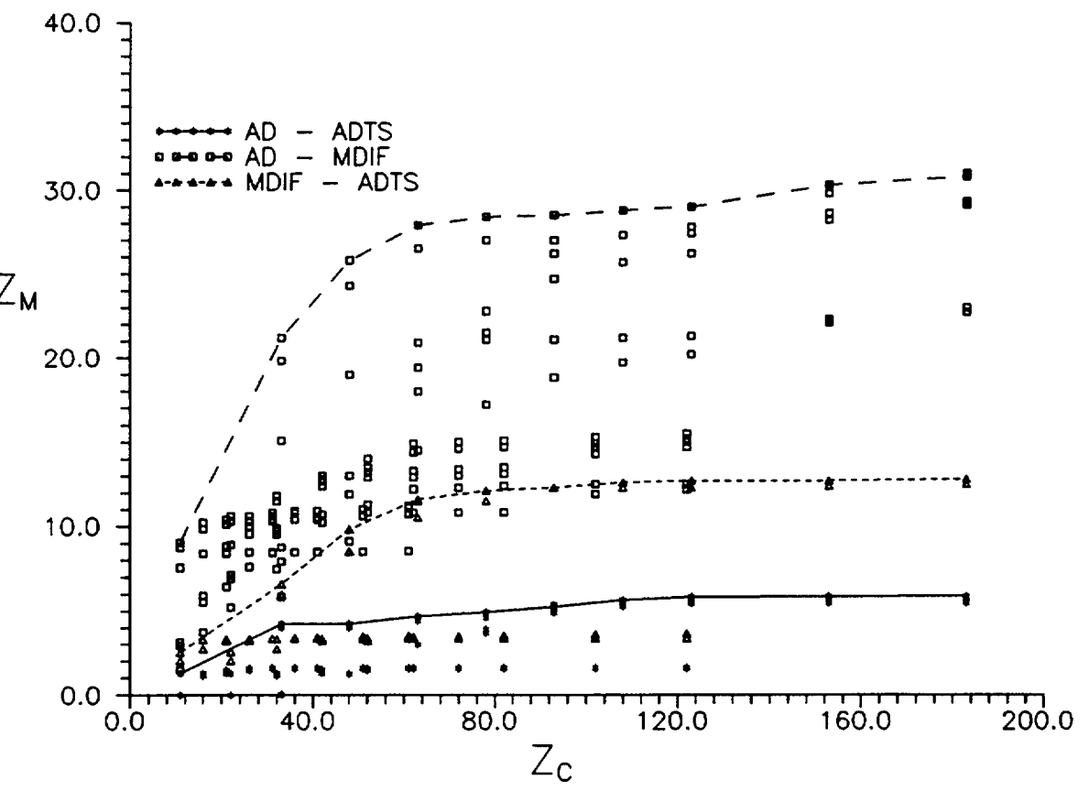

Figure 9–7. Trade–off between the model discrimination objective function for each model pairing (Z_M) and hydraulic disturbance objective (Z_C), using C as the dependent variable. The designs connected by lines are based on three distances and three residence times.

The hydraulic disturbance objective function in the preceding cases was computed with equal weight to sampling distances and water volumes pumped out of the fracture for samples. The calculations in chapter 8 indicated that the residence times for a tracer particles going through a borehole may be delayed by a factor of several times the residence time with no disturbing boreholes. If sample volumes can be kept very small, it is clear that a row of boreholes in the middle of the flow field may have a considerably larger disturbing effect than adding temporal observation points at an existing sampling distance.

The effects of assuming a ratio of $f_d/f_s = 50$, that is, a 50 times greater disturbance from a sampling distance as to a sample taken, are illustrated in Figure 9–8. Figure 9–8 shows a plot of the trade–off between the model discrimination objective function (Z_{MD}) versus the hydraulic disturbance function (Z_C), using C/C_{max} as the dependent variable. Thus, the plotted designs in Figure 9–8 differ from Figure 9–3 only in their values of the hydraulic disturbance objective function (Z_C), causing a shift in the horizontal direction in the graph.

Figure 9–8 shows the same basic feature, as Figure 9–3, that the combined use of several residence times will only give a marginal improvement to the model discrimination objective function (Z_{MD}). However, in this case the non–inferior sets (for the different combinations of residence times) of designs are to large extent made up of designs containing two sampling distances, rather than three. The different combinations of sampling distances appears as separate "clusters" in Figure 9–8, where the designs with only one distance (3 m) is most easily identified in the lower left–hand corner of the graph. In fact, it is only at Z_C–values above approximately 250 units that design involving three sampling distances form part of the boundary of the non–inferior set of designs.

Although the quantification of the disturbance factors, f_d and f_s, at this point to large extent is subjective, the main conclusion from Figure 9–8 is that designs with three sampling distances easily becomes inferior to designs with two distances, as the ratio of borehole/sampling disturbance becomes smaller. On the other hand, the improvement in the objective function, Z_{MD}, when going from one sampling distance to two still is considerable.

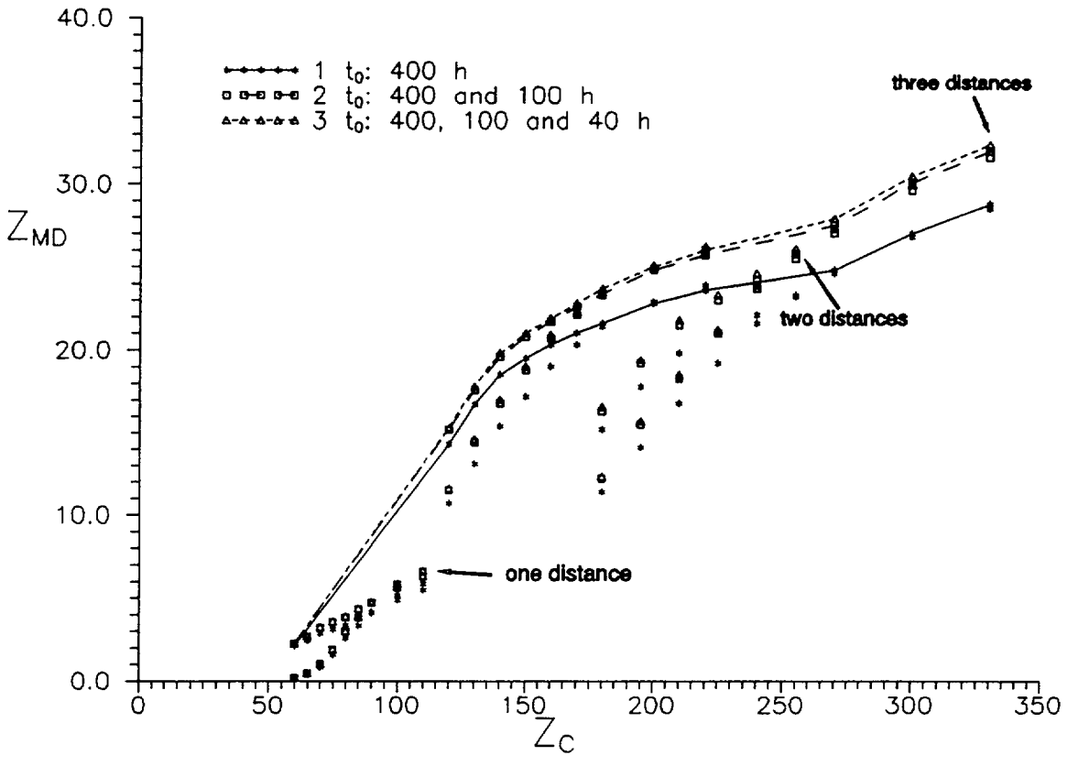

Figure 9–8. Trade–off between the model discrimination objective function (Z_{MD}) and the hydraulic disturbance objective function (Z_C), using C/C_{max}, with a ratio of f_d/f_s = 50. The lines indicate the boundaries of non–inferior designs for each combination of residence times (based on 3 m sampling distance). Arrows indicate the designs with the maximum Z_{MD}–value for each combination of distances.

In summary, some conclusions from the multi–objective optimization calculations can be formulated. It should be repeated that such conclusions are of a general nature, giving basic insight into how the fundamental physics of each model can be utilized for the construction of designs that are likely to be successful. Results from the optimization calculations is a function of the physical characteristics of each model in relation to hypothetical observation locations (in time and space). Thus, the interpretation of results in this chapter is not expected to result in a specific and detailed design, but to give a higher level knowledge how the applied models work in an experimental design context.

In practice, a detailed design would be preceded by on–site characterization, hydraulic tests, etc. In addition, if repeated experiments with different residence times would be attempted in the field, results would be evaluated between tests and the design may be modified, if needed. In that case, optimization calculations need not be parameter–robust, since best–fit

parameter estimates from preceding tests would be used for design of additional tests.

Some of the main conclusions can be stated as follows:

- Repeated experiments with varying residence times are probably necessary for identifying time–dependent processes, since both the objectives of parameter estimation and model discrimination need to be satisfied.

- Using two different residence times may be sufficient, although optimization calculations indicate that three residence times will give even better possibilities.

- Using two sampling distances (3 and 1.5 m) rather than one (3 m) gives a considerable improvement for both the parameter estimation and the model discrimination objectives.

- The method of selecting observation points have a significant effect on the values of the objective functions. It turns out that points selected using the single–objective criterion for parameter estimation does relatively well for both the objectives of parameter estimation and model discrimination.

- Independent information of fracture volume (or cross–section area of transport channel) will enhance the model discrimination possibilities, although this may not be necessary since it is shown that there is a substantial discrimination potential also without a priori knowledge of the fracture volume.

- A relatively large number of sampling points in time are needed for each distance sampled to ensure low correlation between parameters for all the models considered in this study.

- Hydraulic influence of boreholes and pumping for sampling will have a significant effect on the final design decision.

TEST OF DESIGN

A major conclusion of the design calculations was that repeated tracer tests using different average water velocities, in the same flow geometry, are likely to give data that will significantly improve the possibilities to evaluate different time dependent processes. As a demonstration of how the results from such an experiment may be evaluated (according to the design), synthetic tracer tests were run in a two–dimensional, heterogeneous, single fracture. A heterogeneous fracture was represented by generating a single realization of a spatially correlated random field. Naturally it is not possible to definitely prove, even with a very large number of simulated fractures covering a wide range of assumptions about spatial distribution of flow properties, that the design concepts arrived at here actually will work in a real fracture. However, running a tracer test according to the general design principles arrived at above, on a fracture that has some degree of unevenly distributed flow, will give an opportunity to visualize and "practice" the process of evaluating the experiment according to design.

This synthetic experiment also visualizes how rows of boreholes, perpendicular to the direction of the induced uniform gradient, may be used to intercept the main transport conduit(s).

The synthetic fracture was generated using the turning bands method (TUBA) /Zimmerman & Wilson, 1989/. The property that was generated was the transmissivity, assuming a log–normal distribution. The average transmissivity was set to 5×10^{-8} m^2/s, with a variance of one (in log units). A gaussian covariance model was used for the spatial correlation, with an isotropic correlation length of 0.25 m.

The size of the simulated fracture was 5 x 5 m, giving a ratio of 1/20 of correlation length vs scale of fracture. The flow and transport in the fracture was simulated using the SUTRA code /Voss, 1990/, a two–dimensional finite element code, the only transport processes included being advection and dispersion. The simulated transmissivity field is shown i Figure 10–1. The field is plotted using contour lines of equal transmissivity, giving an averaged picture of the simulated field, similar to the averaging done also by the simulation code. The finite element mesh consists of 50 x 50 equally sized elements, thus resulting in elements with a side of 0.1 m.

A uniform gradient was simulated across the fracture by defining a constant head along the vertical sides in Figure 10–1, with no–flow boundaries on the remaining sides, so that a gradient is created in the x–direction. A plot of vectors proportional to the flow rate in Figure 10–2 shows the uneven distribution of flow in the simulated fracture. A tracer pulse injection was simulated by letting the in–flowing water at the mid–point of the left–hand

boundary have a concentration of 1.0 for five minutes, a plausible injection time that may be applied in practice. The injection point is selected somewhat arbitrary, although it is located in a relatively high transmissivity area of the boundary, which also is the preferred option for the actual experiment (see also section 11).

The migration of the injected tracer pulse is monitored in three rows of boreholes, located at distances of 1.5, 3.0, and 4.5 m in the x-direction from the injection point. There were five boreholes in each row, separated from each other by a distance of 0.5 m, symmetrically located around the y-coordinate corresponding to the injection location (y = 2.5 m on the left-hand boundary in Figure 10-1). Tracer breakthrough in each well is obtained by using the calculated concentration in the finite element node associated with each observation borehole. No withdrawal of water is made in the observation points.

One borehole in each row, considered to intersect the main tracer conduit, was selected to represent the distance associated with the row. The boreholes selected were the ones with the highest peak concentration of the tracer breakthrough curve. Three different experiments with different residence times were run. The residence times were approximately the same as was used for the design calculations; 400, 100 and 40 hours. The resulting breakthrough curves for a distance of 3 m, to be used for the evaluation using the 1-D transport models, are shown i Figure 10-3, where the main tracer conduit turned out to be intersected by the observation point at y = 1.5 m in each row of boreholes.

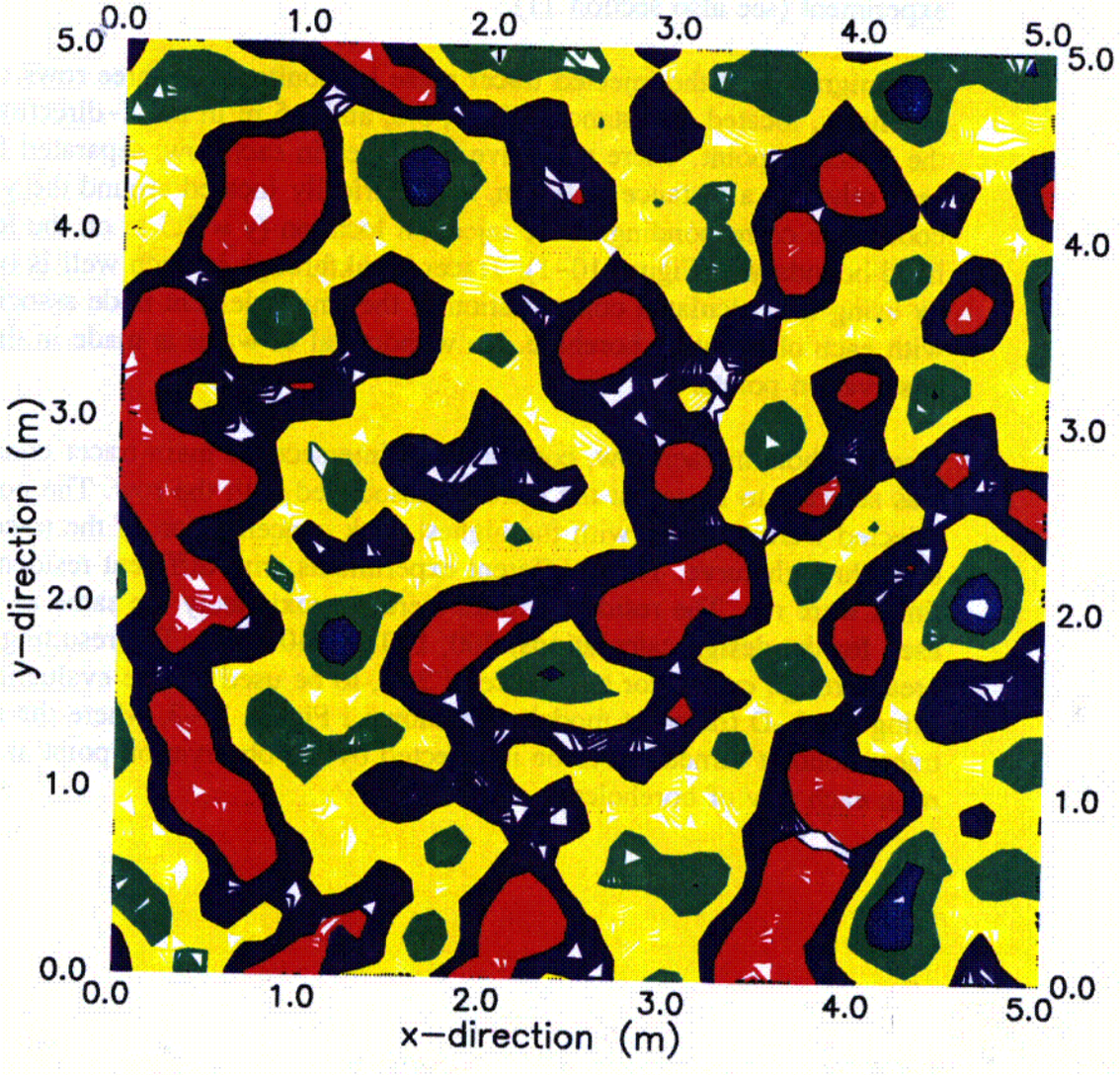

Figure 10–1. Simulated transmissivity field for the synthetic fracture. Colors represent log units ranging from log(T) greater than –6 (red) to log(T) greater than –10 (blue).

C1

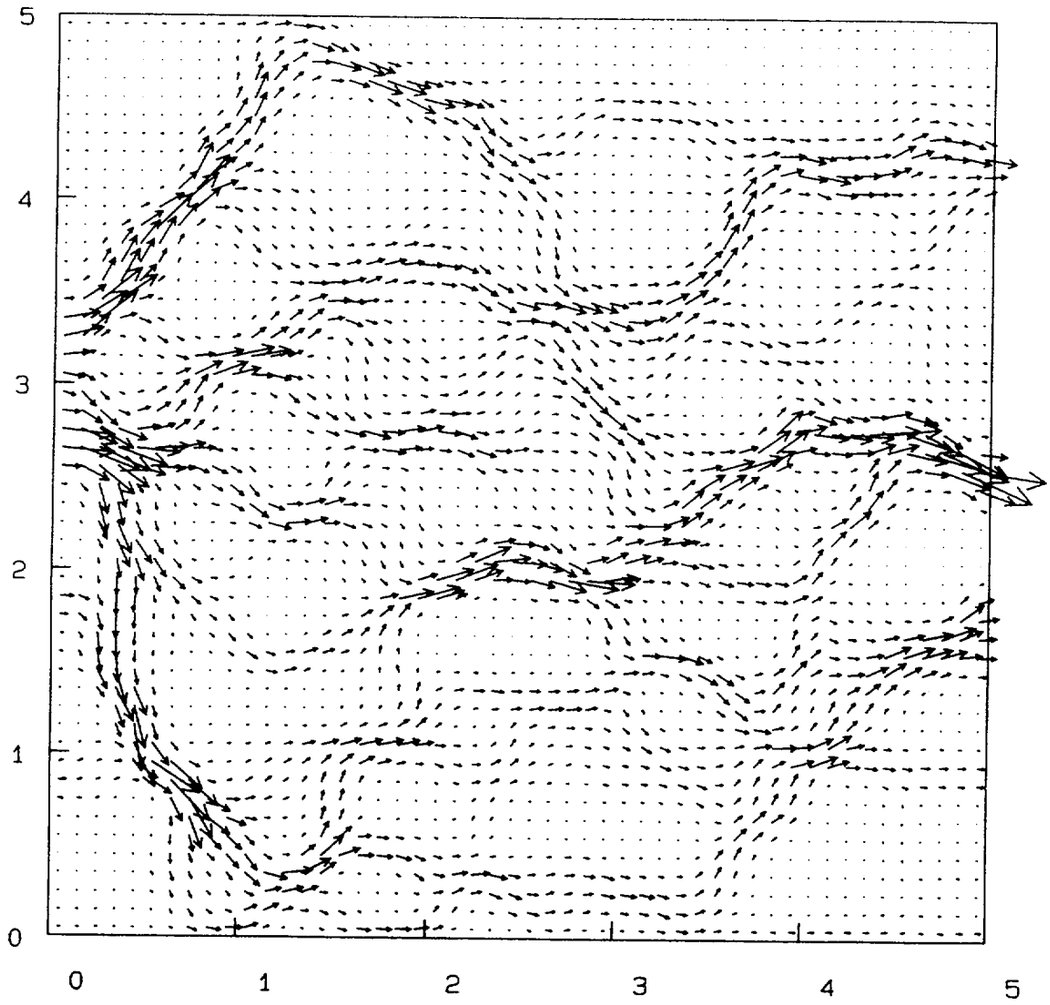

Figure 10–2. Vectors proportional to the flow rate for the simulated system.

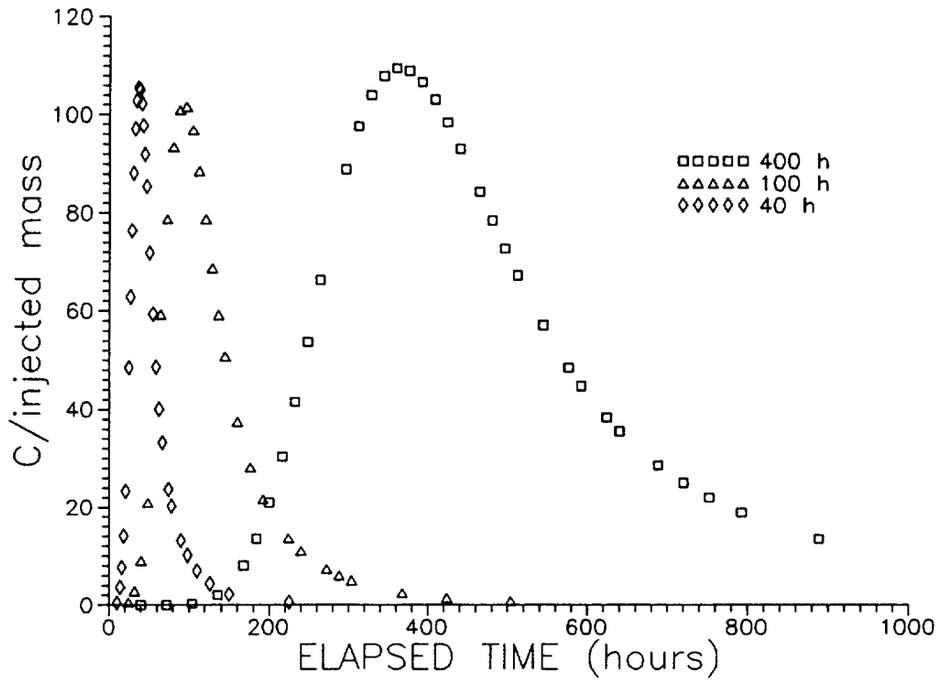

Figure 10–3. Observation data used for the evaluation of the synthetic tracer test.

The evaluation of the breakthrough curves was made with the same three models used for the design. Only one distance, 3 m, was used in this case. The general strategy was to fit each model to the results, and examine if it was possible to determine a single model that best explains the experimental data, and if the other models could be shown to be incorrect. In this case, the only processes simulated are advection and dispersion, and the evaluation should indicate that the advection–dispersion model is the "correct" one. Although in practice model discrimination may involve several different criteria (see section 7), this exercise only considers systematic model errors and some analysis of the estimated parameter values. For the purpose of demonstrating the impact on evaluation by using one or several residence times, each model was evaluated in four different ways:

1. Using the 400 h breakthrough curve only.
2. Using the 400 and 100 h breakthrough curves in combination.
3. Using the 400, 100 and 40 h breakthrough curves in combination.
4. Same as above, but assuming the total tracer volume in the fracture may not be the same for all residence times.

Advection–dispersion model evaluation:

The evaluation using the one–dimensional advection–dispersion model, which presumably would be the correct model in this case, shows that observation data is very well explained in all four cases. This is not surprising, since the breakthrough curves in Figure 10–3 would be almost identical if plotted with dimensionless time (t/t_0). The results from parameter estimation according to 3 above, using 400, 100 and 40 h residence time in combination, are shown in Figure 10–4. The most striking systematic model error, although relatively minor, is in the tailing parts of all three curves. It should be safe to interpret this as mainly an effect of the two–dimensional heterogeneous flow field, which the one–dimensional model is not capable of explaining. However, it is likely that in a real situation the agreement between model and data would have been considered very good.

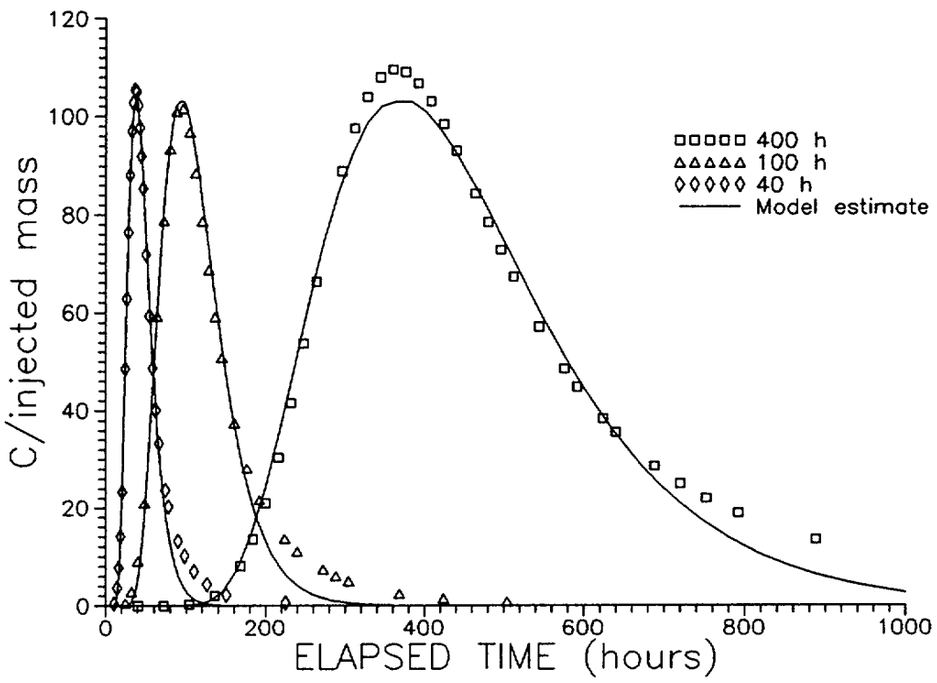

Figure 10–4. Evaluation of observation data from three tracer tests in combination using the AD–model.

Results for the other cases are very similar, and estimated parameter values do not differ substantially. It can be mentioned that the estimated dispersivity is approximately 0.2 m. Satisfactory estimation statistics (estimation variances of parameters and correlation between parameters) are obtained for all cases.

Transient solute storage model evaluation:

This model is presumably incorrect, or rather that it contains too many parameters, in this case, as stagnant zones are not considered in the calculation. However, the spatially distributed variable velocity field may cause effects that might be interpreted, in one dimension, as immobile zone storage. Applying this model according to point 1 above, using the 400 h residence time only, results in a fit of the model to observed data as shown in Figure 10–5.

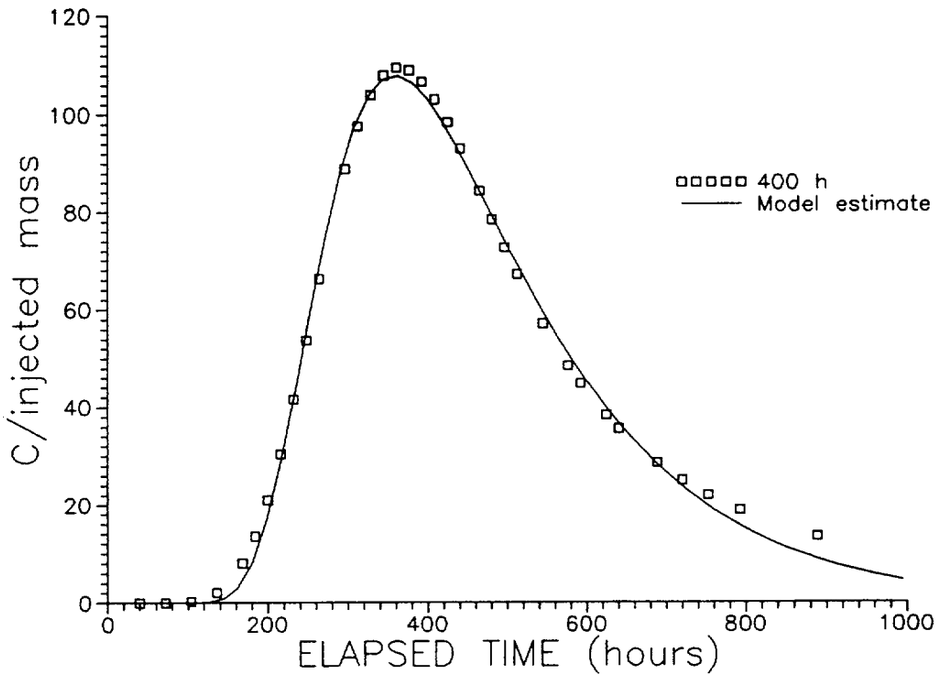

Figure 10–5. Evaluation of observation data from the 400 h residence time tracer test with the transient solute storage model.

From the best–fit estimate in Figure 10–5, it appears as if the ADTS–model is significantly better than the presumably "true" AD–model, as the tailing part of the breakthrough curve shows a better agreement between model and observation data. The estimated residence time with the ADTS–model in this case is 361 hours, and the dispersivity 0.12 m. The estimated stagnant zone parameter values are 0.8 for the flowing fraction (ϕ) and 0.002 h^{-1} for the transfer coefficient (K). Although it is difficult to assign an exact physical meaning to the transfer coefficient, these values seem entirely plausible. The values of ϕ and K, put in relation to the residence time, point to a moderate but significant effect of stagnant zone storage during this experiment. Thus, using one residence time only, the ADTS–model would likely be considered superior to the AD– model. However, this conclusion would be offset by the high correlations between parameters, generally well above 0.9 in this case, contributing to a relatively high estimation variance for some of the parameters.

Applying the ADTS-model to three breakthrough curves, with different residence times, yield completely different results. The best-fit estimate in this case, shown in Figure 10-6, shows an agreement between model and data similar to the AD-model (Figure 10-4).

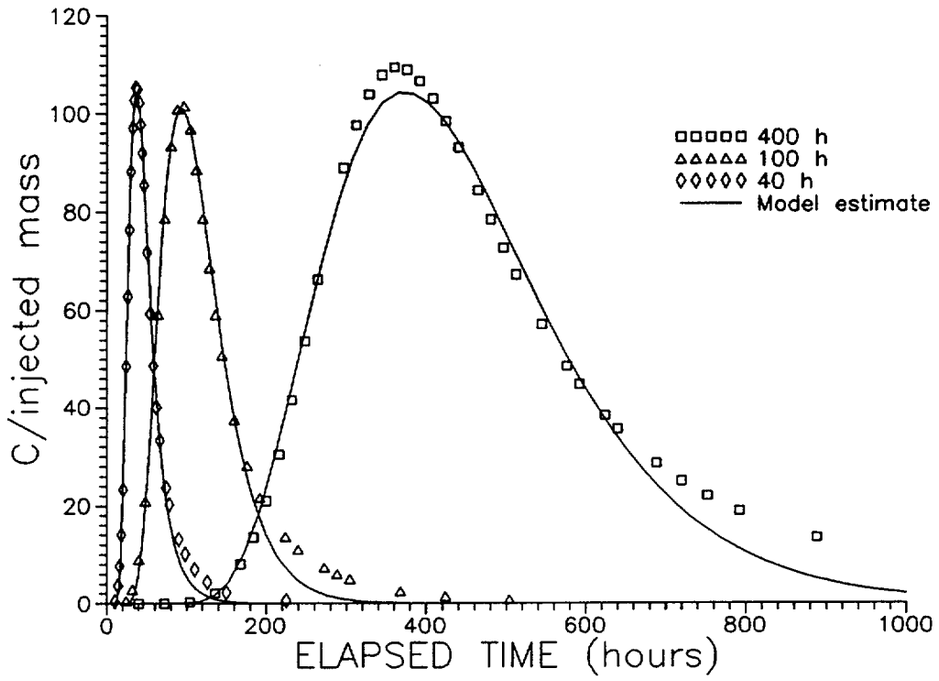

Figure 10-6. Evaluation of observation data from the 400 h, 100 h and 40 h residence time tracers test with the transient solute storage model (ADTS).

The estimated values for the residence times are similar those obtained by the AD-model. However, the values of the dispersivity, and the transfer coefficient differs with roughly a factor two from the application of the ADTS-model to only one breakthrough curve. The estimated flowing fraction parameter, ϕ, is approximately 0.9 compared to 0.8 when using only the 400 h breakthrough curve. Thus, one may conclude the ADTS-model does not explain the observation data satisfactorily, and should be rejected.

The correlation between parameters between parameters is relatively moderate in this case. Thus, although this model may be considered unsatisfactory, the regression statistics is significantly improved, for evaluation with the ADTS-model, by applying breakthrough curves with different residence times.

Matrix diffusion model evaluation:

Similar to the processes in the transient solute storage model, matrix diffusion is likely to be successful in explaining the kind of tailing, in this case caused by the 2-D flow field, that is not explained by the AD-model in

Figure 10–4. Using one breakthrough curve only (400 h residence time), the evaluation with the matrix diffusion model shows, as expected, good agreement with the observation data. This is shown in Figure 10–7, and the best–fit model estimate is very similar to the corresponding one for the ADTS–model in Figure 10–5.

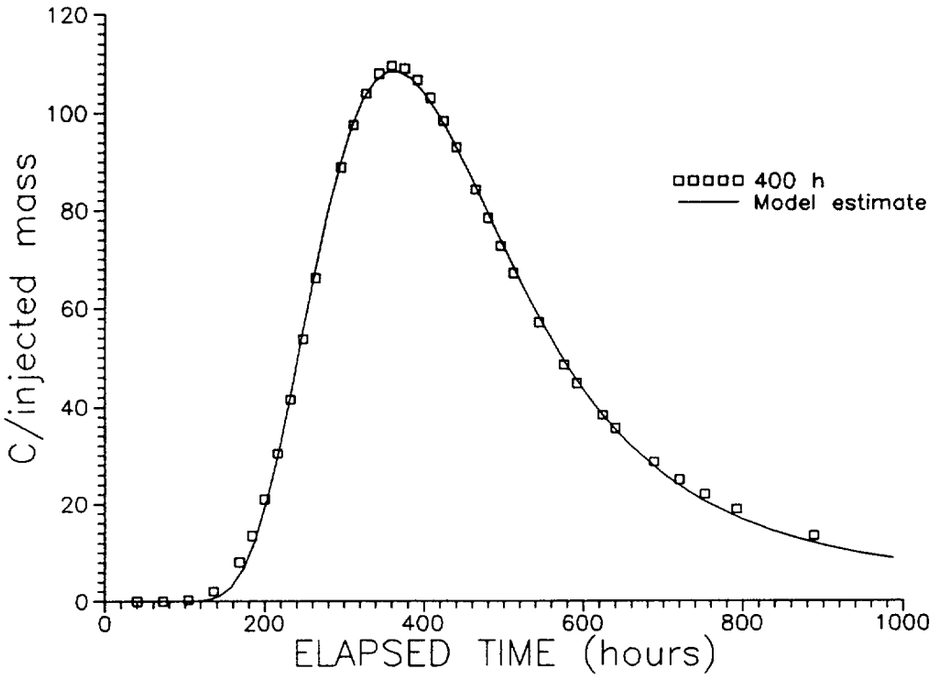

Figure 10–7. Evaluation of observation data from the 400 h residence time tracer test with the matrix diffusion model (MDIF).

The estimated residence time in this case is 377 hours, and the dispersivity 0.14 m. The estimated value for the A–parameter (see section 4.2) is approximately 2×10^{-4}, yielding a moderate but significant effect of matrix diffusion on the tracer transport. Thus, both the ADTS–model and the MDIF–model give very good fits to the observation data, when only using a single residence time. Even the advection–dispersion model may be considered a good model, in spite of the tailing effects. For example, the synthetic breakthrough data was obtained by a simulation with a non–ideal tracer pulse injection, which if incorporated into the applied models also may enable the AD–model to better explain the tailing. However, using one residence time only for model evaluation merely demonstrates the well–known problem that almost any single tracer breakthrough may be explained by a large number of models, and is relatively trivial for the purposes of this analysis, which is to look at the possibilities of repeated experiments with different residence times.

The application of the matrix diffusion model to all three data sets is shown in Figure 10–8. The best–fit model estimate in Figure 10–8 is obtained by assuming that transport volume is the same during all three experiments.

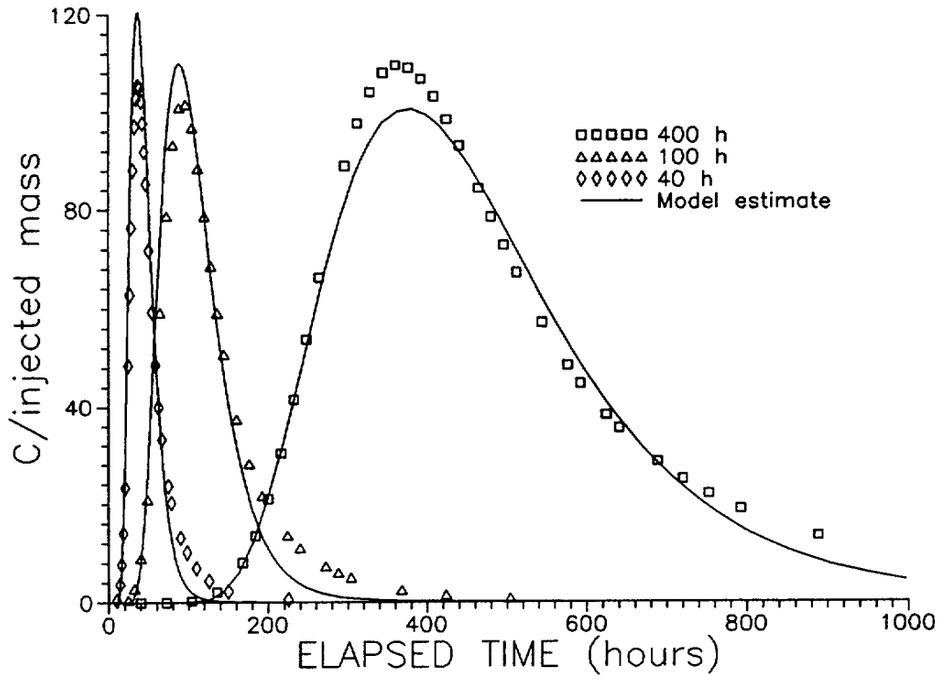

Figure 10–8. Evaluation of observation data from the 400 h, 100 h and 40 h residence time tracer tests with the matrix diffusion model (MDIF).

Assessing the best–fit model estimate from Figure 10–8 only, it would appear as the agreement between model and data is relatively satisfactory, in spite of the discrepancy around the peaks. However, the value of the matrix diffusion parameter, A, is estimated to approximately 3 x 10^{-5} $s^{-1/2}$, almost a magnitude less than for the case of using only the 400 h breakthrough curve (Figure 10–7). In fact, the estimated value is so low that the matrix diffusion model in this case approaches the advection–dispersion model. It may also be mentioned that applying the MDIF–model to two data sets, although not shown, yields a value of approximately 6 x 10^{-5} $s^{-1/2}$ for A. In addition, the estimated values of the residence times, dispersivity, and transport volume are also relatively inconsistent between the estimations in Figure 10–7 and 10–8. The conclusion is that this model, just as the ADTS–model, should be rejected.

In summary, this exercise has been an imitation of a real tracer experiment, where sampling has been performed to a pre–defined experimental design, and results has been evaluated accordingly, as if the synthetic single fracture was a real one. Again, it should be pointed out that the hydraulic and transport properties of the simulated fracture are more or less arbitrary, and the intention has not been to attempt to simulate some "most–likely" fracture. The intention was to generate a fracture that will cause some uneven pattern of tracer concentration, and to demonstrate how the sampling design may function in such a case. At least for this single realization and the models applied, the collected data could actually be used to support the "correct"

model (advection–dispersion) and reject the "incorrect" models. Ideally, a design should be robust enough to give satisfactory data independent of the spatial structure of the fracture, with respect to hydraulic and transport properties.

11 PROPOSED TEST DESIGN FOR THE MWTE

11.1 GENERAL CONSIDERATIONS

Based on the results of the scoping calculations presented in this report a tentative outline of the borehole layout and test program for the MWTE is presented below. The main features of the proposed test design is that:

1. The selected fracture and surrounding rock should be as well characterized as possible hydraulically, geologically, hydrochemically, and geometrically before tracers are added to the system.

2. Repeated tracer tests with different flow velocities should be possible to perform.

3. The tracer tests should be possible to perform in different directions using the same borehole array.

4. A relatively large number of sampling points at different distances within the flow field should be drilled.

5. A linear flow field should be established.

6. The influence of sampling procedures and sampling boreholes should be minimized.

11.2 BOREHOLE LAYOUT

One of the key issues for the success of the MWTE is to locate a suitable single fracture. A detailed test plan for identification and characterization of a suitable fracture for the MWTE is given in Section 11.3. However, it is envisaged that such a fracture is not likely to be continuous or without intersections with other equally transmissive fractures over a large area. The proposed borehole layout is therefore made in order to minimize the area needed for the experiment.

It is clear that a single fracture is preferable but also a set of 2–4 parallel fractures may be acceptable. Such a set of fractures can be quite well characterized given the number of boreholes suggested.

The MWTE is proposed to be performed within an area defined by a number of pilot boreholes which, depending on the site characteristics, should be about 10–20 x 10–20 m. This area is called the "experimental area". A

smaller area of about 5–10 x 5–10 m (the scoping calculations have been made for an area of 8 x 8 m) which is called the "flow area", see Figure 11-1, defined as the fracture area needed to control and create the flow field across the area where the tracer experiments are proposed to be carried out, the "migration area". The "migration area" covers about 2–5 x 2–5 m.

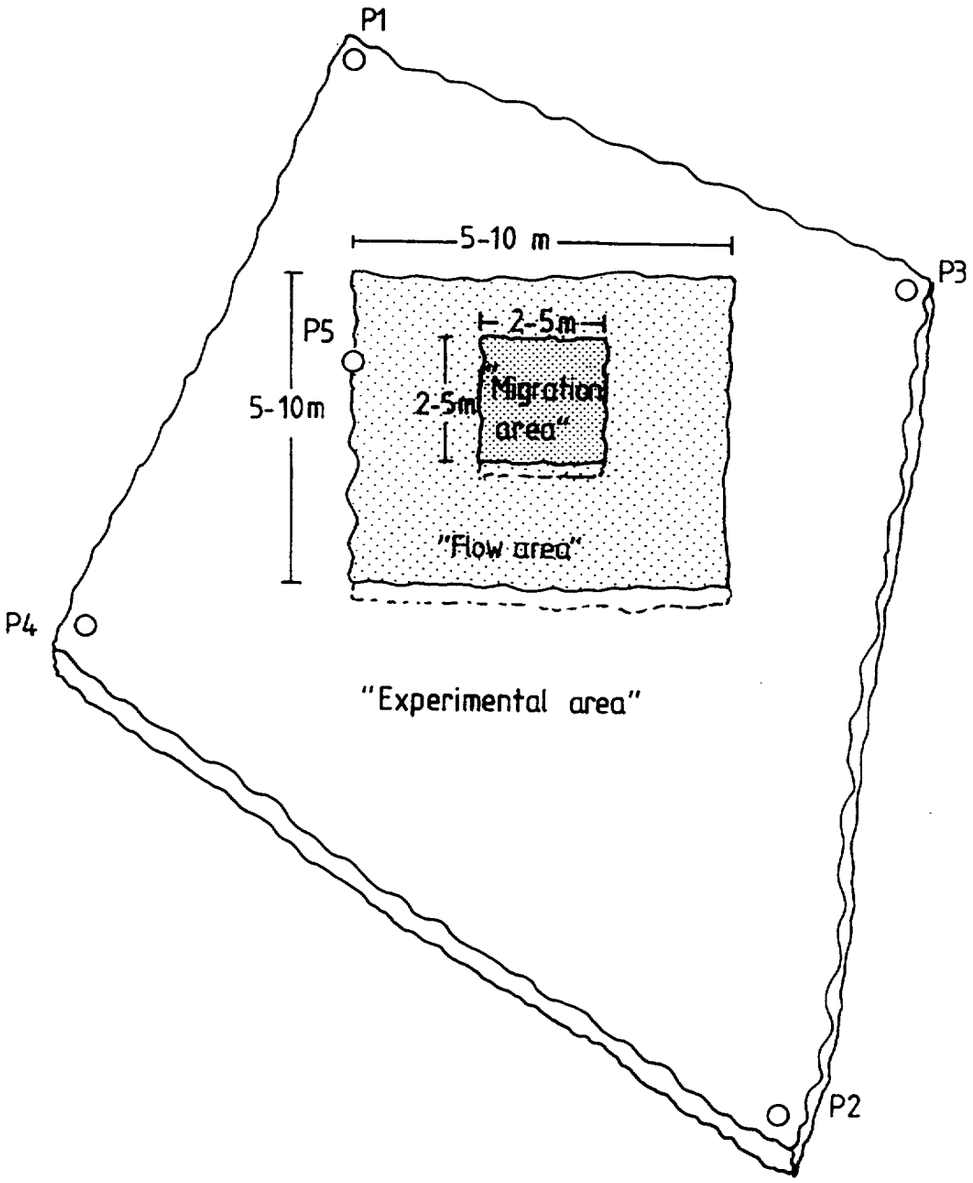

Figure 11–1. Definition of areas in the target fracture together with proposed size and example of pilot hole location.

The proposed borehole layout involves the drilling of 4–6 pilot boreholes (P1–P6), 2–8 "flow boreholes" (F1–F8) and 15–30 "migration boreholes" (M1–M30), see Figures 11–1 and 11–2. The pilot and "flow holes are 76 mm cored holes and the migration holes are 46 mm cored holes. The pilot holes are drilled in order to identify and characterize the geometry and hydraulics of the fracture. The purpose of the "flow boreholes" is mainly to create a linear flow field across the "migration area". Some of the "flow

boreholes" can be identical with the pilot holes as described in Section 11.3. The scoping calculations have shown that an approximately linear flow field could be established over a 4 x 4 m "migration area" by applying a dipole flow field between pairs of boreholes located about 8 m apart, c.f. Section 8. The proposed location of the flow boreholes, F1–F8, are shown in Figure 11–2.

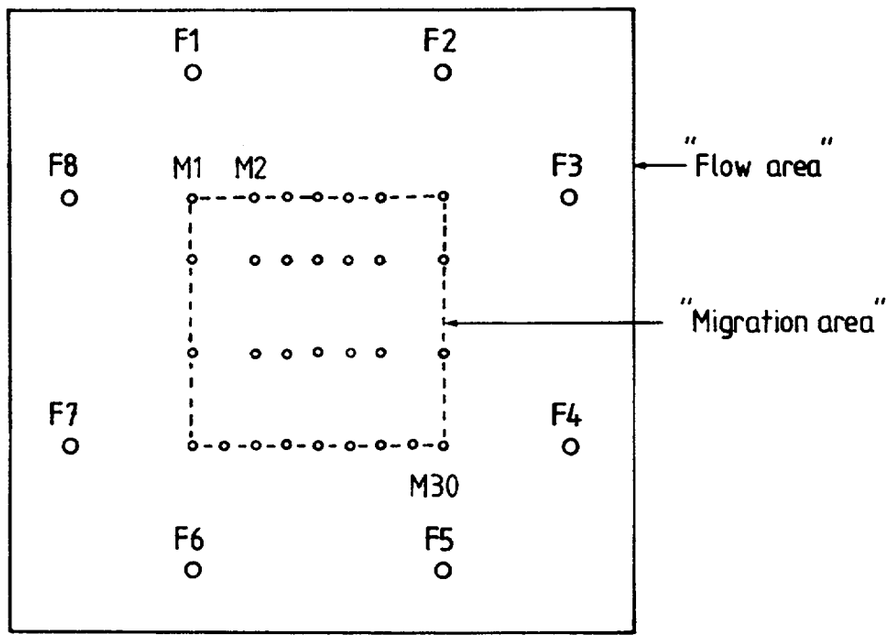

Figure 11–2. Proposed borehole layout for the "flow area" and "migration area".

The purpose of drilling 4 pairs of boreholes in 4 different directions from the "migration area" is to make it possible to alter the direction of flow and perform repeated tracer injections with different flow directions.

The drilling in the "migration area" is not planned in detail. A preliminary layout is shown in Figure 11–2. The final design has to be based on practical and financial considerations. However, based on the scoping calculations only, a design with many observation points is preferred provided that i) borehole volumes can be kept small compared to fracture volume, and ii) sampling can be arranged with minimal disturbance of the flow field. In order to accomplish this, a special sampling technique has to be developed and tested. At the upper and lower boundaries of the "migration area" borehole volumes are not as crucial. These volumes do not contribute to any delay or dispersion of the tracers that cannot be accounted for, but any borehole placed within the migration area will induce a delay, dilution and dispersion of the tracer as it passes through the borehole as shown in Section 8.

.3 IDENTIFICATION AND SELECTION OF A SUITABLE FRACTURE

One of the main difficulties associated with the MWTE is the localization of the single fracture. It is of great importance for the success of the project that a suitable fracture is found and that it is well characterized geologically, geometrically, hydrochemically, and hydraulically. The selection of a fracture should be based on the following criteria:

- Disturbing effects caused by the drift excavation should be minimized, i.e the experimental area should be located outside the "disturbed zone" , i.e at least 5 m from the drift.

- The fracture should preferably not intersect the drift but for the purpose of locating a suitable fracture it may also be possible to choose such a fracture provided that boundary effects in the experimental area are avoided, e.g. by sealing the fracture along the perimeter of the drift.

- The fracture should be continuous over the entire flow area, i.e about 5–10 x 5–10 m, see Figure 11–1.

- There should be no intersections with other fractures having similar or higher hydraulic transmissivities in the proposed "migration area" (2–5 x 2–5 m).

- The fracture should have a mean transmissivity of about $5 \cdot 10^{-8}$ – $5 \cdot 10^{-10}$ m^2/s, i.e a fracture that is possible to accept in the vicinity of a waste canister. The transmissivity of the selected fracture will be dependent on the hydraulic contrast between the fracture and the rock matrix at the site.

The identification of a single fracture that meets all criteria will be difficult. It may very well be necessary to accept the possibility that there are intersecting fractures, but the influence of these have to be assessed before the migration experiment is started.

The basis for identification and selection of a suitable fracture will be:

- drift mapping
- drilling of pilot holes, diameter 76 mm
- core mapping and TV–inspection of pilot holes
- inflow measurements in detailed sections of the pilot borehole, selection of sections based on the core mapping
- head monitoring in other nearby located boreholes during drilling and inflow measurements

The pilot boreholes should be drilled downwards in order to avoid oxygen to penetrate into the fracture. If the approximate location of a potentially suitable fracture is known, careful drilling is recommended at and below the calculated intersection with the fracture. This may diminish the

contamination of water and injection of drilling debris into the fracture. Also, careful monitoring of drilling debris and flushing water (used to cool the drill bit) is recommended. If possible, measurements of both incoming and outflowing water should be made continuously and flushing water should be labelled with a conservative tracer (which is not planned to be used in the tracer experiments). Ideally, a geologist should be present during the drilling with the responsibility of keeping records of drilling water losses and drilling debris recovery, performing continuous core logging, and labelling and sampling of drilling fluid.

Once a suitable fracture has been identified based on drilling and core logging, inflow measurements in detailed sections should be performed. Only tests where water is withdrawn from the fracture are recommended in order to avoid contamination. Also, borehole deviation measurements should be performed in order to determine exact locations of fracture intersections.

At this point, it is necessary to decide whether the site should be abandoned or if the fracture is suitable for further investigations. Further investigations should involve TV–inspection to determine the orientation of the target fracture and of other fractures intersecting the borehole to assess whether they are likely intersect the target fracture or not.

After drilling and inflow measurements the selected fracture should be sealed off by inflatable packers as soon as possible in order to preserve chemical conditions. The packer system should be designed to allow both withdrawal of water as well as pressure measurements within, above and below the target fracture.

Once a potentially suitable fracture has been selected, at least three additional pilot holes should be drilled in different directions from the planned "migration area" in order to determine the geometry and connectivity of the selected fracture. These boreholes may also be used later to establish the flow field in the experimental phase. The boreholes should be drilled to a depth of about 5–10 m below the target fracture in order to characterize the fracture geometry both above and below the target fracture and to assess that no other more transmissive fractures are located close to the target fracture. Continuous pressure registrations should be made in the other (sealed off) boreholes during drilling. At least three intervals of each borehole should be monitored; the target interval, above, and below the target interval. The drilling and measurement program should otherwise be the same as for the first pilot hole.

After drilling of each pilot hole, preliminary investigations including inflow measurements, core mapping, and TV–inspection should be made as well a preliminary analysis of the pressure responses during drilling and inflow measurements in order to assess that the selected site meets the predefined criteria.

4 SITE CHARACTERIZATION

4.1 Characterization of the "Experimental Area"

Based on the drilling and subsequent investigation of the pilot holes a preliminary characterization of the target fracture and surrounding volume of rock has been made. Before migration experiments are started a detailed characterization is needed. One or more of the pilot holes should be selected to define the boundary(ies) of the "flow area". Based on this selection and the averaged transmissivity values determined, 4–8 additional 76 mm cored boreholes are drilled at the boundaries of the "flow area" according to Figure 11–2. The same drilling procedure as used for the pilot holes should be also be applied for these holes. The detailed characterization of the "flow boreholes" and the pilot holes should include the following investigations:

1. Detailed core mapping in combination with TV–inspection in order to assess the geometry and composition (fracture minerals, rock type, etc.) of the fracture system at the site. In particular fractures intersecting the target fracture are essential to identify.

2. Detailed inflow measurements in short sections for identification of other permeable fractures intersecting the boreholes. Pressures should also be monitored in all other holes in at least three sections per borehole as described above in order to locate possible hydraulic connections with the target fracture.

3. Installation of a permanent packer system in the pilot boreholes and "flow boreholes" based on 1) and 2). The packer system should allow injection and withdrawal of water as well as pressure monitoring at arbitrary pressures and in a wide range of flow rates.

4. Preliminary tracer test and interference test between "flow boreholes". This test should be made for two main reasons, i) to assess the impact of the injection and sampling boreholes to be drilled in the "migration area," and the influence of drilling debris, by comparison with a second tracer test performed after drilling, and ii) to assist in the design of the borehole array and detailed design of the migration experiments. Averaged transport parameters such as flow porosity are obtained, which makes it possible to optimize the design of the tracer experiments. The tests should be short–term tests by applying a relatively high gradient to the system. This test will also show that total mass recovery can be obtained in the system, i.e. that no mass is lost in unknown directions. If losses occur, the reasons must be assessed and/or another borehole configuration may have to be considered.

In addition to the above described program for characterization, samples for laboratory analyses of diffusivity and porosity should be taken from the

drillcores.

During the progress of the detailed characterization a conceptual model will be formed. This model should be iteratively calibrated as the investigations proceed. Predictions of the outcome of interference tests as well as the preliminary tracer tests should be made. The model will also be used to determine injection and withdrawal rates and to assist in the design of the borehole array in the "migration area".

11.4.2 Characterization of the "Migration Area"

The detailed design of the "migration area" will be made based on the characterization of the "experimental area" combined with model simulations. Once a suitable borehole array has been defined, a drilling program including at least 15 boreholes within the 2–5 x 2–5 m "migration area". The drilling should preferably be made in such a way that minimal disturbance is obtained, i.e in a similar manner as the pilot holes, c.f Section 11.3. To further minimize the disturbance a smaller borehole diameter, 46 mm, and a thinner drill bit (5 mm) is suggested. In this way a lower pressure can be applied on the drill bit which diminishes the amounts of drilling debris injected into the fracture. Due to the relatively large number of boreholes, detailed inflow measurements in short sections will probably not be possible to perform along the entire length of the boreholes. These measurements should be concentrated to the target fracture while longer sections above and below could be measured.

The following steps are suggested for the detailed characterization of the "migration area":

1. Drilling of all 15–30 boreholes during one drilling campaign using similar procedure as for the pilot holes. Registration of pressure during drilling in all pilot holes and "flow holes".

2. Core mapping and TV–inspection of all cores and boreholes.

3. Sealing of all boreholes with a three–packer system isolating the fracture in as short section as possible. The third packer is placed near the drift to keep ambient pressure in borehole.

3. Inflow measurements/interference tests in three sections/borehole as described above. Simultaneous head monitoring in as many boreholes and sections as possible. Preferably should all boreholes be monitored in three sections, above, below, and at the target fracture. Monitoring should be made using one (or a few) pressure transducer common for all sections.

4. Preliminary tracer test and interference test between "flow holes" across the "migration area", i.e. the same test as before drilling of the "migration holes" as described in Section 11.4.1.

5. Characterization of fracture minerals in the borehole cores. Core samples from the target fracture should be taken for laboratory analyses, c.f. Section 11.6.

Based on these investigations, a selection of suitable tracer injection and observation/sampling boreholes is made. Boreholes with very low hydraulic response and inflow rate may be plugged permanently to avoid stagnant volumes in the fracture plane.

During the progress of the characterization the conceptual model will be updated. Predictions of the outcome of interference tests as well as the preliminary tracer tests should be made. The model will also be used to determine injection and withdrawal rates and to assist in the final design of the tracer tests.

The evaluation of the inflow measurements and interference tests should, besides the transmissivity and the storage coefficient, also be evaluated for dimensionality to get an idea of the degree of channeling within the fracture plane.

5 TRACER TEST DESIGN

5.1 Tracer Tests with Conservative Tracers

Based on the results of the scoping calculations a tentative tracer test design is presented. The final design will most probably be different due to practical and economical considerations. Site specific information from the detailed site characterization also has to be included to obtain an optimal test design.

The proposed design is based on the borehole layout described in Section 11.2 and presented in more detail in Figure 11-3. The main idea of the design is that the flow field and boundary conditions should be well controlled. This is achieved by using two pairs of "flow holes" to create a dipole flow field across the "flow area". By proper selection of flow rates and distances between "flow holes" a linear flow field is created across the "migration area" as shown in Section 8. A linear flow is assumed to most properly mimic the natural undisturbed flow conditions in the rock. The tracer tests are performed in the "migration area" and the "flow boreholes" are used to check the mass balance of the tracers, i.e. that no tracers are lost in unknown directions. Injection of tracers is made in the injection line and observation /sampling is made in three sampling lines at distances 1-5 m from the injection line (Figure 11-3). Sampling is also made in the downstream "flow holes".

A sequence of tests will be performed where different injection and sampling holes are used, flow field is varied, and different tracers are used. The test sequence is designed to vary parameters in the transport models so that distinction can be made between different models. The proposed sequence of tests involves the following steps:

- Detailed design test.
- Tests at two or more different flow velocities.
- Tests in two or more different directions.
- Tests using different tracers.

11.5.1.1 Detailed Design Test

The main purpose of this test is to optimize the test design for the following tests and to test the injection and sampling/observation systems. The test is made by injection of one conservative tracer in the most highly transmissive injection point at the upper boundary of the "migration area". Sampling/observation is made in a few selected boreholes within the "migration area" and in the "flow holes". A relatively large gradient is applied in order to shorten the test time.

The evaluation of the test is mainly concentrated on the distribution of flow paths and travel times in the "migration area". The idea is to optimize how the flow rates in the "flow holes" and how they should be varied in relation to the time available for the tests.

11.5.1.2 Tests at Two or More Different Flow Velocities.

These tests are considered as the main tests with the purpose of model discrimination. The basic idea is to perform identical tracer tests using two or more (depending on time limits, economy, etc.) flow velocities. The flow rates should be chosen so that the lowest flow velocity is as low as possible but still controllable. The second test run should be performed at an approximately 5 times higher velocity and, if possible, a third test at 10 times higher velocity than the lowest.

The tests are made by injecting at least two (3–5 if possible) conservative tracers in boreholes in the injection line (Figure 11–3). The selection of the injection boreholes is made so that boreholes with both high and low transmissivity are chosen. Tracer injection should be made with as low excess pressure as possible to avoid disturbance of the flow field. An option could be to, after the main tests, make an additional tracer run with forced injection in order to study the effects of the injection on transport and flow distribution.

The sampling/observation is made in as many observation points as possible in all three sampling lines. The number of samples and sampling points is based on model simulations performed after the detailed design test. The intention is to minimize the disturbance of the flow field caused by sampling. Ideally, in situ measurements without sampling should be used but this will probably limit the number of possible tracers to only a few. If sampling

without major disturbance of the flow field is shown to be difficult, only one sampling line or a few sampling points in each sampling line may be used. Another alternative might be to sample one sampling line and then repeat the same injection but this time sample the second line and so on. Sampling is also made in the downstream "flow holes" controlling the flow field in order to make mass balance calculations.

After each tracer test run the model predictions will be compared to the experimental results and new predictions based on a updated model will be made.

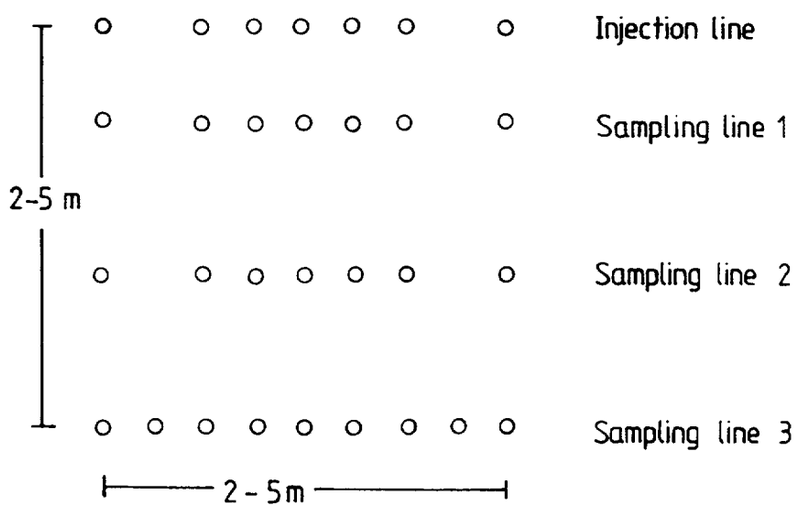

Figure 11-3. Borehole layout in the "migration area".

5.1.3 Tests in Two or More Different Directions

The purpose of changing direction for the tests is to determine the predictive ability of the "best models" calibrated on the tests described above. The tests should be made using the same flow velocity as in one of the earlier tests. A direction perpendicular to the original direction should preferably be used to indicate anisotropy in the fracture. A second alternative would be to alter the direction 180 degrees. The tests should show that results from the earlier tracer tests are consistent with these new tests, i.e any conclusions regarding transport processes should still be valid.

The tests could probably be made using only one or two tracers injected along one of the boundaries of the "migration area" perpendicular to the injection line (Figure 11-3). The possibility of drilling a few more injection or sampling holes along the boundaries or within the area may also be

considered. The tests will otherwise be performed exactly as the earlier tests described in Section 11.5.1.2.

11.5.2 Selection of Conservative Tracers

The selection of conservative tracers will be made based on the method for detection chosen. If in situ measurements are chosen this will require either radioactive tracers or tracers having very much different properties than the native groundwater. If sampling is chosen this will require extremely small samples to be retrieved. The selection of tracers then has to be made so that small volumes may be analyzed or so that a small sample can be diluted to a larger volume and still be detectable.

The selection also has to be based on the groundwater chemistry at the site. The possibly high ionic strength and salinity of the groundwater will make it difficult to use some tracers in ionic form. It is important that supporting laboratory research of these effects are conducted before the start of the tracer injections, c.f Section 11.6.1.

In addition, conservative macromolecular compounds should be injected simultaneously with other conservative tracers in order to make it possible to analyze whether matrix diffusion is important or not.

11.5.3 Tracer Tests with Sorbing Tracers

The migration of fission products and actinides from a repository with spent nuclear fuel will mainly be in the cationic form. This means that the majority of the radioactive elements will sorb on the negatively charged fracture walls of the rock. The sorption behavior will be of different magnitude due to the chemical ability of the radionuclide to be retarded. Most of the cationic radionuclides will not be possible to study within a reasonable time perspective due to the large sorption capacity. This will make tracer tests with the majority of the elements important for the safety assessment more or less impossible.

Based on the results of the tracer tests with conservative tracers, tests will be made with sorptive tracers. The tests should be made with weakly to moderately sorbing tracers in combination with conservative tracers to determine in-situ sorption coefficients. Tests should also be made in order to understand the mechanisms that control the retardation of the radionuclides within the water-rock system. Groundwater chemistry and fracture minerals will be crucial parameters for these tests. A program with supporting research in laboratory will be made to study mechanisms and enhance the knowledge about the local material at the test site.

The sorbing tracer tests will also be predicted using laboratory values of sorption coefficients an diffusivities and the prediction will be compared with the experimental outcome.

The tests will be performed in the same geometry as for the non–sorbing tracers earlier used to calculate and determine the transport parameters for dissolved elements in a flowing fracture system.

Due to the expected long duration of these tests, only a few tracer runs can be made. At least two slightly sorbing tracers are proposed to be injected. These tracer runs will be made parallel to injections with non–sorbing tracers tested and evaluated in earlier runs in the same test configuration. Also macromolecular tracers should be injected to study effects of matrix diffusion and/or filtering effects.

The in–situ cation exchange capacity of the fracture walls is and important factor that controls the interaction between dissolved elements in the groundwater and the fracture walls. The in–situ capacity can be determined by injecting groundwater with a different content of dissolved elements, e.g. a lower TDS, and study the corresponding change of the major elements in the withdrawn water.

After breakthrough of the sorbing tracers have been registered long enough some specific tests are suggested to study the mechanisms of sorption. The migration area within the test flow field makes it possible to vary the parameters of the groundwater chemistry as well as vary the physical environment within the small scale by selecting a tracer/trajectory run by the knowledge enhanced from previous non–sorptive elements. Some of these tests should preferably be made towards the end of the MWTE test as the environment impact can be rather large and affect the next tracer run.

Suggested types of tests to study the mechanisms and in–situ sorption capacities involved in a water–rock system as the MWTE:

- migration behavior by analysis of trace breakthrough curves.
- chemical equilibrium tests
- variable environment test

.5.3.1 Migration Behavior by Tracer Breakthrough Analysis

Sorbing tracers will be injected to study the breakthrough characteristics for some slightly sorbing elements. The tracers will be injected in combination with non–sorbing tracers that also were injected in the previous tests. The outcome will be presented as breakthrough curves that will be used to evaluate transport parameters and retention factors.

The choice of tracers will be made out of the results from the laboratory research program. It is of vital interest that the elements chosen have low sorption capacity to reduce the test times. The high content of dissolved elements in the groundwater at Äspö will probably enhance the transport as the sorptive sites will be occupied and reduce the retention of the migrating

species/tracers.

The migration test should also include the transport of macromolecules to study the effects of filtering processes and matrix diffusion. Their sorptive ability and size can be varied and the latter put in relation to the fracture aperture, channeling proportions and dead ends etc. Colloids or very small particles can also be used as tracers for these studies. The ability for colloids to be transported with groundwater as inert complexes and as carrier for radionuclides is one of the key issues for the safety assessment for the storage of spent nuclear fuel.

11.5.3.2 Chemical Equilibrium Test

The interaction of the fracture minerals with groundwater will be studied as the sorption is dependent on the cation exchange capacity. A groundwater of another type will be injected and the change in the withdrawn water will be studied in respect to the dissolved species that will be interacting with the fracture minerals. The calculations of chemical equilibrium will the be an estimation of the in situ capacity of the fracture walls to exchange cations.

11.5.3.3 Variable Environment Tests

After breakthrough of the sorbing tracers have been registered long enough some specific test are suggested to study the mechanisms of sorption. The migration area within the test flow field makes it possible to vary the parameters of the groundwater chemistry as well as vary the physical environment within the small scale by selecting a tracer/trajectory run by the knowledge enhanced by previous non-sorptive elements. Some of these tests should preferably be made towards the end of the tracer test project as the environment impact can be rather large and affect the next tracer run.

11.6 SUPPORTING RESEARCH

11.6.1 Laboratory Experiments on Core Samples

Laboratory experiments are needed to characterize the rock and fracture minerals in the target fracture. Laboratory values of sorption capacity (K_d) diffusivity, and porosity are needed for model predictions of the sorbing tracer tests. Tests should be made on a number of core samples from the experimental area where the dominant fracture minerals should be represented.

Laboratory experiments with altered chemical conditions should also be performed if these tests are planned to be performed in situ.

6.2 Development and Tests of Equipment for the MWTE

Based on the scoping calculations, it is clear that good injection and sampling/observation techniques are crucial for the success of the project. The most important components of the system that need to be further developed are:

- packer system
- tracer injection system
- tracer sampling/monitoring system

The packer system should be constructed in such a way that both head monitoring and water injection/withdrawal is possible above, below, and within the target fracture. Another option that can be discussed is to install packers that also can be used to block the flow through the target section completely, i.e a system where boreholes can be easily activated or deactivated.

Tracer injection system should be designed to minimize the disturbance, i.e low excess pressures should be used which also implies low injection rates.

Tracer sampling is probably the most critical part of the system. There are several different approaches to this problem that need to be further explored, e.g. retrieval of extremely small volumes, in situ measurements, or sampling in an optimized number of boreholes.

12 REFERENCES

Abelin, H., Birgersson, L., Gidlund, J., Moreno, L., Neretnieks, I., Widén, H., Ågren, T., 1987: 3-D Migration Experiment- Report 3 part 1. Performed Experiments, Results and Evaluation. Stripa Project Technical Report 87-21.

Andersson P., Andersson, J-E., Gustafsson E., Nordqvist R., Voss C., 1993a: Site Characterization in Fractured Crystalline Rock - A Critical Review of Geohydraulic Measurement Methods. SKI Technical Report 93:23.

Andersson P., Nordqvist R., Persson T., Eriksson C-O., Gustafsson E., Ittner T., 1993a: Dipole Tracer Experiment in a Low-Angle Fracture Zone at Finnsjön - Results and Interpretation. SKB Technical Report in prep.

Bear, J., Verruijt, A., 1987: Modeling groundwater flow and pollution. D. Riedel Publishing Company, Dordrecht, Holland.

Cooley, R. L., 1979: A method of estimating parameters and assessing reliability for models of steady state groundwater flow. 2. Application of statistical analysis. Water Resources Research, Vol 15, pp 603-617.

Cooley, R. L., 1985: A comparison of several methods of solving nonlinear regression groundwater flow problems. Water Resources Research, vol 21, no 10, pp 1525-1538.

Draper, N., Smith, H., 1981: Applied regression analysis. John Wiley & Sons, Inc.

Frick, U., Alexander, W. R., Baeyens, B., Bossart, P., Bradbury, M. H., Buhler, Ch., Eikenberg, J., Fierz, Th., Heer, W., Hoehn, E., Mckinley, I. G., Smith, P. A., 1992: The radionuclide migration experiment - overview of investigation 1985 - 1990. Grimsel test site. NAGRA Technical Report 91-04.

Forschungsstelle für Radiohydrometrie, 1966: Jahresbericht 1965, am Institut für allgemeine und angewandte Geologie und Mineralogie der Universität München.

Knopman, D. S., Voss, C. I., 1989: Multiobjective sampling design for parameter estimation and model discrimination in groundwater solute transport. Water Resources Research, Vol 25, pp 2245-2258.

Knopman, D. S., Voss, C. I., 1991: Sampling design for groundwater transport: Test of methods and analysis of Cape Cod tracer test data. Water Resources Research, Vol 27, pp 925–949.

Knopman, D. S., Voss, C. I., 1987: Behaviour of sensitivities in the one–dimensional advection–dispersion equation: Implications for parameter estimation and sampling design. Water Resources Research, Vol 23, pp 253–272.

Knopman, D. S., Voss, C. I., 1988: Further comments on sensitivities, parameter estimation, and sampling design in one–dimensional analysis of solute transport in porous media. Water Resources Research, Vol 24, pp 225–238.

Kreft, A., Zuber, A., 1978: On the physical meaning of the dispersion equation and its solution for different initial and boundary conditions. Chem. Eng. Sci., 33, 1471–1480.

Maloszewski, P., Zuber, A., 1990: Mathematical modeling of tracer behaviour in short–term experiments in fissured rocks. Water Resources Research, Vol 26, pp 1517–1528.

Maloszewski, P., Zuber, A., 1985: On the theory of tracer experiments in fissured rocks with a porous matrix. Journal of Hydrology, 79, pp 333–358.

Marquardht, D. W., 1963: An algorithm for least squares estimation of nonlinear parameters. J. Soc. Ind. Appl. Math., 11(2), pp 431–441.

de Marsily, G., 1986: Quantitative Hydrogeology. Academic Press, Inc.

Moreno, L., Neretnieks, I., Klockars, C–E., 1983: Evaluation of some tracer tests in the granitic rock at Finnsjön. SKB Technical Report, TR 83–38.

Olsson, O., 1992: Draft test plan for flow and transport processes in the detailed scale, Release 0.3, December 1992, SKB, Stockholm, Sweden.

Raven, K. G., Novakowski, K. S., Lapsevic, P. A., 1988: Interpretation of field tracer tests of a single fracture using a transient solute storage model. Water Resources Research, Vol 24, pp 2019–2032.

Skagius, K., Neretnieks, I., 1986: Porosities and diffusivities of some nonsorbing species in crystalline rocks. Water Resources Research, Vol 22, pp 389–398.

Strack O.D.L., 1986: Groundwater Mechanics. Prentice–Hall, 1986.

Van Swaaij, W. P. M., Charpentier, J. P. Villermaux, J., 1969: Residence time distribution in the liquid phase of trickle flow in packed columns.

Chemical Engineering Science, Vol. 24, pp. 1083–1095.

Villermaux, J., Van Swaaij, W. P. M., 1969: Modele representatif de la distribution des temps de sejour dans un reacteur semi–infini a dispersion axiale avec zones stagnantes. Application a l'ecoulement ruisselant dans des colonnes d'anneaux Raschig. Chemical Engineering Science, 1969, Vol 24, pp 1097–1111.

Voss, C.I., 1990: SUTRA – A finite–element simulation model for saturated–unsaturated, fluid–density–dependent groundwater flow with energy transport or chemically–reactive single–species solute transport. Version V06902D. U.S. Geological Survey Water–Resources Investigations Report 84–4369.

Zimmerman, D.A., Wilson, J.L., 1989: Description and Users manual for TUBA. A computer code for generating two–dimensional random fields via the turning bands method. New Mexico Institute of Mining and Technology, Socorro, New Mexico.

APPENDIX A

REFERENCES TO CODES AND OTHER SOFTWARE USED IN SCOPING CALCULATIONS

GRAPHER™. Version 1.77, 1988. Golden Software, Inc. 807 14th Street, P.O. Box 281, Golden, Colorado 80402, U.S.A.

Nordqvist, R., 1994: PAREST: a Fortran code for inverse modeling with an arbitrary model using non-linear least squares regression - users manual. GEOSIGMA GRAP 94005.

Nordqvist, 1994: Documentation of some analytical flow and transport models implemented for use with PAREST - users manual. GEOSIGMA GRAP 94006.

Nordqvist, R., 1994: Notes on a Fortran program for optimization of parameter estimation, model discrimination and sampling cost for arbitrary monitoring networks. GEOSIGMA GRAP 94007.

SLAEM - Single Layer Analytic Element Model. Version 2.1. Otto D.L. Strack, 23 Black Oaks Road, North Oaks, MN 55127, U.S.A.

SURFER™. Version 4.08, 1989. Golden Software, Inc. 807 14th Street, P.O. Box 281, Golden, Colorado 80402, U.S.A.

Voss, C.I., 1990: SUTRA - A finite-element simulation model for saturated-unsaturated, fluid-density-dependent groundwater flow with energy transport or chemically-reactive single-species solute transport. Version V06902D. U.S. Geological Survey Water-Resources Investigations Report 84-4369.

Souza, W.R., 1987: SUTRA-PLOT - Documentation of a graphical display program for the saturated-unsaturated transport (SUTRA) finite-element simulation model. U.S. Geological Survey Water-Resources Investigations Report 87-4245.

Zimmerman, D.A., Wilson, J.L., 1989: Description and Users manual for TUBA. A computer code for generating two-dimensional random fields via the turning bands method. New Mexico Institute of Mining and Technology, Socorro, New Mexico.

APPENDIX B

DOCUMENTATION OF NUMERICAL SIMULATIONS

SKB - ÄSPÖ HARD ROCK LABORATORY

Documentation of numerical simulation by:
Name: Rune Nordqvist
Company: GEOSIGMA AB
Date: September 1993

OBJECT

Modelling Task:	Task No 2A, Scoping Calculations for MWTE
SKB purchase order no:	8-10-170
Title of SKB purchase order:	Äspölaboratoriet - Försök i detaljskala
Author(s) of report:	Nordqvist R., Gustafsson E., Andersson P.
Company:	GEOSIGMA AB
Report Title:	Scoping Calculations for the Multiple Well Tracer Experiment - Efficient Design for Identifying transport Processes.
Report identification:	GEOSIGMA Grap 93 082
Operator of computer and software:	Rune Nordqvist
Company:	GEOSIGMA AB

COMPUTER

Name and version:	486DX - 50 MHz

SOFTWARE

Operative system:	MS-DOS 6.00
Code name:	ODX.FOR
Main Manual(s):	See Code Verification
Program language:	FORTRAN
Compiler:	RM-Fortran
Preprocessor name:	none
Manual:	-
"Postprocessor" name:	GRAPHER, version 1.77, 1988
Manual:	Reference Manual
Subroutine:	none

CODE VERIFICATION

Code:	see above
Distributor:	-
Report/article:	Nordqvist, R, 1994: Documentation of some analytical flow and transport models implemented for use with PAREST - users manual. GEOSIGMA GRAP 94006.

"Code":	GRAPHER™
Distributor:	Golden Software Inc., 807 14th Street, P.O. Box 281, Golden, Colorado 80402, U.S.A.
Report/article:	-

INPUT DATA AND RESULTS

Stored at: All input data and results are stored at GEOSIGMA AB in Uppsala. Files are stored on diskettes.

INPUT DATA: in text

RESULTS:

Ref:	Figure 6–1
Data File name:	ODX61.DAT
HPGL File:	ODX61.OUT

SKB - ÄSPÖ HARD ROCK LABORATORY

Documentation of numerical simulation by:

Name:	Rune Nordqvist
Company:	GEOSIGMA AB
Date:	September 1993

OBJECT

Modelling Task:	Task No 2A, Scoping Calculations for MWTE
SKB purchase order no:	8-10-170
Title of SKB purchase order:	Äspölaboratoriet - Försök i detaljskala
Author(s) of report:	Nordqvist R., Gustafsson E., Andersson P.
Company:	GEOSIGMA AB
Report Title:	Scoping Calculations for the Multiple Well Tracer Experiment - Efficient Design for Identifying transport Processes.
Report identification:	GEOSIGMA Grap 93 082
Operator of computer and software:	Rune Nordqvist
Company:	GEOSIGMA AB

COMPUTER

Name and version:	486DX - 50MHz

SOFTWARE

Operative system:	MS-DOS 6.00
Code name:	ADTSX.FOR
Main Manual(s):	See Code Verification
Program language:	FORTRAN
Compiler:	RM-Fortran
Preprocessor name:	none
Manual:	-
"Postprocessor" name:	GRAPHER, version 1.77, 1988
Manual:	Reference Manual
Subroutine:	none

CODE VERIFICATION

Code:	see above
Distributor:	-
Report/article:	Nordqvist, R, 1994: Documentation of some analytical flow and transport models implemented for use with PAREST - users manual. GEOSIGMA GRAP 94006.
"Code":	GRAPHER™
Distributor:	Golden Software Inc., 807 14th Street, P.O. Box 281, Golden, Colorado 80402, U.S.A.
Report/article:	-

INPUT DATA AND RESULTS

Stored at: All input data and results are stored at GEOSIGMA AB in Uppsala. Files are stored on diskettes.

INPUT DATA: in text

RESULTS:

Ref:	Figure 6–2
Data File name:	ADTSX62.DAT
HPGL File:	ADTSX62.OUT

SKB – ÄSPÖ HARD ROCK LABORATORY

Documentation of numerical simulation by:

Name:	Rune Nordqvist
Company:	GEOSIGMA AB
Date:	September 1993

OBJECT

Modelling Task:	Task No 2A, Scoping Calculations for MWTE
SKB purchase order no:	8–10–170
Title of SKB purchase order:	Äspölaboratoriet – Försök i detaljskala
Author(s) of report:	Nordqvist R., Gustafsson E., Andersson P.
Company:	GEOSIGMA AB
Report Title:	Scoping Calculations for the Multiple Well Tracer Experiment – Efficient Design for Identifying transport Processes.
Report identification:	GEOSIGMA Grap 93 082
Operator of computer and software:	Rune Nordqvist
Company:	GEOSIGMA AB

COMPUTER

Name and version:	486DX – 50MHz

SOFTWARE

Operative system:	MS–DOS 6.00
Code name:	MDIFSFX.FOR
Main Manual(s):	See Code Verification
Program language:	FORTRAN
Compiler:	RM–Fortran
Preprocessor name:	none
Manual:	–
"Postprocessor" name:	GRAPHER, version 1.77, 1988
Manual:	Reference Manual
Subroutine:	none

CODE VERIFICATION

Code:	see above
Distributor:	–
Report/article:	Nordqvist, R, 1994: Documentation of some analytical flow and transport models implemented for use with PAREST – users manual. GEOSIGMA GRAP 94006.
"Code":	GRAPHER™
Distributor:	Golden Software Inc., 807 14th Street, P.O. Box 281, Golden, Colorado 80402, U.S.A.
Report/article:	–

INPUT DATA AND RESULTS

Stored at: All input data and results are stored at GEOSIGMA AB in Uppsala. Files are stored on diskettes.

INPUT DATA: in text

RESULTS:

Ref:	Figure 6–3
Data File name:	MDIFX63.DAT
HPGL File:	MDIFX63.OUT

SKB – ÄSPÖ HARD ROCK LABORATORY

Documentation of numerical simulation by:

Name:	Rune Nordqvist
Company:	GEOSIGMA AB
Date:	September 1993

OBJECT

Modelling Task:	Task No 2A, Scoping Calculations for MWTE
SKB purchase order no:	8–10–170
Title of SKB purchase order:	Äspölaboratoriet – Försök i detaljskala
Author(s) of report:	Nordqvist R., Gustafsson E., Andersson P.
Company:	GEOSIGMA AB
Report Title:	Scoping Calculations for the Multiple Well Tracer Experiment – Efficient Design for Identifying transport Processes.
Report identification:	GEOSIGMA Grap 93 082
Operator of computer and software:	Rune Nordqvist
Company:	GEOSIGMA AB

COMPUTER

Name and version:	486DX – 50MHz

SOFTWARE

Operative system:	MS–DOS 6.00
Code name:	ODX.FOR, ADTSX.FOR, MDIFSFX.FOR
Main Manual(s):	See Code Verification
Program language:	FORTRAN
Compiler:	RM–Fortran
Preprocessor name:	none
Manual:	–
"Postprocessor" name:	GRAPHER, version 1.77, 1988
Manual:	Reference Manual
Subroutine:	none

CODE VERIFICATION

Code:	see above
Distributor:	–
Report/article:	Nordqvist, R, 1994: Documentation of some analytical flow and transport models implemented for use with PAREST – users manual. GEOSIGMA GRAP 94006.
"Code":	GRAPHER™
Distributor:	Golden Software Inc., 807 14th Street, P.O. Box 281, Golden, Colorado 80402, U.S.A.
Report/article:	–

INPUT DATA AND RESULTS

Stored at: All input data and results are stored at GEOSIGMA AB in Uppsala. Files are stored on diskettes.

INPUT DATA: in text

RESULTS:

Ref:	Figure 7–1
Data file names:	DDDA1.DAT
	DDDA5.DAT
HPGL File:	MDIS71.OUT
Ref:	Figure 7–2
Data file names:	DDDA1.DAT
	DDDA3.DAT
	DDDA5.DAT
	DDDA7.DAT
HPGL File:	MDIS72.OUT
Ref:	Figure 7–3
Data File names:	DDDA1.DAT
	DDDA5.DAT
	MDIF7.DAT
	MDIF8.DAT
HPGL File:	MDIS73.OUT
Ref:	Figure 7–4
Data file names:	DDDA3.DAT
	DDDA7.DAT
	MDIF7.DAT
	MDIF8.DAT
HPGL File:	MDIS74.OUT

SKB – ÄSPÖ HARD ROCK LABORATORY

Documentation of numerical simulation by:
Name: Rune Nordqvist
Company: GEOSIGMA AB
Date: September 1993

OBJECT

Modelling Task:	Task No 2A, Scoping Calculations for MWTE
SKB purchase order no:	8–10–170
Title of SKB purchase order:	Äspölaboratoriet – Försök i detaljskala
Author(s) of report:	Nordqvist R., Gustafsson E., Andersson P.
Company:	GEOSIGMA AB
Report Title:	Scoping Calculations for the Multiple Well Tracer Experiment – Efficient Design for Identifying transport Processes.
Report identification:	GEOSIGMA Grap 93 082
Operator of computer and software:	Rune Nordqvist
Company:	GEOSIGMA AB

COMPUTER

Name and version: 486DX – 50MHz

SOFTWARE

Operative system:	MS–DOS 6.00
Code name:	ADTSX.FOR
Main Manual(s):	See Code Verification
Program language:	FORTRAN
Compiler:	RM–Fortran
Preprocessor name:	none
Manual:	–
"Postprocessor" name:	GRAPHER, version 1.77, 1988
Manual:	Reference Manual
Subroutine:	none

CODE VERIFICATION

Code:	see above
Distributor:	–
Report/article:	Nordqvist, R, 1994: Documentation of some analytical flow and transport models implemented for use with PAREST – users manual. GEOSIGMA GRAP 94006.
"Code":	GRAPHER™
Distributor:	Golden Software Inc., 807 14th Street, P.O. Box 281, Golden, Colorado 80402, U.S.A.
Report/article:	–

INPUT DATA AND RESULTS

Stored at: All input data and results are stored at GEOSIGMA AB in Uppsala. Files are stored on diskettes.

INPUT DATA: in text

RESULTS:

Ref:	Figure 7–5
Data File names:	5H75.DAT
	20H75.DAT
	50H75.DAT
HPGL File:	ADTS75.OUT

SKB – ÄSPÖ HARD ROCK LABORATORY

Documentation of numerical simulation by:
Name: Rune Nordqvist
Company: GEOSIGMA AB
Date: September 1993

OBJECT

Modelling Task:	Task No 2A, Scoping Calculations for MWTE
SKB purchase order no:	8–10–170
Title of SKB purchase order:	Äspölaboratoriet – Försök i detaljskala
Author(s) of report:	Nordqvist R., Gustafsson E., Andersson P.
Company:	GEOSIGMA AB
Report Title:	Scoping Calculations for the Multiple Well Tracer Experiment – Efficient Design for Identifying transport Processes.
Report identification:	GEOSIGMA Grap 93 082
Operator of computer and software:	Rune Nordqvist
Company:	GEOSIGMA AB

COMPUTER

Name and version:	486DX – 50MHz

SOFTWARE

Operative system:	MS–DOS 6.00
Code name:	PAREST
Main Manual(s):	See Code Verification
Program language:	FORTRAN
Compiler:	LAHEY
Preprocessor name:	none
Manual:	–
"Postprocessor" name:	GRAPHER, version 1.77, 1988
Manual:	Reference Manual
Subroutine:	none

CODE VERIFICATION

Code:	see above
Distributor:	–
Report/article:	Nordqvist, R, 1994: PAREST: a Fortran code for inverse modeling with an arbitrary model using non–linear least squares regression – users manual. GEOSIGMA GRAP 94005.
"Code":	GRAPHER™
Distributor:	Golden Software Inc., 807 14th Street, P.O. Box 281, Golden, Colorado 80402, U.S.A.
Report/article:	–

INPUT DATA AND RESULTS

Stored at: All input data and results are stored at GEOSIGMA AB in Uppsala. Files are stored on diskettes.

INPUT DATA:

Ref:	Figure 7-6
Data file names:	50H75.DAT

RESULTS:

Ref:	Figure 7-6
Data File names:	21.SUM
HPGL File:	21X.OUT

INPUT DATA:

Ref:	Figure 7-7
Data file names:	50H75.DAT
	20H75.DAT
	5H75.DAT

RESULTS:

Ref:	Figure 7-7
Data File names:	23.SUM
HPGL File:	23X.OUT

INPUT DATA:

Ref:	Figure 7-8
Data file names:	50H75.DAT
	20H75.DAT
	5H75.DAT

RESULTS:

Ref:	Figure 7-8
Data File names:	27.SUM
HPGL File:	27X.OUT

SKB – ÄSPÖ HARD ROCK LABORATORY

Documentation of numerical simulation by:
Name: Erik Gustafsson
Company: GEOSIGMA AB
Date: September 1993

OBJECT

Modelling Task:	Task No 2A, Scoping Calculations for MWTE
SKB purchase order no:	8–10–170
Title of SKB purchase order:	Äspölaboratoriet – Försök i detaljskala
Author(s) of report:	Nordqvist R., Gustafsson E., Andersson P.
Company:	GEOSIGMA AB
Report Title:	Scoping Calculations for the Multiple Well Tracer Experiment – Efficient Design for Identifying transport Processes.
Report identification:	GEOSIGMA Grap 93 082
Operator of computer and software:	Erik Gustafsson
Company:	GEOSIGMA AB

COMPUTER

Name and version:	Samsung SD830 386 – 33MHz

SOFTWARE

Operative system:	MS–DOS 6.2 / WINDOWS 3.11
Code name:	SLAEM, version 2.1 (Single Layer Analytic Element Model)
Main Manual(s):	SLAEM Manual and SLAEM Help–Files
Program language:	FORTRAN
Compiler:	LAHEY
Preprocessor name:	none
Manual:	–
"Postprocessor" name:	SURFER, version 4.08, 1989
Manual:	Reference Manual
Subroutine:	none

CODE VERIFICATION

Code:	SLAEM
Distributor:	Otto D.L. Strack, 23 Black Oaks Road, Norths Oaks, MN 55127, U.S.A.
Report/article:	Strack O.D.L. 1986. Groundwater Mechanics. Prentice–Hall.
"Code":	SURFER™
Distributor:	Golden Software Inc., 807 14th Street, P.O. Box 281, Golden, Colorado 80402, U.S.A.
Report/article:	–

INPUT DATA AND RESULTS

Stored at: All input data and results are stored at GEOSIGMA AB in Uppsala. Files are stored in directory: C:\SLAEM\DAT and B:\SLAEM\DAT

Numerical simulation number refers to Table 8–1, page 34 in Grap 93 082.

ılation	Input file to SLAEM	Result file / Input to SURFER	Output file from SURFER	Presentation of output
	MWTE01.DAT	MWTE01H.DAT	MWTE01H.OUT	Figure 8–1
	MWTE02.DAT	MWTE02H.DAT	MWTE02H.OUT	in text
	MWTE03.DAT	MWTE03H.DAT	MWTE03H.OUT	in text
	MWTE04.DAT	MWTE04H.DAT	MWTE04H.OUT	in text
	MWTE04.DAT	MWTE04H.DAT	MWTE04H2.OUT	in text
	MWTE05.DAT	MWTE05H.DAT	MWTE05H.OUT	in text
	MWTE06.DAT	MWTE06H.DAT	MWTE06H.OUT	Figure 8–2, 8–3

SKB - ÄSPÖ HARD ROCK LABORATORY

Documentation of numerical simulation by:

Name:	Rune Nordqvist
Company:	GEOSIGMA AB
Date:	September 1993

OBJECT

Modelling Task:	Task No 2A, Scoping Calculations for MWTE
SKB purchase order no:	8-10-170
Title of SKB purchase order:	Äspölaboratoriet - Försök i detaljskala
Author(s) of report:	Nordqvist R., Gustafsson E., Andersson P.
Company:	GEOSIGMA AB
Report Title:	Scoping Calculations for the Multiple Well Tracer Experiment - Efficient Design for Identifying transport Processes.
Report identification:	GEOSIGMA Grap 93 082
Operator of computer and software:	Rune Nordqvist
Company:	GEOSIGMA AB

COMPUTER

Name and version:	486DX - 50MHz

SOFTWARE

Operative system:	MS-DOS 6.00
Code name:	OPT.FOR
Main Manual(s):	See Code Verification
Program language:	FORTRAN
Compiler:	LAHEY
Preprocessor name:	none
Manual:	-
"Postprocessor" name:	GRAPHER, version 1.77, 1988
Manual:	Reference Manual
Subroutine:	none

CODE VERIFICATION

Code:	see above
Distributor:	-
Report/article:	Nordqvist, R, 1994: Notes on a Fortran program for optimization of parameter estimation, model discrimination and sampling cost for arbitrary monitoring networks. GEOSIGMA GRAP 94007.
"Code":	GRAPHER™
Distributor:	Golden Software Inc., 807 14th Street, P.O. Box 281, Golden, Colorado 80402, U.S.A.
Report/article:	-

INPUT DATA AND RESULTS

Stored at: All input data and results are stored at GEOSIGMA AB in Uppsala. Files are stored on diskettes.

INPUT DATA:

Data file names:
1A.DAT
1B.DAT
2A.DAT
2B.DAT
2C.DAT
2D.DAT
2F.DAT
2G.DAT
2H.DAT
3A.DAT
3B.DAT
3C.DAT
3D.DAT

RESULTS:

Ref: Figure 9-1 to 9-6
Data File name: OPTRES4.DAT

HPGL Files:
PEVSC4XX.OUT (9-1)
1T092.OUT (9-2a)
2T092.OUT (9-2b)
3T092.OUT (9-2c)
MDVSC4X.OUT (9-3)
MDVSPE4X.OUT (9-4)
ZDVSC4X.OUT (9-5)
ZMVSC4X.OUT (9-6)

Ref: Figure 9-7
Data file name: OPTRES1.DAT
HPGL file: ZMVSC1X.OUT

Ref: Figure 9-8
Data file name: OPTRES3.DAT
HPGL file: ZMVSC3X.OUT

SKB – ÄSPÖ HARD ROCK LABORATORY

Documentation of numerical simulation by:
Name: Rune Nordqvist
Company: GEOSIGMA AB
Date: September 1993

OBJECT

Modelling Task:	Task No 2A, Scoping Calculations for MWTE
SKB purchase order no:	8–10–170
Title of SKB purchase order:	Äspölaboratoriet – Försök i detaljskala
Author(s) of report:	Nordqvist R., Gustafsson E., Andersson P.
Company:	GEOSIGMA AB
Report Title:	Scoping Calculations for the Multiple Well Tracer Experiment – Efficient Design for Identifying transport Processes.
Report identification:	GEOSIGMA Grap 93 082
Operator of computer and software:	Rune Nordqvist
Company:	GEOSIGMA AB

COMPUTER

Name and version:	486DX – 50MHz

SOFTWARE

Operative system:	MS–DOS 6.00
Code name:	TUBA
Main Manual(s):	See Code Verification
Program language:	FORTRAN
Compiler:	LAHEY
Preprocessor name:	none
Manual:	–
"Postprocessor" name:	SURFER, version 4.08, 1989
Manual:	Reference Manual
Subroutine:	none

CODE VERIFICATION

Code:	see above
Distributor:	–
Report/article:	Zimmerman, D.,A., Wilson, J.L., 1989: Description and Users manual for TUBA. A computer code for generating two–dimensional random fields via the turning bands method. New Mexico Institute of Mining and Technology, Socorro, New Mexico.
"Code":	SURFER™
Distributor:	Golden Software Inc., 807 14th Street, P.O. Box 281, Golden, Colorado 80402, U.S.A.
Report/article:	–

INPUT DATA AND RESULTS

Stored at: All input data and results are stored at GEOSIGMA AB in Uppsala. Files are stored on diskettes.

INPUT DATA: in text

RESULTS:

Ref:	Figure 10–1
Data File name:	TL101.DAT
HPGL File:	TL101.OUT

SKB – ÄSPÖ HARD ROCK LABORATORY

Documentation of numerical simulation by:
Name: Rune Nordqvist
Company: GEOSIGMA AB
Date: September 1993

OBJECT

Modelling Task:	Task No 2A, Scoping Calculations for MWTE
SKB purchase order no:	8–10–170
Title of SKB purchase order:	Äspölaboratoriet – Försök i detaljskala
Author(s) of report:	Nordqvist R., Gustafsson E., Andersson P.
Company:	GEOSIGMA AB
Report Title:	Scoping Calculations for the Multiple Well Tracer Experiment – Efficient Design for Identifying transport Processes.
Report identification:	GEOSIGMA Grap 93 082
Operator of computer and software:	Rune Nordqvist
Company:	GEOSIGMA AB

COMPUTER

Name and version:	486DX – 50MHz

SOFTWARE

Operative system:	MS–DOS 6.00
Code name:	SUTRA
Main Manual(s):	See Code Verification
Program language:	FORTRAN
Compiler:	LAHEY
Preprocessor name:	none
Manual:	–
"Postprocessor" name:	GRAPHER, version 1.77, 1988
Manual:	Reference Manual
"Postprocessor" name:	SUREA–PLOT
Manual:	See Code verification

CODE VERIFICATION

Code:	see above
Distributor:	U.S.G.S
Report/article:	Voss, C.I., 1990: SUTRA – A finite element simulation model for saturated–unsaturated, fluid–density–dependent groundwater flow with energy or chemically–reactive single–species solute transport. Version V06902D. U.S. Geological Survey Water–Resources Investigations Report 84–4369.
Code:	SUTRA–PLOT
Report/article:	Souza, W.R., 1987: SUTRA–PLOT – Documentation of a graphical display program for the saturated–unsaturated transport (SUTRA) finite–element simulation model. Version V06902D. U.S. Geological Survey Water–

Resources Investigations Report 87–4245.
"Code": GRAPHER™
Distributor: Golden Software Inc., 807 14th Street, P.O. Box 281, Golden, Colorado 80402, U.S.A.

INPUT DATA AND RESULTS

Stored at: All input data and results are stored at GEOSIGMA AB in Uppsala. Files are stored on diskettes.

INPUT DATA:

Data file names: MWTE2D.D5
MWTE2D.D55

RESULTS:

Ref: Figure 10–2
Data File name: MWTE2DV.DAT
HPGL File: MWTE2DV.OUT

Ref: Figure 10–3
Data file names: TTMP40.DAT
TTMP100.DAT
TTMP400.DAT
HPGL file: 2DINVDAT.OUT

SKB - ÄSPÖ HARD ROCK LABORATORY

Documentation of numerical simulation by:
Name: Rune Nordqvist
Company: GEOSIGMA AB
Date: September 1993

OBJECT

Modelling Task:	Task No 2A, Scoping Calculations for MWTE
SKB purchase order no:	8-10-170
Title of SKB purchase order:	Äspölaboratoriet - Försök i detaljskala
Author(s) of report:	Nordqvist R., Gustafsson E., Andersson P.
Company:	GEOSIGMA AB
Report Title:	Scoping Calculations for the Multiple Well Tracer Experiment - Efficient Design for Identifying transport Processes.
Report identification:	GEOSIGMA Grap 93 082
Operator of computer and software:	Rune Nordqvist
Company:	GEOSIGMA AB

COMPUTER

Name and version:	486DX - 50MHz

SOFTWARE

Operative system:	MS-DOS 6.00
Code name:	PAREST
Main Manual(s):	See Code Verification
Program language:	FORTRAN
Compiler:	LAHEY
Preprocessor name:	none
Manual:	-
"Postprocessor" name:	GRAPHER, version 1.77, 1988
Manual:	Reference Manual
Subroutine:	none

CODE VERIFICATION

Code:	see above
Distributor:	-
Report/article:	Nordqvist, R, 1994: PAREST: a Fortran code for inverse modeling with an arbitrary model using non-linear least squares regression - users manual. GEOSIGMA GRAP 94005.
"Code":	GRAPHER™
Distributor:	Golden Software Inc., 807 14th Street, P.O. Box 281, Golden, Colorado 80402, U.S.A.
Report/article:	-

INPUT DATA AND RESULTS

Stored at: All input data and results are stored at GEOSIGMA AB in Uppsala. Files are stored on diskettes.

INPUT DATA:

Data file names: TTMP40.DAT
TTMP100.DAT
TTMP400.DAT

RESULTS:

Ref: Figure 10–4
Data File name: 2DINV12.SUM
HPGL File: 2DINV12.OUT

Ref: Figure 10–5
Data file name: 2DINV5C.SUM
HPGL file: 2DINV5C.OUT

Ref: Figure 10–6
Data file name: 2DINV7.SUM
HPGL file: 2DINV7.OUT

Ref: Figure 10–7
Data file name: 2DINV9.SUM
HPGL file: 2DINV9.OUT

Ref: Figure 10–8
Data file name: 2DINV11.SUM
HPGL file: 2DINV11.OUT

List of ICR Reports 1993

ICR 93-01
Flowmeter measurement in borehole KAS 16
P Rouhiainen
June 1993
Supported by TVO, Finland

ICR 93-02
Development of ROCK-CAD model for Äspö Hard Rock Laboratory site
Pauli Saksa, Juha Lindh, Eero Heikkinen
Fintact KY, Helsinki, Finland
December 1993
Supported by TVO, Finland

ICR 93-03
Scoping calculations for the Matrix Diffusion Experiment
Lars Birgersson[1], Hans Widén[1], Thomas Ågren[1], Ivars Neretnieks[2], Luis Moreno[2]
1 Kemakta Konsult AB, Stockholm, Sweden
2 Royal Institute of Technology, Stockholm, Sweden
November 1993
Supported by SKB, Sweden

ISSN 1104-3210
ISRN SKB-ICR--93/4--SE
CM Gruppen AB, Bromma 1994